



2014

# EVALUATION OF THE PHYSIOLOGICAL EFFECTS OF REDUCED HYDROXOCOBALAMIN ON ACUTE CARBON MONOXIDE TOXICITY

Alden Newcomb  
*Virginia Commonwealth University*

Follow this and additional works at: <https://scholarscompass.vcu.edu/etd>



Part of the [Physiology Commons](#)

© The Author

---

**Downloaded from**

<https://scholarscompass.vcu.edu/etd/3560>

This Thesis is brought to you for free and open access by the Graduate School at VCU Scholars Compass. It has been accepted for inclusion in Theses and Dissertations by an authorized administrator of VCU Scholars Compass. For more information, please contact [libcompass@vcu.edu](mailto:libcompass@vcu.edu).

**© Alden Newcomb 2014**  
**All Rights Reserved**

EVALUATION OF THE PHYSIOLOGICAL EFFECTS OF REDUCED  
HYDROXOCOBALAMIN ON ACUTE CARBON MONOXIDE TOXICITY

A thesis submitted in partial fulfillment for the degree of Master of Science in Physiology  
& Biophysics at Virginia Commonwealth University

By

ALDEN H. NEWCOMB

Bachelor of Science, Biochemistry, Virginia Polytechnic Institute and State University,  
2012

Director: DR. BRUCE SPIESS, MD, FAHA

DIRECTOR VIRGINIA COMMONWEALTH UNIVERSITY REANIMATION SHOCK  
CENTER, DEPARTMENT OF ANESTHESIOLOGY, VCU SCHOOL OF MEDICINE

Virginia Commonwealth University  
Richmond, VA  
July, 2014

## Acknowledgements

I would like to thank Dr. Bruce Spiess for granting me the incredible opportunity to become a part of the VCURES family and providing me with the support, encouragement, and funds to bring this project to fruition. Additional heartfelt thanks go out to Dr. Christina Marmarou and Dr. Brandon Wills, for their tireless support and encouragement through this process. Thanks to Dr. Penny Reynolds, Dr. Jiepei Zhu, and Mr. Brian Berger for their willingness to share their endless expertise and answer my equally endless questions. I feel truly blessed to be a part of the VCURES team and could not have asked for more brilliant and supportive educators. From the bottom of my heart, thank you. I also cannot possibly articulate how grateful I am for the continuous support from my family. Without the emotional and financial support from my mother, grandmother, and sister, I know that I couldn't have made it this far. Finally, I would like to thank and dedicate this work to my friend, mentor and guardian angel, Dr. Cheryl Haas, who will forever motivate me.



## TABLE OF CONTENTS

|   |      |
|---|------|
| LIST OF FIGURES .....   | vi   |
| LIST OF TABLES .....  | vii  |
| LIST OF ABBREVIATIONS .....   | viii |
| ABSTRACT .....  | xiv  |
| 1. INTRODUCTION AND BACKGROUND.....                                     |      |
| 1.1 Carbon Monoxide – A Global Health Threat.....                       | 1    |
| 1.2 Carboxyhemoglobin .....   | 4    |
| 1.3 Effects of CO on the Vascular & Cardiopulmonary Systems .....       |      |
| 1.3.1 CO & The Vasculature .....  | 8    |
| 1.3.2 CO-Induced Myocardial Damage .....                                | 9    |
| 1.3.3 CO-Induced Myocardial Damage – Cellular Toxicity .....            | 10   |
| 1.3.4 The Respiratory System & Blood Chemistry in CO Poisoning .....    | 13   |
| 1.4 Effects of CO on the Brain .....                                    |      |
| 1.4.1 Acute Pathophysiology.....  | 15   |
| 1.4.2 Delayed Pathophysiology.....                                      | 17   |
| 1.5 Clinical Presentation, Diagnosis, & Treatment of CO Poisoning ..... |      |
| 1.5.1 Clinical Presentation .....                                       | 18   |
| 1.5.2 Diagnostic Workup & Common Findings .....                         | 19   |
| 1.5.3 Current Treatment Modalities & Controversies .....                | 20   |
| 1.6 A Potential Antidote .....  |      |
| 1.6.1 Hydroxocobalamin .....  | 25   |

|  |    |
|--|----|
| 1.6.2 Reduced Hydroxocobalamin & CO .....                          | 26 |
| 1.7 Hypotheses & Specific Aims .....                               | 27 |
| 1.8 Basic Approach.....  |    |
| 1.8.1 Non-Survival Surgery .....                                   | 28 |
| 1.8.2 Brain Tissue Oxygen Tension Monitoring .....                 | 30 |
| 1.9 Summary of Findings .....                                      | 32 |
| 2. MATERIALS & METHODS.....  |    |
| 2.1 Materials .....  | 34 |
| 2.2 Production of Reduced Hydroxocobalamin .....                   | 37 |
| 2.3 Animals & Ethics Statement .....                               | 38 |
| 2.4 Non-Survival Surgical Procedure.....                           |    |
| 2.4.1 Experimental Group Assignment & Procedural Preparation ..... | 38 |
| 2.4.2 Femoral Artery Cannulation .....                             | 39 |
| 2.4.3 Licox® Placement .....                                       | 41 |
| 2.4.4 Insult, Treatment, & Post-Treatment Monitoring .....         | 44 |
| 2.5 Statistical Analysis .....                                     | 46 |
| 3. RESULTS.....  |    |
| 3.1 Brain Tissue Oxygen Tension Results.....                       | 47 |
| 3.2 Mean Arterial Pressure Results .....                           | 53 |
| 3.3 Arterial Blood Gas Results.....                                | 59 |
| 3.4 Respiratory Rate Results .....                                 | 63 |
| 4. DISCUSSION .....  |    |
| 4.1 CO Poisoning, Perfusion, & Oxygenation .....                   | 66 |

|  |    |
|--|----|
| 4.2 Post-Exposure & Treatment .....      | 74 |
| 4.3 Limitations & Sources of Error ..... | 78 |
| 4.4 Future Work .....                    | 79 |
| 4.5 Summary .....                        | 80 |
| 4.4 Conclusion .....                     | 81 |
| Bibliography.....                        | 83 |
| Vita .....                               | 96 |

## LIST OF FIGURES

|  |       |
|--|-------|
| Figure 1: Schematic of %COHb Changes in Maternal and Fetal Hb .....                  | 5     |
| Figure 2: Overview of CO-Mediated Pathophysiology .....                              | 7     |
| Figure 3: Pathophysiology of CO-Mediated Cardiotoxicity .....                        | 12    |
| Figure 4: Visual Representation of Surgical Procedure Timeline .....                 | 29    |
| Figure 5: Licox® Brain Tissue Oxygen Tension Electrode.....                          | 31    |
| Figure 6: Surgical Equipment for Arterial Line Placement.....                        | 35    |
| Figure 7: Surgical Equipment for Licox® Electrode Placement & Monitoring .....       | 36    |
| Figure 8: Bilateral Craniotomy Holes.....  | 43    |
| Figure 9: Licox® PbtO <sub>2</sub> Electrode Preparation & Placement .....           | 44    |
| Figure 10: Mean PbtO <sub>2</sub> and Standard Deviations of the Mean Over Time..... | 50    |
| Figure 11: Individual PbtO <sub>2</sub> Trajectories by Experimental Group .....     | 51-52 |
| Figure 12: Mean MAP and Standard Deviations of the Mean Over Time .....              | 57    |
| Figure 13: Individual MAP Trajectories by Experimental Group .....                   | 58-59 |
| Figure 14: Mean Respiratory Rate and Standard Deviations of the Mean Over Time ...   | 65    |
| Figure 15: Correlation of PbtO <sub>2</sub> and MAP during CO Exposure.....          | 69    |
| Figure 16: Correlation of PbtO <sub>2</sub> with MAP – Hemphill et al. ....          | 70    |
| Figure 17: Overlay of Pre- & Post-Treatment PbtO <sub>2</sub> /MAP.....              | 76    |
| Figure 18: Mean PbtO <sub>2</sub> /MAP for all Groups and Times.....                 | 77    |

## LIST OF TABLES

|   |    |
|---|----|
| Table 1: Experimental Exposure-Treatment Groups and Sample Sizes .....          | 38 |
| Table 2: B12r Dosing Protocol .....   | 45 |
| Table 3: Mean PbtO <sub>2</sub> Values and Standard Deviations of the Mean..... | 12 |
| Table 4: Summary Statistical Data for PbtO <sub>2</sub> Analysis .....          | 49 |
| Table 5: Mean MAP Values and Standard Deviations of the Mean .....              | 55 |
| Table 6: Summary Statistical Data for MAP Analysis .....                        | 56 |
| Table 7: Mean ABG Parameter Values and Standard Deviations of the Mean.....     | 62 |
| Table 8: Summary Statistical Data for ABG Parameter Analysis .....              | 63 |
| Table 9: Mean Respiratory Rate and Standard Deviations of the Mean .....        | 64 |
| Table 10: Summary Statistical Data for Respiratory Rate Analysis .....          | 64 |

## LIST OF ABBREVIATIONS

**AA** – Ascorbic acid, ascorbate, or vitamin C. Reducing agent used to reduce hydroxocobalamin.

**ALS** – Advanced Life Support. An abbreviation used to refer to the level of training of an emergency medical services provider. ALS providers include EMT-Intermediates and Paramedics. These providers are capable of performing procedures above that of an emergency medical technician including intravenous drug administration, endtracheal intubation, and cardiac monitoring.

**ATP** – Adenosine Triphosphate. A high-energy nucleoside triphosphate that serves as an energy source for intracellular processes.

**B12** – Hydroxocobalamin, or vitamin B12.

**B12r** – Reduced form of hydroxocobalamin formed when AA is mixed with B12 in proper proportions.

**BKCa** – Large (Big) Conductance Calcium-Activated Potassium Channel. Potassium channel characterized by large conductance of potassium that are essential for smooth muscle tone and neuronal excitability.

**BLS** – Basic Life Support. Refers to the lowest and most basic level of training for emergency medical technicians. BLS providers are only able to provide non-invasive treatments including oral medication administration and oxygen administration.

**C<sub>a</sub>O<sub>2</sub>** – Arterial Content of Oxygen. Calculated as:

$$C_aO_2 = ctHb \times 1.34 \times S_aO_2 + 0.003 \times p_aO_2$$

**CvO<sub>2</sub>** – Venous Content of Oxygen. Calculated as:

$$C_vO_2 = ctHb \times 1.34 \times S_vO_2 + 0.003 \times p_vO_2$$

**CBF** – Cerebral Blood Flow. The amount of blood flowing into the brain, calculated as the difference between mean arterial pressure and intracranial pressure.

**cGMP** – Cyclic Guanosine Monophosphate. A cyclic nucleotide formed from guanosine triphosphate that functions as a key second messenger in many intracellular processes.

**CMRO<sub>2</sub>** – Cerebral Oxygen Consumption Rate. The amount of oxygen consumed by the brain. Calculated as:  $CMRO_2 = CBF(C_aO_2 - C_vO_2)$

**CO** – Carbon monoxide

**CO<sub>2</sub>** – Carbon dioxide

**COHb** – Carboxyhemoglobin. Hemoglobin bound to carbon monoxide in place of, or in addition to oxygen.

**COHb%** - Percentage of carboxyhemoglobin.

**ctHb** – Total concentration of hemoglobin. Amount of hemoglobin in a blood sample, typically expressed in g/dL.

**DNS** – Delayed Neurological Sequelae. A term used to refer to the lasting neurological effects demonstrated following resolution of carbon monoxide exposure symptoms. Also referred to as “Prolonged Neurological Sequelae,” or PNS.

**DO<sub>2</sub>** – Oxygen Delivery. Refers to the amount of oxygen delivered to the whole body or specific organ. In the context of the brain, it is calculated as  $DO_2 = CBF \times C_aO_2$

**ED** – Emergency Department. Hospital department responsible for examination and treatment of patients experiencing a medical emergency.

**EMS** – Emergency Medical Services. Refers to systems in place across the United States and world that provide ambulance-based emergency medical care. EMS providers are trained at the emergency medical technician level or higher.

**EMT** – Emergency Medical Technician. An abbreviation used to refer to emergency responders trained to provide BLS pre-hospital medical care.

**ER** – Emergency Room. Used interchangeably with ED to refer to hospital emergency departments.

**FCOHb** – Fraction of Carboxyhemoglobin. An alternative abbreviation for %COHb.

**GTP** – Guanosine Triphosphate. A high-energy purine nucleoside triphosphate that serves as an energy source for intracellular processes.

**HEMS** – Helicopter EMS. The abbreviation used to refer to helicopter-based EMS care, which typically offers significantly more advanced care and monitoring than ground ambulances.

**Hb** – Hemoglobin. The protein responsible for transport of diatomic oxygen within the body. It is comprised of four subunits, each of which contain a porphyrin ring with a central ferrous iron core. Each subunit is capable of binding and transporting a single diatomic oxygen molecule.

**HBO** – Hyperbaric Oxygen Therapy. Abbreviation used to describe the process of using a sealed chamber to deliver high-concentration oxygen at 2-3 times above normal atmospheric pressure to provide an increased partial pressure of oxygen in order to drive off carbon monoxide from hemoglobin in CO poisoned patients. Considered the current gold standard in CO poisoning treatment.



**HCO<sub>3</sub><sup>-</sup>** - Bicarbonate ion. The anion of carbonic acid. Can refer to the ion itself or the calculated value of bicarbonate in a blood sample, expressed as mEq/L.

**HO** – Heme-Oxygenase Enzyme responsible for endogenous CO production via degradation of heme into protoporphyrin IX.

**HVAC** – Heating, Ventilation, and Air Conditioning. Used to refer to systems that control and supply indoor temperature control, ventilation, and air quality.

**IP** – Intraperitoneal. Administration of a drug via injection into the abdominal cavity for absorption by the peritoneum.

**IRB** – Institutional Review Board. The university department responsible for oversight and approval of all projects involving the use of human subjects in research.

**IV** – Intravenous. Administration of a drug via injection into the venous system.

**MAC** – Minimum Alveolar Concentration. A relative concentration of anesthetic gas required to sedate 50% of a given species or population to an adequate anesthetic plane to tolerate surgical pain

**NBO** – Normobaric Oxygen Therapy. The application of high-concentration oxygen to patients at normal atmospheric.

**NO** – Nitric Oxide. An endogenous gaseous signaling molecule that plays an important role in vascular smooth muscle tone.

**NS** – Normal Saline. An isotonic 0.9% saline solution.

**O<sub>2</sub>** – Diatomic Oxygen.

**O<sub>2</sub>Hb** – Oxyhemoglobin. Hemoglobin bound to oxygen.

**OHcbl** – Hydroxocobalamin. A form of vitamin B12 containing a hydroxyl group bound to the upper axial ligand binding site. Refers specifically to the non-reduced form.

**OSHA** – Occupational Health and Safety Administration. The government agency responsible for establishing guidelines for safe workplace environments.

**PbO<sub>2</sub>** – Brain Tissue Oxygen Tension. A measurement of oxygen tension within brain tissue as measured by Licox® Clark-type polarographic electrode, expressed in mmHg.

**pCO<sub>2</sub>** – Partial Pressure of Carbon Dioxide. A measure of the pressure of dissolved carbon dioxide within a blood sample relative to the pressure of other gases within the same sample. Expressed in mmHg.

**pH** – A measure of the concentration of hydrogen atoms in a solution on a logarithmic scale.

**pO<sub>2</sub>** – Partial Pressure of Oxygen. A measure of the pressure of dissolved oxygen within a blood sample relative to the pressure of other gases within the sample. Expressed in mmHg.

**PNS** – Prolonged Neurological Sequelae. See DNS.

**PPM** – Parts Per Million.

**Q** – Cardiac Output. The product of stroke volume and heart rate. Commonly abbreviated CO, but substituted for the physiological abbreviation to avoid confusion with carbon monoxide.

**RBC** – Red Blood Cell.

**ROS** – Reactive Oxygen Species. Commonly known as “free radicals.” Produced as a natural byproduct of respiration, accumulation of these compounds is cytotoxic.

**RR** – Respiration Rate. The number of respiratory cycles in a given time frame.

**RRS** – Raman Resonance Spectroscopy. An analytical technique that uses monochromatic laser light directed onto a sample to identify chemical components.

Used to verify the production of B12r in B12+AA mixtures.

**sGC** – Soluble Guanylyl Cyclase. A heme-containing protein responsible for the conversion of GTP to cGMP.

**T<sub>1/2</sub>** – Half-life. Time required for a compound to decay to half of the original concentration.

**VO<sub>2</sub>** – Oxygen consumption. Refers to whole body oxygen consumption in the context of this paper. Calculated according to the Fick equation:  $VO_2 = Q \times (C_aO_2 - C_vO_2)$

## **Abstract**

### **EVALUATION OF THE PHYSIOLOGICAL EFFECTS OF REDUCED HYDROXOCOBALAMIN ON ACUTE CARBON MONOXIDE TOXICITY**

By: Alden H. Newcomb, B.S.

A thesis submitted in partial fulfillment of the requirements for the degree of Master of  
Science at Virginia Commonwealth University

Virginia Commonwealth University, 2014

Major Advisor: Dr. Bruce Spiess, MD, FAHA  
Director, Virginia Commonwealth University Reanimation Shock Center  
Affiliate Professor, Department of Physiology & Biophysics

Carbon monoxide (CO) poisoning represents a global health threat responsible for hundreds of thousands of hospital visits and tens of thousands of deaths annually. Oxygen therapy is the only current approved treatment for CO poisoning. Previous work published in the 1970's and research conducted in the VCURES lab group has indicated that a reduced form of vitamin B12, hydroxocobalamin (B12r), can potentially serve as an antidote for CO poisoning by converting CO bound to hemoglobin to carbon dioxide (CO<sub>2</sub>) and mitigating the deleterious neurological effects of CO poisoning. For the first time in documented literature we successfully used a Clark-type polarographic oxygen-sensitive electrode to demonstrate CO-induced decreases in brain tissue oxygen tension in anesthetized rats. Additionally, we demonstrated that B12r is capable of rescuing this CO-induced hypoxia and hypotension within 15 minutes of intraperitoneal administration with no adverse effects on blood chemistry.

## INTRODUCTION AND BACKGROUND

### 1.1 Carbon Monoxide Poisoning – A Global Health Threat

The toxic and fatal effects of carbon monoxide (CO) have been known for thousands of years; ancient Greeks and Romans used the gas for execution purposes. Known as “the silent killer” due to its lack of color, odor, or taste, CO forms from the incomplete combustion of hydrocarbons and other carbon-containing compounds.<sup>1</sup> The Occupational Health and Safety Administration (OSHA) requires workplace atmospheric CO concentrations to be less than 0.0035%, or 35 parts per million (ppm), indicating how toxic CO truly is.<sup>2</sup> Common sources of CO production include exhaust from internal combustion engines, improperly ventilated gas appliances, malfunctioning HVAC systems, and structure fires. Most recently, a faulty ventilation system in a New York restaurant led to a mass CO exposure that caused one death and hospitalized dozens of employees and restaurant patrons.<sup>3</sup> In the United States alone between 2000 and 2009, non-fire related CO exposures accounted for over 15,000 emergency department (ED) visits and over 500 deaths annually.<sup>4–6</sup> The World Health Organization reported over 140,000 non-fire related CO deaths in European member states from 1980-2008.<sup>7</sup> When fire-related CO exposures are accounted for, these numbers increase drastically. Each year, a reported 310,000-670,000 persons are exposed to structure fire smoke and 20,000-23,000 die from smoke inhalation in the United States alone.<sup>8</sup> Structure fire smoke can contain CO levels of greater than 70,000 parts per million (ppm) in an enclosed room.<sup>9</sup> The actual number of annual carbon monoxide exposures and deaths is assumed to be much higher than the reported numbers because CO exposure

symptoms are often mistaken for benign pathologies like acute viral illnesses, acute anxiety, or clinical depression.<sup>10</sup> Across the globe, carbon monoxide is thought to account for over 50% of deaths by poisoning.<sup>10,11</sup>

Incidences of CO poisoning vary seasonally in temperate climates. Cold seasons are often associated with higher numbers of CO exposures due to improperly ventilated hydrocarbon-powered heating appliances.<sup>10</sup> Natural disasters such as hurricanes, tornadoes, and snowstorms also bring about an increase in CO poisonings due to the use of generators and other fossil fuel-powered appliances indoors with poor ventilation. Between 1991 and 2009, there were 1888 reported cases of disaster-related CO exposure with 75 fatalities.<sup>12</sup> In the two weeks following Hurricane Sandy in 2012, there were 437 CO exposures reported to 911 call centers in New York City alone due to indoor grilling and indoor use of gasoline generators.<sup>13</sup> Gasoline powered generators are the most common culprit behind hurricane and tornado related CO exposures; vehicle exhaust is the most common cause of CO exposures related to snowstorms.<sup>14–16</sup> Countries in tropical climates, particularly developing countries, have reported CO exposures resulting from the use of indoor charcoal cooking devices.<sup>17</sup> Gas geysers, a type of gas-powered water heater popular in India, have been linked to multiple deaths and CO poisonings. However, the true number of CO-related deaths and exposures in India is unknown due to improper reporting of suspected cases.<sup>18,19</sup>

The abovementioned CO poisonings and deaths do not account for intentional exposures, that is, attempted and successful suicides. Intentional CO exposures account for over 15,000 ED visits annually and two thirds of all CO-related deaths in the United States.<sup>20</sup> In New Zealand, over 60% of the reported 1,302 intentional poisoning

deaths between 1999 and 2008 were due to CO inhalation.<sup>21</sup> Suicide by intentional CO inhalation is common across the globe, with vehicle exhaust and charcoal smoke as the two most common CO sources.<sup>22–34</sup> Intentional vehicle exhaust exposures can take place both indoors and outdoors. Indoor exposures generally involve idling a vehicle in an enclosed space, often a garage, with the vehicle windows down and garage door shut. Outdoor exhaust inhalations require slightly more creative methods – a vacuum hose or similar tubing is run from the vehicle tailpipe into the passenger compartment of the automobile and exhaust fumes are allowed to accumulate within the cabin. Similar methods have been reported in the United States, across Europe, and Asia.<sup>29,30,32,34,35</sup> This method of intentional CO exposure has witnessed a decline over the past two decades as modern catalytic converters can effectively scrub up to 99% of CO from automobile exhaust.<sup>34</sup>

Although the incidence of vehicle exhausted-related CO exposures has declined, the popularity of suicide by carbon monoxide has not. A simple Google search of “commit suicide by carbon monoxide” yields multiple websites that provide detailed instructions on how to do so.<sup>36,37</sup> The most recent global trend in intentional CO exposures involves burning charcoal inside of a small room, often a bathroom, that has been sealed with duct tape.<sup>23</sup> This method of suicide has gained popularity across the world, but most notably so in Asian countries. Indoor charcoal burning accounted for 33.5% of all suicides in Taiwan in 2006.<sup>31,33</sup> In Hong Kong, charcoal burning accounted for 24.1% of suicides between 2002 and 2004.<sup>38</sup> A startling Internet trend known as a “suicide pact” has emerged in Japan and spread to China, in which strangers exchange online messages vowing to commit suicide together. The cause of death in over 90% of

these “internet suicides” in China and Japan was carbon monoxide poisoning due to indoor charcoal burning.<sup>28,39</sup>

## 1.2 Carboxyhemoglobin

The central dogma of CO toxicity, herein referred to as the “hypoxic theory,” was first described by Douglas and Haldane in the turn of the 20<sup>th</sup> century.<sup>40,41</sup> Their work has stood the test of time and is still taught in medical schools, nursing schools, and allied health programs across the world. Carbon monoxide is nonpolar and therefore lipophilic, diffusing rapidly across pulmonary epithelium when inhaled and binding tightly to the central iron atom in the heme moiety of heme-containing proteins such as hemoglobin (Hb), myoglobin, cytochromes, and NADH reductase.<sup>42</sup> Binding of CO to Hb forms carboxyhemoglobin (COHb), which is incapable of binding and transporting oxygen (O<sub>2</sub>), thus causing a functional anemia by reducing the amount of oxyhemoglobin (O<sub>2</sub>Hb). Carboxyhemoglobin formation also alters the conformation of hemoglobin, reducing its ability to release O<sub>2</sub> to tissue. The increased oxygen affinity of Hb in CO poisoning is known as the “Haldane effect.”<sup>43</sup>

This displacement of oxygen from hemoglobin and alteration of O<sub>2</sub> release leads to a decrease in tissue O<sub>2</sub> delivery causing hypoxic injury, especially to organs that are heavily oxygen dependent such as the brain and heart. Due to the high affinity of CO for Hb, COHb exhibits a half-life ( $t_{1/2}$ ) of approximately 6 hours when an exposed patient is removed from the environment containing CO and allowed to breathe ambient air. Because of this long half-life, patients exposed to CO can potentially still suffer its harmful effects hours after exposure.<sup>44–46</sup> This holds especially true in pregnant patients



due to the higher affinity of fetal Hb for both CO and O<sub>2</sub>. Thus, at equilibrium for a given partial pressure of dissolved CO in blood, fetal COHb levels (%COHB) will be higher than that of the mother and can continue to rise even while maternal %COHb drops.<sup>43</sup> A representative schematic of this phenomenon is depicted in Figure 1.

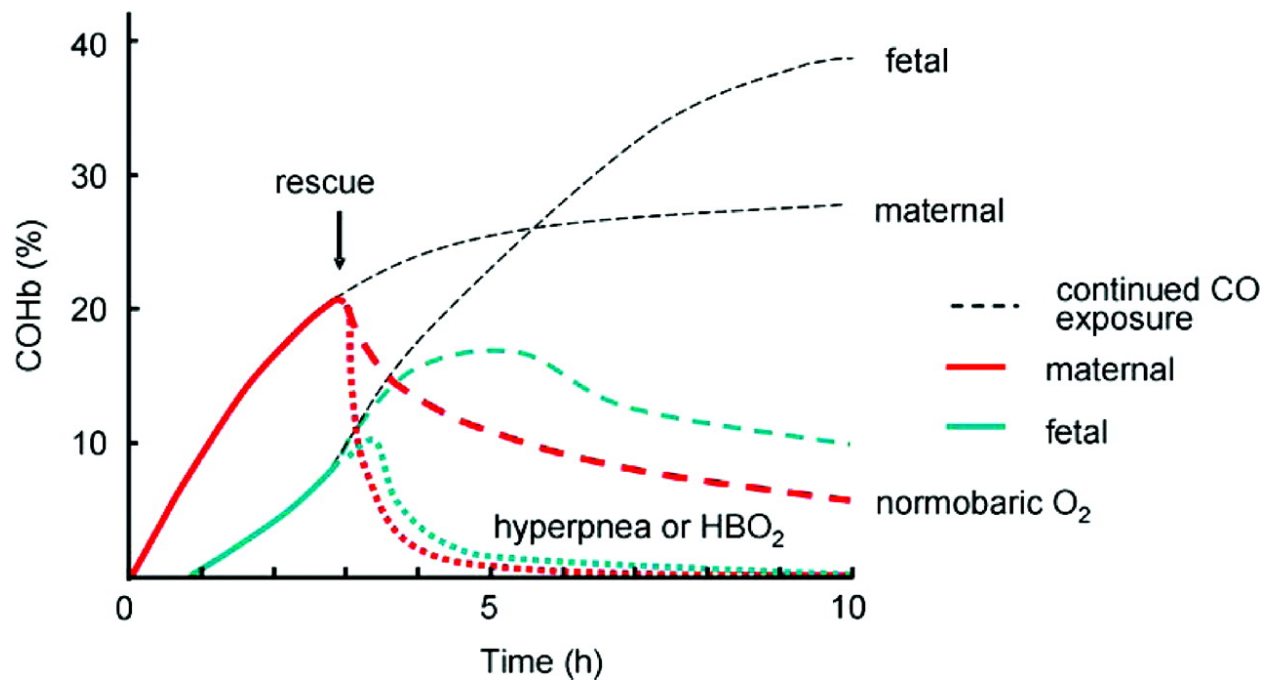


**Figure 1 – Schematic of %COHb Changes in Maternal and Fetal Hb.** Black broken lines indicate %COHb steady-state equilibrium. Colored broken lines represent immediate post-exposure treatment with normobaric O<sub>2</sub>. Colored dotted lines represent immediate treatment with hyperbaric O<sub>2</sub>. Adapted from “Rapid Elimination of CO from the Lungs: coming full circle 100 years on” by Fisher et al., 2011, *Experimental Physiology OA*, 96:12, 1262-1269. Copyright 2011 by the authors. Adapted with permission.

The amount of COHb formed during CO inhalation varies with the concentration of the inhaled gas, time exposed, cardiac output, respiratory rate, and tidal volume. COHb formation continues during exposure until a steady-state equilibrium %COHb is reached with the partial pressure of inhaled CO.<sup>40,41,46</sup>

Mammals form CO endogenously during the breakdown of heme via heme oxygenase (HO) proteins. As such, humans will generally have a baseline %COHb from 0-3%. Smokers and people in urban environments can exhibit %COHb of greater than 10%.<sup>47</sup> While it is generally accepted that high %COHb levels are associated with more severe exposures and poor clinical outcomes, there is interestingly no correlation between %COHb and prognosis.<sup>44,46,48–50</sup> This phenomenon was first described by John Haldane's son in 1927, who reported that CO mortality was not related to the formation of COHb.<sup>51</sup> Patients presenting with a seemingly fatal %COHb can make complete recoveries, just as those presenting with mildly increased %COHb may die or suffer from lasting neurological and/or cardiac complications.<sup>44,46–48</sup> The variances seen between initial %COHb and prognosis are evidence that there is much more to CO poisoning than COHb-dependent tissue hypoxia, and this is indeed true. A visual representation of COHb-mediated pathophysiology and additional mechanisms to be discussed in the proceeding sections is given in Figure 2.

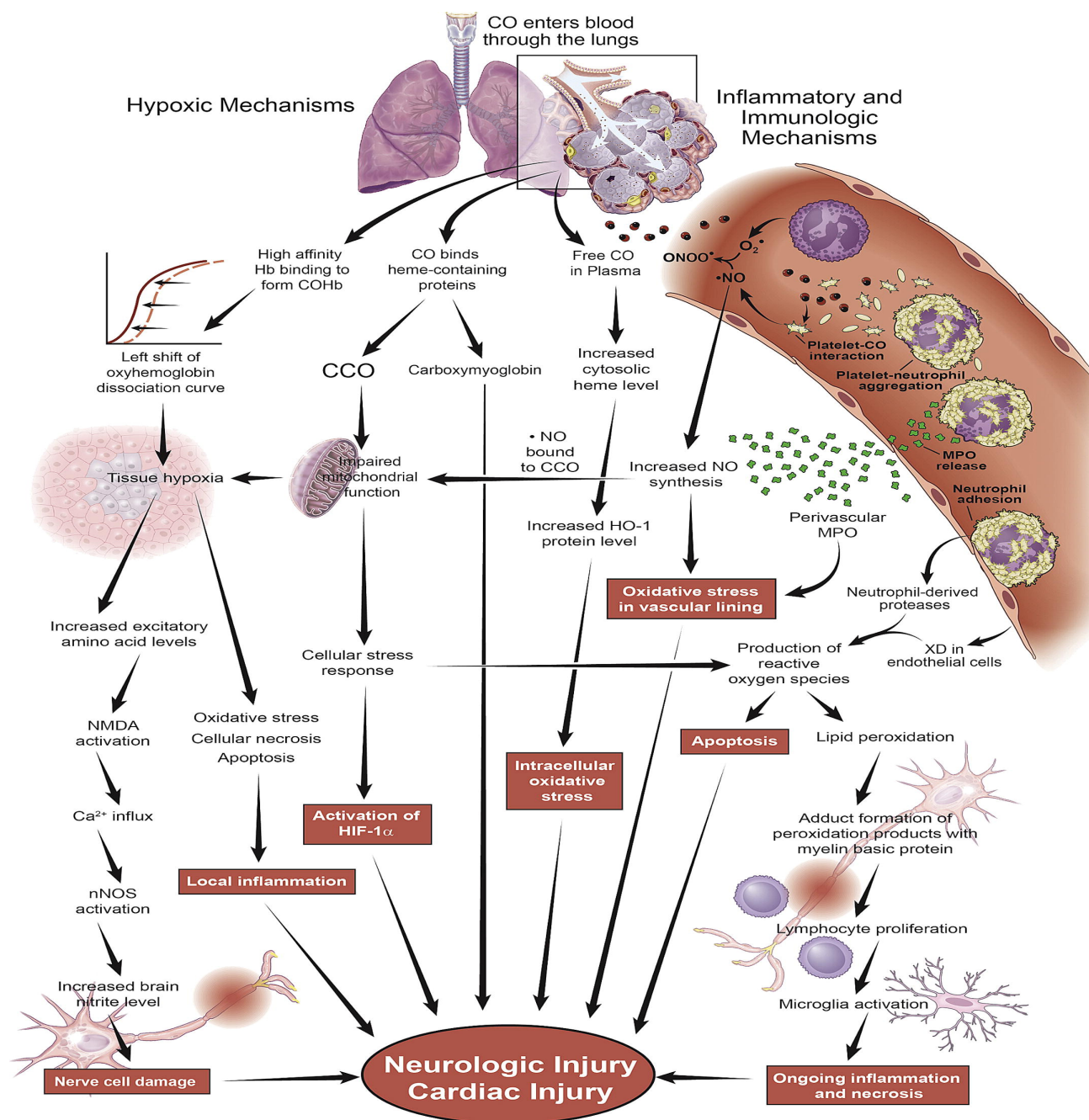


**Figure 2 – Overview of CO-Mediated Pathophysiology.** Adapted from: “Carbon Monoxide Poisoning” by Guzman, J. *Critical Care Clinics*, 2012, 98:537-548. Copyright 2012, Elsevier. Adapted with permission.

## **1.3 Effects of CO on the Vascular & Cardiopulmonary Systems**

### **1.3.1 CO & Vasculature**

Simple physics dictates that the formation of COHb requires a partial pressure of dissolved CO in the bloodstream in order to form and stabilize the COHb complex. This dissolved CO readily diffuses across endothelial membranes and into surrounding tissue. CO exhibits potent vasodilatory effects in vascular tissue similar to those of nitric oxide (NO) and hypotension is commonly seen in CO poisoned patients as a result.<sup>42,44,52</sup> Much like NO, CO is also produced endogenously. Endogenous CO forms from the breakdown of heme via HO proteins that are expressed ubiquitously in the body.<sup>53,54</sup> Once synthesized by HO, CO binds and activates soluble guanylyl cyclase (sGC), a heme-containing protein responsible for the conversion of guanosine triphosphate (GTP) to cyclic guanosine monophosphate (cGMP). Activation of sGC increases cGMP concentration in vascular smooth muscle cells, which decreases intracellular calcium ( $\text{Ca}^{2+}$ ) concentrations by blocking  $\text{Ca}^{2+}$  entry, blocks potassium ( $\text{K}^{+}$ ) entry into the cell (thereby hyperpolarizing the membrane potential), and stimulates myosin light chain phosphatase pathways resulting in smooth muscle relaxation and vasodilation.<sup>53–55</sup> NO production is also increased during exposure to low concentrations (nanomolar levels) of CO. At low concentrations, CO binds to the heme moiety and activates nitric oxide synthase (NOS), the enzyme responsible for NO production. This increase in NO production ceases at higher CO concentrations (micromolar levels), at which point CO actually inhibits NOS activity.<sup>42</sup> CO also causes release of NO from

platelets and triggers platelet-neutrophil aggregation causing neutrophil diapedesis into the endothelium and free radical-mediated endothelial injury.

In addition to the NO-cGMP-dependent pathway described above, CO has also been shown to activate large-conductance calcium channels (BKCa). Although the exact mechanism of the interaction between BKCa and CO remains elusive, multiple studies have shown that activation of BKCa by CO results in a reduction of intracellular  $\text{Ca}^{2+}$  via closing of voltage dependent  $\text{Ca}^{2+}$  channels, resulting in membrane hyperpolarization and vasodilation.<sup>56,57</sup>

### **1.3.2 CO-Induced Myocardial Damage**

Myocardial damage is common following moderate to severe CO exposure and presents in approximately 35% of these patients.<sup>58</sup> Chronic exposure to CO has been shown to cause myocardial fibrosis and stunning; severe acute exposure is more closely associated with lethal arrhythmias.<sup>52,58–60</sup> Ventricular dysfunction and heart failure have also been reported following CO exposure. These patients demonstrated a strong negative correlation between left ventricular ejection fraction and %COHb ( $r = -0.660$ ) and duration of CO exposure ( $r = -0.630$ ).<sup>58</sup> Satran et al. reported that over one in three patients hospitalized for CO exposure demonstrated elevated serum levels of troponin I (TnI) and creatine-kinase MB fraction (CKMB), which are sensitive and specific biological markers of cardiac injury.<sup>52,61</sup> Fracasso and colleagues demonstrated increased expression of two known markers of acute myocardial injury, fibronectin and complement complex C5b-9, in the right ventricles of 26 out of 26 CO fatality victims.<sup>61</sup>

The toxicity exerted on cardiac tissue by CO is twofold and additive; decreased  $\text{O}_2$  delivery causes a hypoxia/ischemia injury and a toxic injury forms from the direct

cytotoxic effects of CO on cellular metabolism. This unique injury pattern is outlined in Figure 2. CO-induced vasodilation causes a compensatory increase in heart rate, cardiac output (Q), and contractility that has been well documented since the mid-19<sup>th</sup> century.<sup>42,62</sup> Coronary blood flow increases as well during CO exposure.<sup>59</sup> Interestingly, subendocardial blood flow only displays a marginal increase during CO exposure. This indicates the possibility of subendocardial hypoperfusion playing a role in the cardiac pathology of CO poisoning.<sup>63</sup> Hypoxic stress from the formation of COHb is further exacerbated by the increase in myocardial oxygen demand caused by the associated changes in contractility and Q and can result in eventual cardiac failure. This CO-induced cardiac hypoxia/ischemia injury pattern displays pathological and diagnostic similarities to ischemic cardiac injury seen in the context of coronary artery disease.<sup>52,61,64</sup> Population studies and case reports have indicated that CO exposure can create a pro-thrombotic state, leading to an increased risk of arterial, venous, and stent thrombosis. The mechanism behind this is not known.<sup>42</sup>

### **1.3.3 CO-Induced Myocardial Damage – Cellular Toxicity**

The specific cytotoxic effects of CO on cardiac tissue are complicated and still not fully understood. At the subcellular level, CO is both directly and indirectly toxic to the mitochondria. When dissolved CO diffuses into the myocardium, it binds to the heme complex of the intracellular O<sub>2</sub> carrier myoglobin with an affinity 60-times greater than that of O<sub>2</sub>. This displaces O<sub>2</sub> and rapidly depletes the O<sub>2</sub> supply to the mitochondria, impairing oxidative phosphorylation.<sup>44</sup>

Direct mitochondrial toxicity of CO is once again, multifaceted and complex. CO specifically binds and inhibits the terminal electron acceptor of the electron transport

chain (ETC), cytochrome c oxidase (CcO), which causes uncoupling of the ETC and impaired adenosine triphosphate (ATP) production.<sup>65,66</sup> Cardiac muscle is then forced to switch to anaerobic glycolysis to produce energy, resulting in lactic acidosis.<sup>59</sup>

Mitochondria continuously produce reactive oxygen species (ROS), commonly known as “free radicals,” as a normal byproduct of oxidative phosphorylation. These ROS are normally scavenged by the natural antioxidant glutathione. However, CO exposure depletes glutathione levels in cardiac tissue, leading to unchecked ROS production, lipid peroxidation, and tissue damage.<sup>59,67,68</sup> At tissue concentrations greater than 88nM, CO has also been shown to trigger apoptosis in endothelial cells via NO-mediated activation of the pro-apoptotic enzyme caspase-1.<sup>69</sup>

Cardiac ion channels have recently been shown to be susceptible to modulation by CO, however the effects and mechanisms are again poorly understood and no fully comprehensive data on this phenomenon has yet been published.<sup>70</sup> Acute CO exposure is closely associated with the development of atrial and ventricular arrhythmias, elongated QT intervals, and ischemic ST and T wave changes.<sup>44,59,61,70–73</sup> The risk of arrhythmia in CO poisoning increases if additional stress is placed on the heart and in patients with existing cardiac pathology.<sup>71</sup> The current leading theory behind the development of arrhythmias in CO poisoning indicates that CO prolongs the late inward Na<sup>+</sup> flux of the Na<sub>v</sub>1.5 channel and the associated Ca<sup>2+</sup> transient via NO-mediated pathways, leading to action potential prolongation and early after-depolarization-like arrhythmias.<sup>74,75</sup>

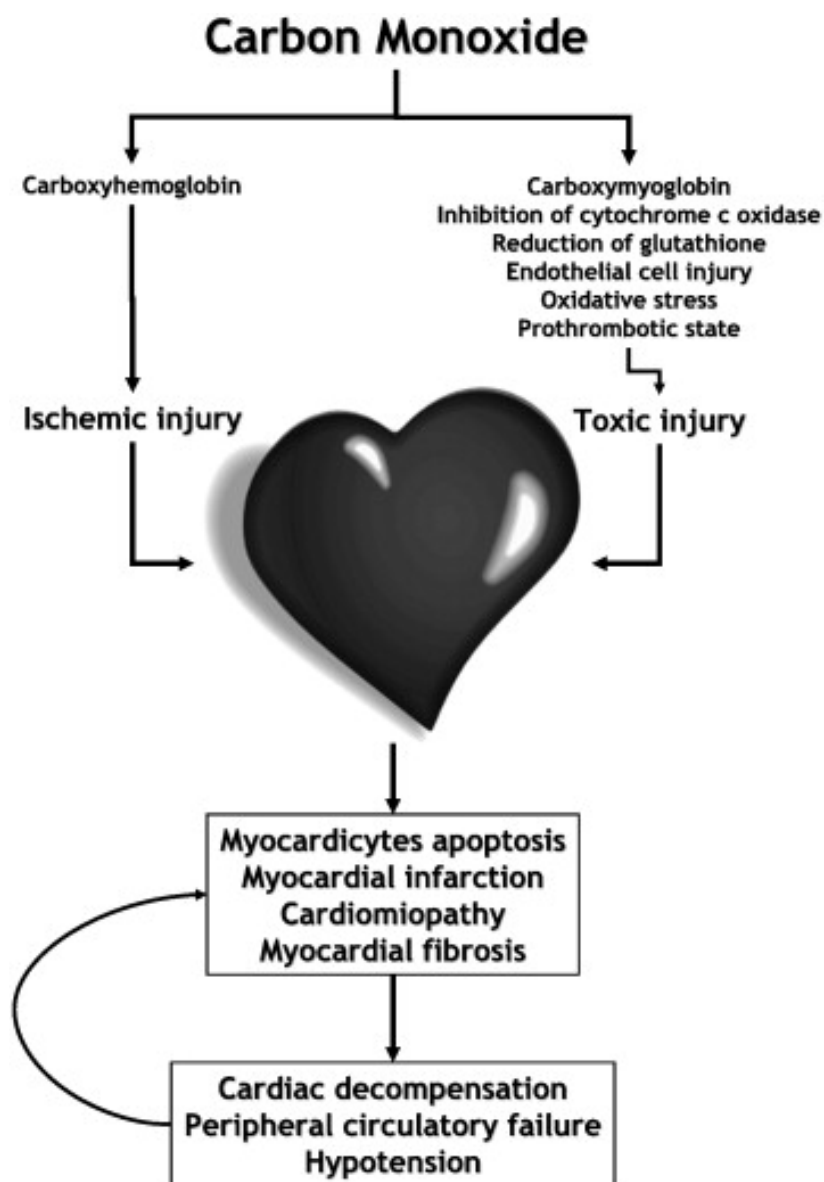


**Figure 3 – Pathophysiology of CO-Mediated Cardiotoxicity.**

Adapted from: "Pathophysiology, clinics, diagnosis, and treatment of heart involvement in carbon monoxide poisoning" by Lippi et al., 2012, *Clinical Biochemistry*, 96:1278-1285. Copyright 2012, Elsevier. Adapted with permission.



### 1.3.3 The Respiratory System & Blood Chemistry in CO Poisoning

As expected with any hypoxic insult, CO poisoning is associated with a compensatory increase in minute volume (MV) to attempt to compensate for the tissue O<sub>2</sub> deficit. This hyperventilation response to CO poisoning has been well documented in human and animal subjects.<sup>76–79</sup> But unlike hypoxic-hypoxia, such as from nitrogen asphyxiation, pure CO poisoning is not associated with a significant decrease in the arterial partial pressure of O<sub>2</sub> (pO<sub>2</sub>) as the concentration of atmospheric O<sub>2</sub> remains relatively unchanged despite the presence of CO.<sup>76</sup> In fact, CO poisoned victims tend to demonstrate normal or increased arterial pO<sub>2</sub> values and stable or decreased arterial pCO<sub>2</sub> values.<sup>76,77,80</sup> However, accurate *in vivo* blood gas data on acute pure CO exposure is limited and unreliable as many studies combined CO exposure with decreased concentrations of O<sub>2</sub> or attempted to model CO exposure using hypoxic-hypoxia alone.<sup>81,82</sup> Pure CO poisoning differs from CO poisoning associated with smoke inhalation, as other components of smoke will displace atmospheric O<sub>2</sub> and create a hypoxic environment.<sup>9</sup>

The MV increase seen in hypoxic-hypoxia is mediated by peripheral aortic pO<sub>2</sub> chemoreceptors, whereas it is believed that the MV increase in CO poisoning is mediated via central pH chemoreceptors that respond to the decrease in cerebrospinal fluid (CSF) pH that accompanies cerebral lactic acidosis.<sup>76,77</sup> Doblar and colleagues also proposed that cerebral cortex hypoxia could lead to release of the normal inhibitory influence of higher brain centers on respiratory drive.<sup>76</sup>

Acute pulmonary edema commonly accompanies severe CO poisoning and is noted during autopsy in 66% of CO fatalities.<sup>48,83,84</sup> While the exact mechanism(s)

behind this remain elusive, rabbits exposed to 8000ppm CO balanced in air demonstrated an increase in alveolar epithelium permeability resulting in noncardiogenic pulmonary edema similar to that seen in humans.<sup>85</sup> But given the cardiotoxic effects of CO and left ventricular dysfunction seen severe CO poisoning, the possibility of cardiac involvement in CO-induced edema formation has been reported and cannot be ruled out without further research.<sup>86</sup>

The little reliable data on arterial blood gases in CO poisoning do not provide a clear indication as to the presence and/or magnitude of arterial pH changes that may or may not take place during exposure.<sup>76,76,80,87,88</sup> Goats exposed to 10,000ppm CO in 40% O<sub>2</sub> for 10 minutes demonstrated no significant changes in arterial pH, although CSF pH did drop significantly.<sup>76,76</sup> Sheep exposed to 10,000ppm CO in air for 35 minutes showed no changes in blood lactate levels or pH. CSF pH and brain tissue lactate were not measured in this study, as the authors did not believe that appreciable pH differences could be observed between blood and cerebral tissue compartments.<sup>89</sup> Rats exposed to 10,000ppm CO in 40% O<sub>2</sub> for 10 minutes showed decreases in arterial pH from 7.47 to 7.24.<sup>87</sup> Human studies have concluded that blood pH does not correlate with %COHb, severity of exposure, patient acuity, or prognosis and has thus been deemed of limited to no use in the clinical setting.<sup>88,90</sup>

Data on blood lactic acid levels in animal models of CO exposure are inconclusive. No significant changes in lactate levels were appreciated in rat, dog, goat, porcine and sheep models of CO poisoning. However, the concentration of CO used and exposure time varied drastically between these studies.<sup>62,89,91–93</sup> Unlike the published animal models, lactic acid elevation has shown to be an effective indicator of

prognosis following CO poisoning in human patients.<sup>49,94</sup> Moon and colleagues reported elevated lactate levels in 70% of CO poisoned patients that required inpatient admission. There was no correlation between %COHb and prognosis in this study.<sup>49</sup>

## **1.4 Effects of CO on the Brain**

### **1.4.1 Acute Pathophysiology**

CO poisoning is associated with a broad spectrum of acute and chronic neurological sequelae ranging from mild to severe. Mild CO exposure victims often present with headaches, dizziness, nausea, and behavioral changes. Moderate and severe CO exposures are associated with seizures, altered mental status, loss of consciousness, cerebral edema and neuronal necrosis. The brain is the single most oxygen-demanding organ in the body with approximately 50% of that oxygen being utilized by the Na<sup>+</sup>/K<sup>+</sup> ATP-ase, which maintains resting neuronal membrane potential.<sup>95</sup> Proper neuronal function depends on the presence of resting membrane potentials, thus making cerebral tissue extremely sensitive to any hypoxic insult. Irreparable neuronal damage results within 10 minutes of oxygen deprivation.<sup>96</sup>

Multiple lab groups hypothesized that COHb hypoxia causes quantifiable decreases in animal whole body (VO<sub>2</sub>) or cerebral oxygen consumption (CMRO<sub>2</sub>) and oxygen delivery (DO<sub>2</sub>), but these animal model data are conflicting. Smithline et al. reported that whole body VO<sub>2</sub> remained constant in a canine model of acute CO exposure despite decreased DO<sub>2</sub>, however this study did not specifically examine cerebral metabolism.<sup>62</sup> Langston et al. reported just the opposite; their analysis of cerebral metabolism in sheep showed that CO exposure caused a decrease in CMRO<sub>2</sub> while DO<sub>2</sub> was maintained.<sup>89</sup> The literature review by Raub and Benignus concluded

that cerebral  $\text{DO}_2$  remains stable and  $\text{CMRO}_2$  decreases in a statistically significantly manner with  $\%\text{COHb} > 30\%$ .<sup>98</sup> However, a paper by Doblar et al. that was cited in this review did demonstrate significant decreases in both  $\text{DO}_2$  and  $\text{CMRO}_2$  in goats when  $\%\text{COHb}$  rose above 30%, and no change in OER was noted.<sup>76</sup>

Analyses of the nicotinamide adenine dinucleotide (NADH) redox state with reflectance fluorometry during CO exposure in rat brains sought to expose cerebral hypoxia at the mitochondrial level. These studies failed to demonstrate significant indicators of mitochondrial stress. Despite the absence of outward signs of cerebral hypoxia, these rat studies curiously showed increased extracellular  $\text{K}^+$  concentrations and spontaneous neuronal depolarizations, indicating dysfunction of the  $\text{Na}^+/\text{K}^+$  ATP-ase. This was accompanied by decreased cerebral pH, which was hypothesized to be a product of aerobic lactic acidosis.<sup>95,98</sup> More recent investigations into the effect of CO on mitochondria have provided convincing evidence that CcO inhibition may be the primary acute effect of CO on cerebral metabolism.<sup>65,66,99–103</sup>

The stable  $\text{DO}_2$  seen in CO poisoning is due to a  $\%\text{COHb}$ -proportionate compensatory increase in cerebral blood flow (CBF) (with regional variations within the brain) that has been well documented in small animals, large animals, and human studies.<sup>89,104–107</sup> In multiple human and animal studies on regional CBF immediately following acute CO exposure, the cerebral cortex demonstrated the highest increases in CBF while the basal ganglia, specifically the globus pallidus, demonstrated the lowest relative increases in CBF.<sup>105–108</sup> Perfusion of capillary beds increases uniformly throughout the brain as well.<sup>87</sup> The mechanism(s) behind the CBF increase have been widely debated, with theories in published literature implicating tissue hypoxia, acidosis

and hemoglobin-oxygen affinities.<sup>106,109–111</sup> However, multiple recent studies have shown that effects of CO on cerebrovascular modulation can be blocked to the aforementioned NO-cGMP dependent pathways.<sup>54,112–114</sup> Additionally, an increase in the oxygen extraction rate (OER) is seen along with the increase in CBF, indicating that the body is utilizing a rarely-used functional reserve of hemoglobin to sustain oxygen delivery.<sup>62</sup> Although current data on acute CO-mediated cerebral pathology implicates mechanisms other than hypoxia, to the best of our knowledge, no published literature on changes in brain tissue oxygen tension (PbtO<sub>2</sub>) during CO poisoning exists.

#### **1.4.2 Delayed Pathophysiology**

Despite the return of %COHb to normal physiological levels after exposure, mitochondrial dysfunction can persist for days, leading to neuronal damage and death via necrosis and apoptosis.<sup>99</sup> This produces neurological deficits in up to in up to 33% of patients that can last for months following exposure. Symptoms generally appear within a week following exposure and can include, but are not limited to, dyskinesias, Parkinsonian tremors, depression, learning impairments, difficulty focusing, and amnesia.<sup>115,116</sup> These prolonged neurological deficits are known as delayed neurological sequelae (DNS) or prolonged neurological sequelae (PNS).<sup>115,117</sup> DNS is closely associated with lesions in the cerebral cortex, globus pallidus, and hippocampus, which is not surprising given the functions of these regions of the brain in coordinating higher learning, fine motor control and memory, respectively.<sup>97,118–121</sup> These lesions are most clearly seen *in vivo* using magnetic resonance imaging (MRI) techniques.<sup>121</sup> Bilateral globus palladi lesions with marked diffusion restriction on diffusion weighted (DW) MRI

protocols are considered to be the “classic” radiological indicator of CO-induced pathology in the days and weeks following CO poisoning.<sup>44,120,122,123</sup>

The mechanisms behind DNS are not fully understood, but are believed to be immune-mediated secondary to unchecked ROS production and membrane lipid peroxidation.<sup>113,115,117,118,124,125</sup> As COHb dissociates following exposure, there is a redistribution of dissolved CO into extravascular tissue driven by the CO partial pressure gradient and high binding affinity of CO for intracellular targets like CcO.<sup>43</sup> ROS are produced during uncoupling of the ETC and upregulation of NO synthesis by neuronal NOS, resulting in the production of damaging peroxynitrite radicals.<sup>113</sup> Unlike cardiac tissue, brain tissue does not express myoglobin, a known CO buffer, and is therefore more sensitive to the increase in ROS production, especially when coupled with CO-mediated antioxidant depletion.<sup>124,126</sup> A chain reaction of membrane lipid peroxidation ensues, which disrupts normal membrane properties and triggers pro-apoptotic pathways.<sup>113,115,117</sup>

The variability seen between DNS prevalence and initial presentation has made determination of DNS risk factors difficult. Although not 100% predictive, DNS has been correlated with %COHb >25%, age >36 years, and exposure time >24 hours.<sup>127,128</sup>

## **1.5 Clinical Presentation, Diagnosis & Treatment of CO Poisoning**

### **1.5.1 Clinical Presentation**

The symptoms of CO poisoning are often vague. The most common complaints of CO-poisoned patients are headache, dizziness, nausea, weakness, and vertigo. Syncope, altered mental status, seizures, and decreased level of consciousness are not uncommon with more severe exposures and are associated with poorer

prognoses.<sup>44,48,97,129,130</sup> Additional findings on presentation can include arrhythmias, diarrhea, and abdominal pain.<sup>44,48</sup> The often-described “cherry red” appearance of CO victims taught to clinicians for decades is rare.<sup>131,132</sup> This originated with the observation that COHb exhibits a distinctly brighter red color than O<sub>2</sub>Hb by Hoppe in 1857.<sup>133</sup> The assumption was made that an increase in %COHb could be noted in the skin and mucus membranes. Lethal levels of %COHb must be present before any changes in epithelial color are noticed.<sup>134</sup>

Diagnosis of CO poisoning is difficult, if not impossible, to make based just on symptoms alone and therefore requires accurate history taking sharp clinical acumen to raise the index of suspicion and to avoid misdiagnosis. Acute CO poisoning can easily go misdiagnosed as other acute low-acuity pathology like viral illnesses, acute anxiety, or migraine headache. Chronic CO exposure can present similarly to psychiatric illnesses like depression and psychosis.<sup>97,135,136</sup> Misdiagnosis of CO poisoning can endanger not only the patient, but clinicians and first responders as well if entry is made into a hazardous environment, which was demonstrated when 12 fire-rescue personnel were admitted for CO poisoning after treating a patient in a CO-filled house.<sup>136</sup>

### **1.5.2 Diagnostic Workup & Common Findings**

Once suspicion of CO exposure has been raised, simple diagnostic confirmation of CO exposure can be carried out via invasive or non-invasive %COHb analysis. Both %COHb analysis techniques make use of the unique differences between the spectrophotometric absorbance spectra of O<sub>2</sub>Hb and COHb to quantify %COHb, and each has advantages and pitfalls.<sup>136–138</sup> Invasive %COHb testing is considered the gold standard of accuracy, but requires laboratory equipment and a blood sample. Non-

invasive COHb-oximetry is portable, easy to use and interpret, and uses a finger probe to assess %COHb. This technology has been reported to be less accurate than laboratory testing, although still useful as a screening tool for occult poisoning.<sup>136</sup> Many fire departments and EMS agencies use this technology in conjunction with handheld atmospheric CO detectors in both the emergency medical and fireground setting. These allow for simple and rapid pre-hospital confirmation of CO poisoning which can aid in determination of most appropriate patient destination in the field.<sup>137–139</sup> Abnormal %COHb levels are >3% for non-smokers and >10% for smokers, however it must again be reiterated that %COHb holds no correlation to patient acuity.<sup>44,48,129,140</sup>

Patients with positive %COHb levels should undergo a full ED cardiac workup to include ECG with close examination for ischemic changes and QT elongation, cardiac biomarker evaluation, and chest x-ray.<sup>58,71,129,141</sup> Elongated T-peak-T-end time has recently been reported to be a reliable indicator of CO-induced cardiac injury as well.<sup>87</sup> The utility of arterial blood gas analysis has been disputed, but lactate levels correlate well to prognosis and should be evaluated.<sup>49,94</sup> An echocardiogram is also recommended for patients with signs of pulmonary edema.<sup>42,59</sup> Patients presenting with syncope, altered mental status, seizures, and decreased levels of consciousness should undergo neurological imaging studies unless radiological studies would delay transfer to a more appropriate treatment center.<sup>129,130</sup> If available, magnetic resonance imaging (MRI) is the preferred imaging modality for CO poisoning as it offers higher soft tissue detail than computerized tomography (CT). Hypodensities in the basal ganglia and cerebral edema are common acute findings in brain MRI and CT studies.<sup>120,121</sup>



### 1.5.3 Current Treatment Modalities & Controversies

Despite over a century of medical research on CO poisoning, the treatment remains unchanged. Oxygen therapy is currently the only accepted therapeutic agent used for the treatment of CO poisoning. The goal of oxygen therapy is to decrease %COHb using simple chemistry; providing an increased atmospheric  $pO_2$  to a CO-poisoned patient shifts the equilibrium of COHb formation and favors dissociation of CO from Hb.<sup>43,129,130</sup> Although oxygen therapy is considered the gold standard of treatment, it is based on the century-old theory that CO pathology comes from COHb formation alone.

The most common method of  $O_2$  administration for CO victims is via the non-rebreather mask (NRB). At an  $O_2$  flow rate of 10-15L/min, the NRB is capable of delivering 95-100%  $O_2$  at ambient atmospheric pressure to a patient and reducing COHb  $t_{1/2}$  from 5 hours (breathing ambient air) to 60-90 minutes.<sup>9,129,142–144</sup> In patients unable to maintain their airway and/or respiratory drive, airway support and artificial ventilation using high flow  $O_2$  must take the place of a NRB. This is otherwise known as normobaric  $O_2$  (NBO). Equipment required to administer NBO is simple and cheap to operate, readily portable, and easily accessible in hospitals, clinics, and EMS systems. All emergency medical first responders are trained to administer NBO and the required equipment to do so is required on any emergency response vehicle staffed by any trained emergency medical technician (EMT) or higher.<sup>145</sup> Administration of NBO pre-hospital reduces the time exposed patients have to wait to receive treatment, which is considered to be equally, if not more important than treatment itself.<sup>43</sup> American EMS systems have a median BLS response time of less 10 minutes, which allows for

extremely rapid O<sub>2</sub> administration if CO exposure is suspected.<sup>146–148,148</sup> Increased time to treatment after CO exposure is associated with decreased efficacy of O<sub>2</sub> therapy and increased mortality and morbidity.<sup>43,131,149,150</sup>

The only significant advancement made in CO poisoning therapy was the addition of hyperbaric O<sub>2</sub> therapy (HBO) to existing O<sub>2</sub> therapy protocols over 50 years ago.<sup>151</sup> HBO further exploits the mass-action effect of COHb equilibrium by application of O<sub>2</sub> at 2-3 times normal atmospheric pressure, further driving dissociation of CO from Hb and can reduce COHb t<sub>1/2</sub> to 15-30 minutes.<sup>48</sup> While the optimal HBO dose is still yet to be determined and protocols vary between facilities, most facilities employ a multi-therapy protocol of 2.5-3.0atm for periods of 60-90 minutes in the days following exposure.<sup>127,152–154</sup> Criteria for HBO therapy generally include severe exposures, loss of consciousness or syncope, neurological symptoms other than headache, age >36 years and %COHb >25%. Pregnant patients are also HBO candidates due to the high affinity of fetal Hb for CO discussed previously.<sup>48,127,154</sup> However, no standardized criteria for HBO therapy currently exist, and thus vary widely between facilities equipped to provide it.<sup>155</sup>

HBO therapy is considered the modern gold standard for severe CO exposure, but it is not without limitations. Few hospitals are equipped with critical care hyperbaric chambers and the cost of operation is exorbitant. Patients often require transfer to a tertiary facility and the logistics of interfacility transport and hyperbaric chamber preparation can further increase time to HBO therapy, which is associated with a decrease in HBO efficacy and an increase in morbidity and mortality.<sup>131,149,150</sup>

Interfacility critical care transport is also expensive, with helicopter EMS transport (HEMS) costs of approximately \$20,000 per flight.<sup>156,157</sup>

There is no question that both modalities hasten the dissociation of CO from Hb through basic biochemical mechanisms; this phenomenon has been well documented since the early 20<sup>th</sup> century.<sup>127,154,158,159</sup> But despite decades of use, the efficacy of both O<sub>2</sub> therapy modalities remains widely debated in the literature. Recent studies have found that the data on %COHb reduction with NBO are unreliable and that NBO does not offer any protection from DNS compared to breathing ambient air.<sup>159–161</sup> Efficacy of HBO compared to NBO also remains to be definitively elucidated. Due to a 3% mortality rate of CO-exposed patients presenting to hospitals and no published data demonstrating that HBO decreases mortality, the goal of HBO therapy is to prevent DNS, not to prolong short-term survival.<sup>127</sup> Published studies on the efficacy of HBO are fraught with methodological limitations that make drawing conclusions difficult, but some indicate that HBO provided without delay is effective at ameliorating cellular damage and DNS in human and animal models.<sup>66,115,127,128,131,153,161,162,162,163</sup> Other studies and retrospective reviews of existing data were unable to demonstrate any benefit from HBO therapy.<sup>43,160,164,165</sup>

Additional arguments have been made that O<sub>2</sub> therapy can actually exacerbate CO-induced oxidative stress. Oxygen therapy, particularly HBO, induces ROS production in proportion to the pO<sub>2</sub> in the chamber and time of treatment, leading to DNA damage, membrane lipid peroxidation, and activation of pro-apoptotic pathways.<sup>166–170</sup> CO-mediated ROS formation, antioxidant depletion, and subsequent cellular damage have been implicated as major pathophysiological mechanisms in CO

poisoning.<sup>59,67,68,113,117,118,124,125</sup> Although it remains to be definitively studied, it is therefore likely that the oxidative stresses from O<sub>2</sub> therapy and CO poisoning are additive, which could exacerbate pathology.<sup>125</sup> Oxygen is also a potent respiratory stimulant. Hyperoxia-induced hyperventilation results in hypocarbia, triggering vasoconstriction in CO<sub>2</sub>-sensitive vascular beds in the heart and brain, reducing blood flow.<sup>43</sup> This phenomenon occurs even in the presence of CO and can result in decreased DO<sub>2</sub> to these tissues despite the increase in pO<sub>2</sub>.<sup>43,171</sup>

Exploration into therapies other than O<sub>2</sub> has, much like O<sub>2</sub> therapy, hinged upon the hypoxic theory of CO poisoning. Attempts to increase oxygen delivery have included the use of artificial oxygen carriers (perfluorocarbons and hyper-oxygenated saline) and early attempts using blood transfusions, but these have not been adopted into clinical practice.<sup>172–175</sup> Recent studies have found success in utilizing extracorporeal membrane oxygenation (ECMO) to reduce COHb and reverse acidosis in severe cases of CO poisoning, but no data exists on the effects of ECMO therapy on long-term outcomes.<sup>176,177</sup> Before the rise of HBO as the standard of care in the 1960's, an inhaled mixture of oxygen and CO<sub>2</sub> (carbogen) was employed to decrease %COHb by triggering hyperoxic hyperventilation while maintaining a normocarbic state. Fisher and colleagues are attempting to bring this treatment modality back into favor.<sup>43</sup>

Few attempts have been made to target the effects of CO not mediated by COHb formation. Qingsong and colleagues successfully demonstrated amelioration of DNS pathology following CO exposure using the free radical scavenger edavarone, but no further data is available on this.<sup>178</sup>

The current lack of therapy options for CO-poisoned patients presents a clear and present need for a replacement or adjuvant therapeutic options. The ideal treatment would be portable, robust, safe, and easily deployed in the field by paramedics. It would be efficacious at mediating the well known harmful effects of COHb formation as well as the less understood but ever present cytotoxic mechanisms.

## **1.6 A Potential Antidote**

### **1.6.1 Hydroxocobalamin**

Hydroxocobalamin (OHCbl) is a member of the vitamin B12 family, a group of four compounds (hydroxocobalamin, cyanocobalamin (CNCbl), methylcobalamin, and adenosylcobalamin) that differ only by a single upper axial side chain. These compounds exhibit a marked structural similarity to the heme moiety of Hb, differing only by one carbon atom and a central cobalt atom instead of iron.<sup>179</sup> Physiologically, cobalamins serve as cofactors for the methylmalonyl-CoA mutase catalyzed isomerization of methylmalonic acid to succinate and the methionine synthase-catalyzed synthesis of methionine from homocysteine and 5-methyltetrahydrofolate.<sup>180</sup>

For the past 40 years it has been used in high doses (5-15g) as a safe and effective antidote for cyanide exposure, acting similarly to a chelating agent by binding cyanide to become CNCbl.<sup>181,182</sup> Hydroxocobalamin is also capable of scavenging free NO and inhibiting NOS resulting in vasoconstriction and an increase in blood pressure.<sup>183-185</sup> This effect has been shown to mitigate endotoxin-induced hypotension in rats and has most recently been employed to counteract vasoplegic syndrome in a human case study following cardiac surgery by Roderique and colleagues.<sup>186,187</sup> The

vitamin B12 family also demonstrates remarkable anti-inflammatory and antioxidant properties, capable of scavenging free radicals and downregulating the expression of pro-inflammatory cytokines and transcription factors.<sup>188,189</sup>

### 1.6.2 Reduced Hydroxocobalamin & CO

In the late 1960's, the lab group of Schrauzer and co-workers postulated that OHCbl would be capable of reacting with CO, given the affinity of CO for heme-containing proteins and the structural similarities between heme moieties and OHCbl. They successfully demonstrated that OHCbl is capable of reacting with free CO and forming CO<sub>2</sub>, but only when OHCbl was in its reduced state, that is, with the central cobalt atom reduced from the Co<sup>3+</sup> state to Co<sup>2+</sup>. Reduced OHCbl will herein be referred to interchangeably as B12r, with OHCbl referring to the unreduced form of the compound. The same reaction was attempted with carboxyhemoglobin, but was unable to produce decarbonylation from Hb-bound CO.<sup>190</sup> No further investigation into this phenomenon was published until 2013.

Based on the work performed by Schrauzer in the 1960's, a second attempt at reacting B12r with carboxyhemoglobin was undertaken by Roderique and colleagues at Virginia Commonwealth University to test the viability of B12r as a potential therapy for CO exposure. B12r was produced by combining OHCbl with ascorbic acid (vitamin C, AA) as a reducing agent in an nitrogenous environment.<sup>191</sup> Ascorbic acid was chosen because of its powerful action as a reducing agent and safety when administered in large doses.<sup>192</sup> Confirmation of the presence of B12r was performed by Raman resonance spectroscopy (RRS). Using a closed-loop circulatory system containing

whole human blood and a CO<sub>2</sub> analyzer, they were able to demonstrate increased release of CO<sub>2</sub> from CO-poisoned blood after B12r injection compared to unpoisoned blood. It was hypothesized that B12r was reacting with COHb, catalyzing the dissociation of CO from Hb and oxidizing CO to CO<sub>2</sub> via an unknown mechanism<sup>191</sup> Further *in vitro* work by Somera and co-workers probed these findings using additional Raman analysis techniques. The data from these experiments indicate a significant %COHb decrease in CO-poisoned human whole blood following B12r administration.<sup>193</sup> The *in vitro* data from the work by Roderique and Somera indicate that B12r could potentially function as a therapeutic agent for CO poisoning by interacting with and driving dissociation of COHb.

## 1.7 Hypotheses & Specific Aims

The data obtained from work by Roderique and Somera et al. suggest that B12r is capable of reacting with CO in blood and decreasing %COHb *in vitro*.<sup>191,193</sup> Hydroxocobalamin also a potent NO scavenger and NOS inhibitor, causing an increase in blood pressure when administered.<sup>183–185,187</sup> Additionally, OHCbl is a powerful antioxidant and anti-inflammatory capable of neutralizing ROS and downregulating pro-inflammatory mediators.<sup>188,189</sup> This trifecta of pharmacological mechanisms implicates B12r as a potential therapy for CO poisoning. This work was a direct outgrowth of the work by Roderique and Somera..

Additionally, there are currently no published data on changes in brain tissue oxygen tension (PbtO<sub>2</sub>) during and after CO exposure despite ongoing literature debate about cerebral perfusion and metabolic changes in CO poisoning. Using a

multiparametric monitoring approach in a non-survival surgical model, we aimed to characterize the physiological effects associated with acute CO exposure in a rat model by examining changes in brain tissue oxygen tension, mean arterial blood pressure (MAP), respiratory rate, and arterial blood gas chemistry. We also aimed to evaluate the efficacy of B12r as a therapeutic agent for CO poisoning by observing for rescue from CO pathology in comparison to control rats administered a normal saline vehicle.

Specifically, we hypothesized that:

1. CO poisoning will decrease PbtO<sub>2</sub> significantly in rats exposed to CO as measured by a Licox® Clark-type polarographic electrode placed into the cerebral cortex.
2. Administration of B12r could rescue PbtO<sub>2</sub> of CO-exposed rats within 20 minutes of administration. Additionally, B12r administration would cause a MAP increase within 20 minutes and/or demonstrate blood chemistry improvement within 60 minutes in comparison to controls.
3. B12r would produce the same increase in CO<sub>2</sub> off-gassing *in vivo* as seen in prior *in vitro* work, demonstrated by an increase in observed respiratory rate and/or increase in arterial pCO<sub>2</sub> within 20 minutes in comparison to controls.

## **1.8 Basic Approach**

### **1.8.1 Non-Survival Surgery**

Physiological parameters of anesthetized rats were recorded during a non-survival procedure. Parameters monitored included PbtO<sub>2</sub> via microelectrode, arterial blood pressure via femoral artery catheter, respiration rate, and arterial blood gas (ABG)



chemistry. Rats were anesthetized using inhaled isoflurane and were not intubated in order to preserve natural compensatory changes in respiratory drive. Following surgical placement of monitoring equipment and stabilization, rats were randomly assigned to an exposure group to receive either 3000ppm CO balanced in medical air or medical air (sham exposure), both of which were mixed with 2% isoflurane. After exposure, all rats were switched back to breathing medical air and administered a randomly assigned intraperitoneal (IP) injection of either 100mg/kg B12r (50mg OHCbl+50mgAA/mL in deoxygenated saline) or equivalent volume of normal saline (vehicle) and monitored for 60 minutes. Respiratory rate and PbtO<sub>2</sub> were recorded every 5 minutes during exposure and after treatment. Serial ABG samples were taken prior to exposure and at three time points after exposure. Rats were humanely euthanized after 60 minutes of monitoring. A visual representation of the procedure timeline is below in Figure 4.

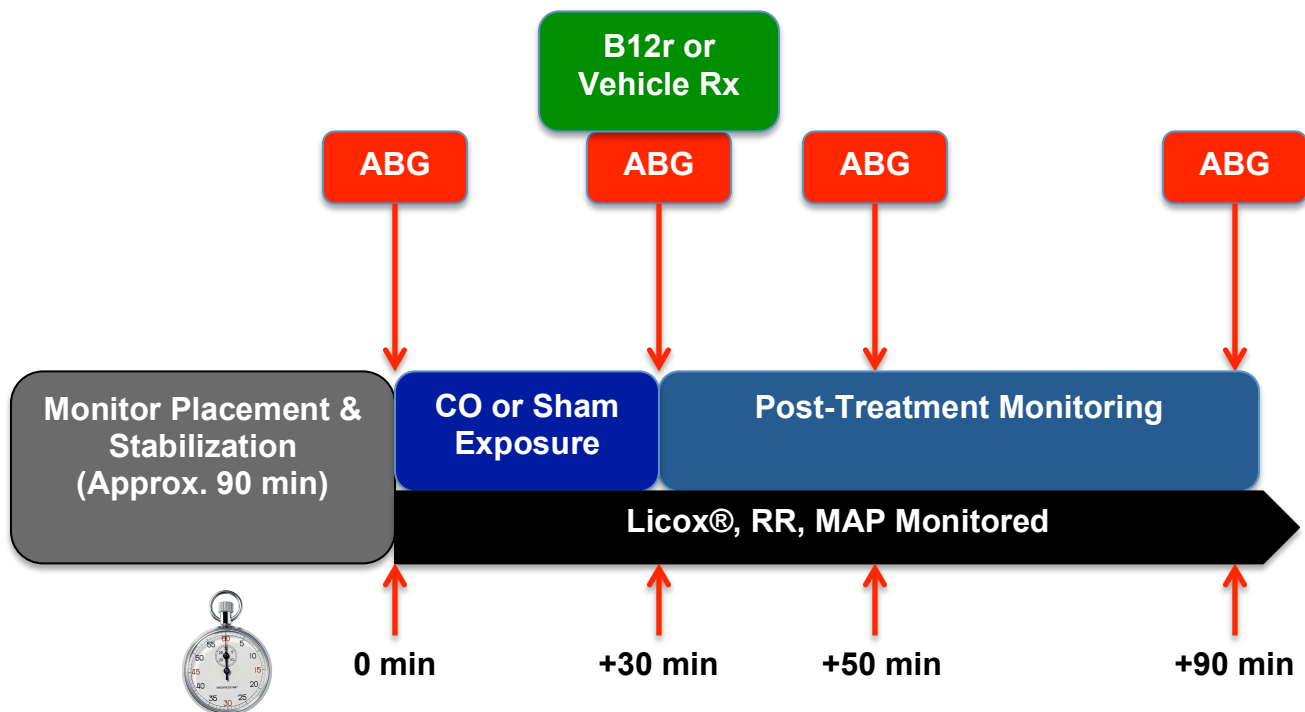


**Figure 4 – Visual Representation of Surgical Procedure Timeline.**

### 1.8.2 Brain Tissue Oxygen Tension Monitoring

We measured PbtO<sub>2</sub> via a Licox® (Integra Neuroscience™) CC1.R Clark-type polarographic oxygen-sensitive electrode and associated AC31 monitoring system placed into the cerebral cortex of anesthetized rats at -1mm anteroposterior, -3mm mediolateral with respect to Bregma using stereotaxic technique. This region of the brain was chosen for evaluation due to the prevalence of literature on rat cerebral cortex pathology in CO exposure.<sup>95,98,119,194</sup> Licox® technology has been used extensively in clinical treatment and research of stroke and traumatic brain injury.<sup>195–198</sup> The microcatheter contains a 1mm oxygen-sensitive electrode that consists of gold and silver electrodes within an oxygen-permeable membrane and measures the partial pressure of dissolved oxygen in the extracellular space. Dissolved oxygen diffuses across the membrane and is reduced by the electrode in a temperature-dependent reaction, creating a current proportional to the concentration of oxygen.<sup>199</sup>

This device allows for real-time analysis of PbtO<sub>2</sub>, which is believed to represent the balanced between O<sub>2</sub> delivery and consumption, reflecting the availability of O<sub>2</sub> for metabolic processes. Normal PbtO<sub>2</sub> range is 20-35mmHg, although this can vary depending on the study and species evaluated. Reported mean normal PbtO<sub>2</sub> values were 29.4mmHg in a murine study, 28mmHg in dogs, 42mmHg in cats, and 33-36 in humans.<sup>200</sup> The critical PbtO<sub>2</sub> for normal human brain tissue is between 15-20mmHg, below which infarction can occur.<sup>201</sup> Values below 15mmHg are considered hypoxic and are associated with poor outcomes.<sup>199</sup>

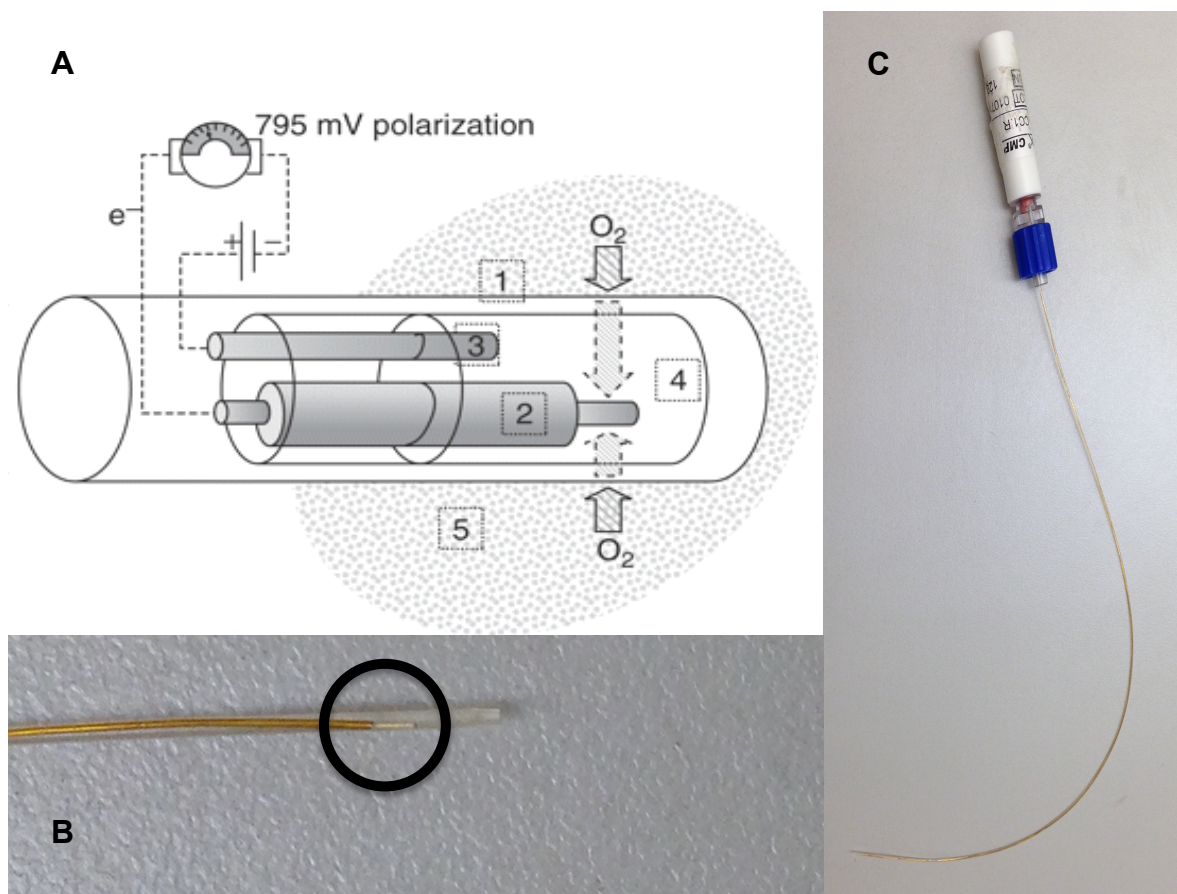


**Figure 5 – Licox® Brain Tissue Oxygen Tension Electrode.** (A) Schematic representation of Licox® electrode oxygen-sensitive tip. 1, Polyethylene tube with oxygen-permeable membrane; 2, gold cathode; 3, silver polarographic anode; 4, electrolyte chamber; 5, brain tissue. (B) Photograph of the tip of the Licox® electrode used. Black circle is placed around the oxygen-sensitive portion. (C) Photograph of the entire electrode assembly.

## 1.9 Summary of Findings

There were no deaths during the procedures. There were no significant differences between baseline parameters of groups. All rats exposed to CO demonstrated marked decreases in PbtO<sub>2</sub> and MAP during exposure. Mean PbtO<sub>2</sub> values decreased from 31.3±1.2 to 18.3±1.0 mmHg and 31.2±0.7 to 18.3±1.3 mmHg at end of CO exposure in B12r-treated (n=10) and vehicle-treated rats (n=10), respectively (p<.0001). Baseline MAP recordings were 88.23±3.24 in CO-B12r and 89.32±3.54 in CO-Vehicle groups. Post-exposure, CO-B12r and CO-vehicle MAP recordings were 46.23±1.81 and 45.35±2.01, respectively (p<.0001, compared to sham-exposed groups). Lactic acid levels were significantly increased after exposure in CO-exposed groups with mean lactate levels >3.0mM. This was associated with significant hypocarbia and decreases in HCO<sub>3</sub><sup>-</sup> (p<.05). Exposure to CO caused a decrease in respiration rates with observed tidal volume increase and Kussmaul-like respiration pattern in CO-exposed groups. Rats not exposed to CO did not demonstrate appreciable changes in PbtO<sub>2</sub> or MAP during sham exposure. Respiration rates remained constant in Sham-B12r and Sham-vehicle groups.

PbtO<sub>2</sub> values remained <25mmHg for 40 minutes after exposure and remained below baseline levels in the CO-Vehicle group. The CO-B12r group demonstrated rapid recovery of PbtO<sub>2</sub> to >25mmHg and MAP to >75mmHg within 15 minutes of treatment. CO-Vehicle group MAP was significantly lower than sham-exposed groups during the entirety of post-exposure monitoring (p<.001). A significant transient MAP increase was seen in the Sham-B12r group 5 minutes after treatment that persisted for 15 minutes (p<.05). No significant blood chemistry differences were noted between CO-B12r and

CO-vehicle rats after treatment. Lactic acid levels in CO-exposed groups decreased throughout monitoring without significant difference between the groups. Respiratory rate remained significantly lower in the CO-B12r compared to the CO-Vehicle group for 25 minutes after treatment. Sham-B12r and sham-vehicle groups demonstrated normal arterial blood gas composition at all time points and did not exhibit lactic acidosis, indicating adequate surgical technique and anesthetic management.

## MATERIALS & METHODS

### 2.1 Materials

Ascorbic acid and hydroxocobalamin were obtained from Sigma-Aldrich and were of analytical grade. All gases were obtained from Airgas™ and contents certified by the manufacturer. Gases used were medical air, USP and 2500ppm CO balanced with medical air. Licox® components were obtained from Integra Neuroscience™; a CC1.R probe (0.5mm diameter, 1.0mm sensitive tip) was used to measure PbtO<sub>2</sub> in conjunction with the AC31 PbtO<sub>2</sub> monitor and calibrated for temperature using the C8.B temperature probe. The stereotaxic frame used was a Stoelting™ model 51500 single-arm dual rat/mouse frame. Blood pressure was monitored using the MP150® hardware system in conjunction with AcqKnowledge 4.0® software. Blood gas analysis was performed using a Radiometer™ ABL 800 Flex clinical blood gas analyzer.

Surgeries were performed inside of a fume hood in order to minimize any escape of carbon monoxide. Inside of the fume hood was a full compliment of surgical lights, instruments, and an electric homeothermic heating pad with rectal probe. The surgical suite setup for arterial line placement is depicted in Figure 6, setup for Licox® monitoring is depicted in Figure 7.

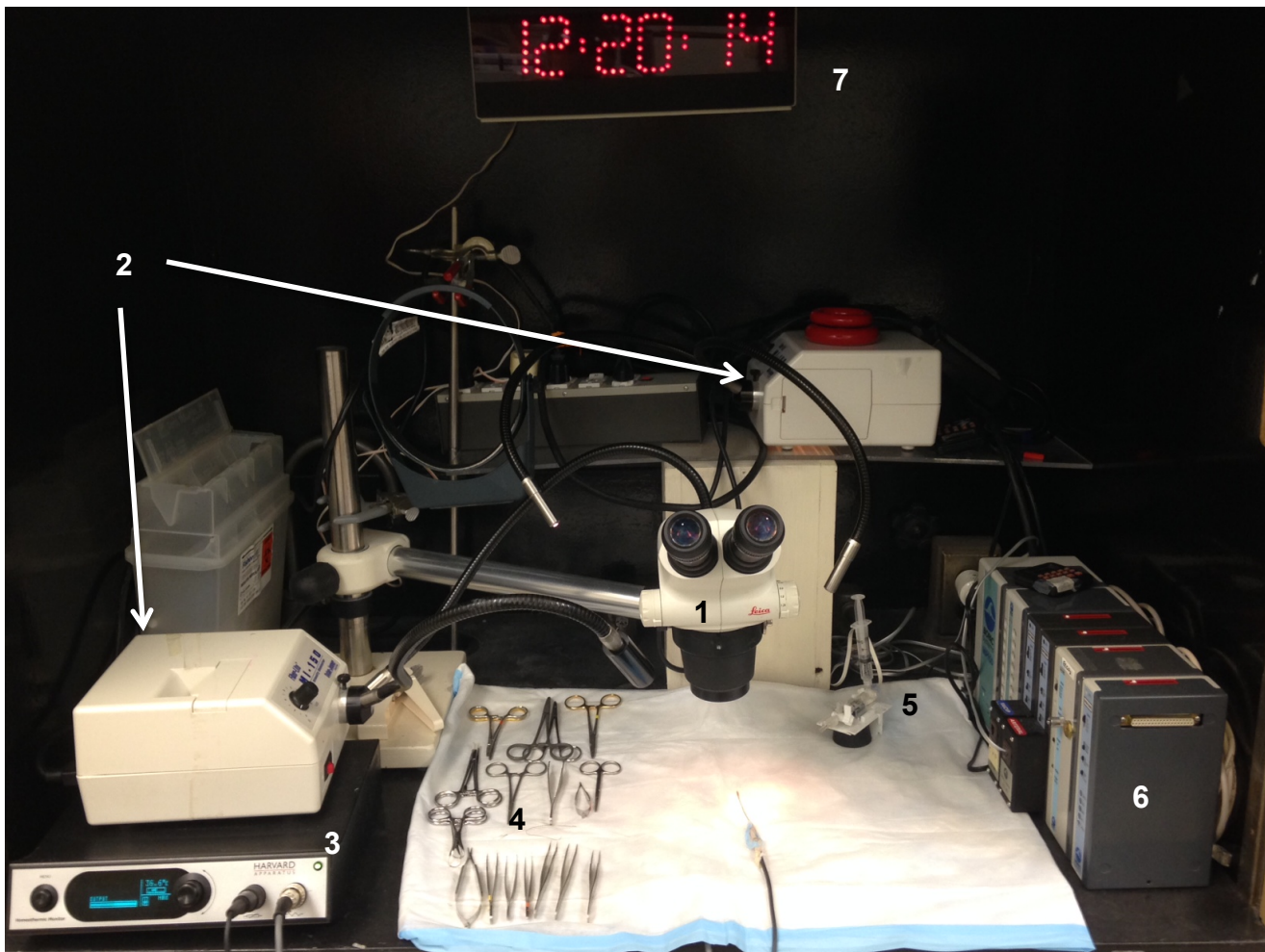


**Figure 6 – Surgical Equipment for Arterial Line Placement.** (1) Dissecting microscope; (2) lights, (3) homeothermic warming unit (warming pad underneath drape, rectal probe in center of drape); (4) surgical instruments, catheter material, suture material; (5) pressure transducer; (6) BioPac™ MP150®; (7) digital clock. Not pictured: anesthesia equipment, gas tanks.



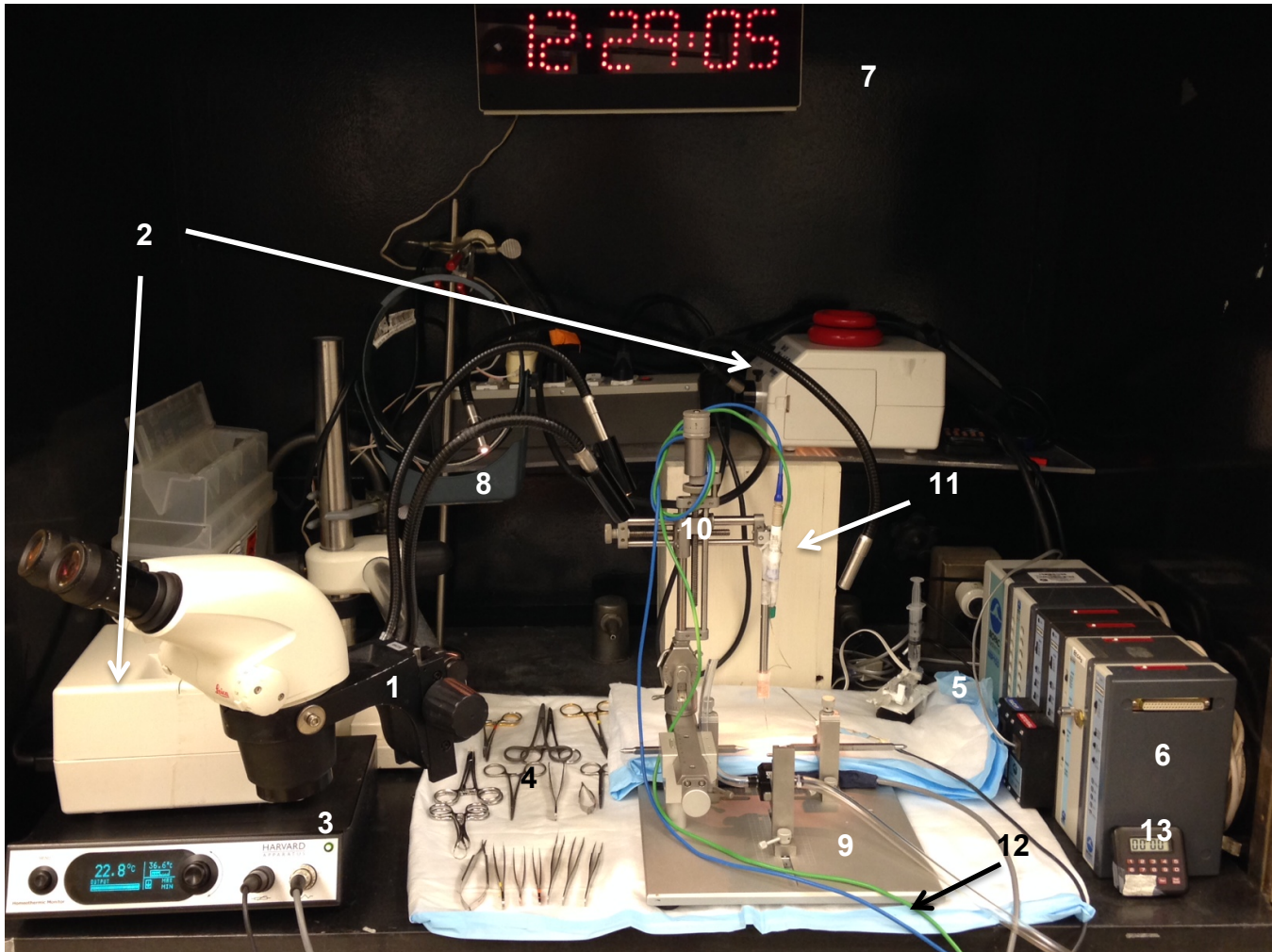


**Figure 7 – Surgical Equipment for Licox® Electrode Placement & Monitoring.** (1) Dissecting microscope, moved out of suite; (2) lights; (3) homeothermic heating equipment; (4) surgical instruments; (5) pressure transducer; (6) BioPac™ MP150®; (7) digital clock; (8) loupes; (9) stereotaxic frame and anesthetic nose cone; (10) stereotaxic manipulator arm; (11) Licox® oxygen and temperature probes taped to manipulator arm; (12) Licox® cables; (13) digital timer. Not pictured: Licox® AC31 monitor, Dremel® tool, anesthesia machine.



## 2.2 Production of Reduced Hydroxocobalamin

Powdered hydroxocobalamin and ascorbic acid (AA) were obtained from Sigma-Aldrich. Hydroxocobalamin was stored in a dark brown glass bottle at 4°C in a dark refrigerator until needed. Ascorbic acid (AA) was stored in a sealed polypropylene container at ambient temperature until needed. Deoxygenated saline was produced by bubbling nitrogen through a 0.9% saline solution in an Erlenmeyer flask under a vacuum for 90 minutes before transfer into the nitrogenous environment within an airtight glove box. Antidote was produced using 50mg OHCbl and 50mg AA per mL of deoxygenated saline. This 1:1 mass ratio ensured adequate reduction of the OHCbl to B12r as noted by Raman analysis with the assistance of Capt. Leo Somera.<sup>193</sup>

Each dose of antidote was created individually. Using an analytical balance, 50mg of OHCbl and AA was measured out into separate 5mL syringes with plungers removed. The two syringes were then placed into the airlock of our glove box and the airlock was flushed with gaseous nitrogen for a minimum of seven minutes to remove any ambient air. The syringes were then moved into the glove box, which contained a 100% nitrogen environment to prevent oxidation of the antidote from atmospheric O<sub>2</sub>. Using a third syringe, a 1mL aliquot of deoxygenated saline was injected into the syringe containing the AA. This syringe was then connected to a three-way stopcock along with the syringe containing the OHCbl. The AA/saline solution was flushed back and forth between the two syringes for a minimum of 30 seconds to agitate the reagents and allow proper mixing. The mixture was then transferred into one syringe and capped with a needle. Antidote preparations were left in the nitrogenous environment until needed and were warmed on the heating pad prior to administration.

## 2.3 Animals & Ethics Statement

All procedures followed the guidelines established in the Guide for the Care and Use of Laboratory Animals (U.S. Department of Health and Human Services) and were approved by the Institutional Animal Care and Use Committee of Virginia Commonwealth University (Protocol Number AD10000569). The surgical procedure was observed and approved by VCU Department of Animal research veterinary staff. Male Sprague-Dawley Rats (SD rats) were used for surgical procedures. Rats were obtained from Harlan Laboratories, Inc, and weighed 315-370g on the day of the procedure. All rats were housed two per cage in a 12-hour on/off light cycle vivarium with ad libitum access to food and water. VCU Department of Animal Resources staff carried out all cage maintenance and provided enrichments. Rats were acclimated to the lab and vivarium with weights monitored daily for a minimum 7 days prior to surgical procedures. During acclimation, rats were habituated to handling by experimenters.

## 2.4 Non-Survival Surgical Procedure

### 2.4.1 Experimental Group Assignment & Procedural Preparation

Rats were divided into 4 groups according to assigned exposure (CO or sham) and treatment (B12r or normal saline “vehicle”) received. Experimental groups are outlined in Table 1. Assignment of rats to experimental groups was randomized.

**Table 1 – Experimental Exposure-Treatment Groups and Sample Sizes**

| Exposure-Treatment | Sample Size (n) |
|--------------------|-----------------|
| CO-B12r            | 10              |
| CO-Vehicle         | 10              |
| Sham-B12r          | 5               |
| Sham-Vehicle       | 5               |

Prior to the start of surgeries, all instruments and work areas were cleaned. All equipment was prepped and checked for proper function. The blood pressure transducer was calibrated at 0mmHg using ambient air pressure and 120mmHg using a mercury sphygmomanometer. Each rat was weighed prior to anesthesia induction. This surgery was a non-survival procedure, so aseptic technique was used, as opposed to sterile technique.

Anesthesia induction took place in an induction chamber mounted to the anesthesia machine. Rats were induced with 4% isoflurane balanced in medical air for 3 minutes. Following induction, the rat was then removed from the chamber and hair was clipped over the left inguinal area and superior aspect of the head. If the animal moved during clipping, it was placed back into induction chamber at 4% isoflurane until cessation of movement. The rat was then placed supine on the surgical table and the nose inserted into a nose cone delivering anesthetic gas. Isoflurane was reduced to 2% after induction. A digital homeothermic heating pad placed dorsally on the rat and rectal temperature probe were used to maintain a core temperature of 36.6°C. Anesthesia checks were performed every 15 minutes by pinching the toes and observing for a pain-withdrawal response.

#### **2.4.2 Femoral Artery Cannulation**

The arterial catheter was prepared prior to the start of surgery and consisted of a 3-4" length of PE-50 tubing with a one-way pin port connected to one end. The volume of the catheter was determined using a 1mL syringe; catheter volume was between 40-70µL. Each catheter was flushed with a 4u/mL heparinized saline solution.

Using forceps and blunt dissection scissors, a 2cm incision was made into the left inguinal crease. Skin and subcutaneous tissue were then retracted. The entire surgical site was irrigated with 0.25% bupivacaine warmed on the homeothermic heating pad and allowed to sit on tissue for minimum 1 minute before removal with gauze. The femoral artery was located and dissected away from the femoral vein and sciatic nerve using microsurgical forceps under a dissecting microscope. The artery was ligated proximal to the bifurcation of the epigastric artery using a surgeon's knot in 4-0 silk. A hemostat was clipped to the ligature tail and gently retracted to pull distal traction. A second ligature of using 4-0 silk was passed underneath the artery proximal to the initial ligature. A single overhand knot was placed into the thread, which was then clipped to hemostats and retracted towards the midline to close off the arterial lumen. Using microsurgical scissors, an incision was cut across 1/3 of the arterial wall between the ligatures. The opening was retracted using microsurgical forceps and a short length of PE-50 tubing was threaded into the arterial lumen. Proximal ligature traction was reduced, and the catheter advanced approximately 1-2cm. The catheter was then aspirated for blood return and flushed with 4u/mL heparinized saline to prevent coagulation. The proximal ligature was then tightened and secured with a surgeon's knot. The incision was closed with staples or continuous suture using 2-0 nylon. The rat was then moved back into induction chamber with 2% isoflurane maintained in order to prepare the surgical area for Licox probe insertion. Isoflurane concentration was adjusted in small percentages in order maintain non-responsiveness to foot pinches. Blood loss during arterial cannulation was estimated to be less than 100 $\mu$ L for each rat by using 1 or less cotton-tipped applicators for bleeding control. This technique was

adapted from Jespersen, et al. with additional technical guidance provided by VCURES professors Dr. Jiepei Zhu and Dr. Penny Reynolds.<sup>202</sup>

### **2.4.3 Licox® Placement**

The dissection microscope was swung out of the surgical suite and the heating pad removed. The stereotaxic frame was placed centrally into the surgical suite and the heating pad placed on top of the frame platform then covered with a clean drape. A stereotaxic nose cone was used to deliver anesthetic gas. The rat was placed onto the stereotaxic frame and the head secured in a level position via ear bars and nose cone. Once secured, the pin port of the arterial cannula was connected to the pressure transducer and arterial pressure monitoring was initiated. Arterial blood pressure was monitored continuously for the remainder of the procedure.

A midline incision was made down the length of the skull using a #11 scalpel and the incision was retracted using microsurgical retractors. The periosteum was peeled away from the skull using forceps. A 19-gauge needle taped to the arm of the stereotaxic frame served as a navigation guide. Under 10x loupe magnification, the Bregma point was located on the skull by locating the intersection of the coronal and sagittal sutures. The coordinates of the Bregma point were recorded. The region of interest (ROI) coordinates were then calculated by moving the needle 1mm posterior and 3mm lateral (written as -1mm AP, -3mm ML) with respect to Bregma to allow for access to the primary somatosensory cortex. The right side of the skull was used on each rat to maintain consistency. This location was marked with a felt-tip pen and the stereotaxic manipulator arm was removed. This location would be used for insertion of the Licox® oxygen-sensing electrode. A second location was marked contralaterally at

the approximate same location to serve as the insertion point of the temperature probe; placement of this probe did not require specific stereo taxic coordinates.

Access to the cranial vault was achieved using a Dremel™ tool with a 2mm burr drill bit. In order to prevent major damage to brain tissue caused by the Dremel™ drill, a technique was devised to safely drill burr holes. Using two hands, the drill was slowly advanced through the roof of the cranium until a thin, pliable film of bone remained. A small hook was created on the end of a 19-guage needle by applying repetitive blunt force to the tip of the needle against the lab bench in order bend the tip of the needle towards the bevel. The bent tip of the needle was then used to gently puncture the edge of the thin bony film and gently lift it away from the underlying brain tissue. Forceps were then used to extract the disk. This process was repeated for both marked sites. The dura mater was gently pierced and incised using the same bent tip of the needle used to remove the film from the craniotomy site. Bilateral craniotomy burr holes are pictured in Figure 8.

The Licox® CC1.R electrode hub was then taped to the top of the manipulator arm and the electrode tip taped to the end of the arm with an approximately 1cm overhang of the probe tip. The hub of the temperature probe was then taped to the shaft of the manipulator arm, as shown in Figure 9A. The manipulator arm was positioned with the CC1.R probe tip over the insertion site and the tip was lowered to the surface of the brain tissue. Using loupe magnification and fine adjustment knobs of the manipulator arm, the probe was then lowered into the brain parenchyma to a depth of 2.3mm. This depth ensured that the 1mm oxygen-sensitive portion of the electrode would be positioned within the cortex. Catheter placement is depicted in Figure 9B. The

temperature probe was then inserted into the respective insertion site and both probes were connected to the Licox® AC31 monitor, which was then powered on. The probes were then allowed to equilibrate and stabilize for 30 minutes. Anesthetic gas was maintained at 2% for the remainder of the procedure to ensure consistency. All rats were stable at this concentration of isoflurane.

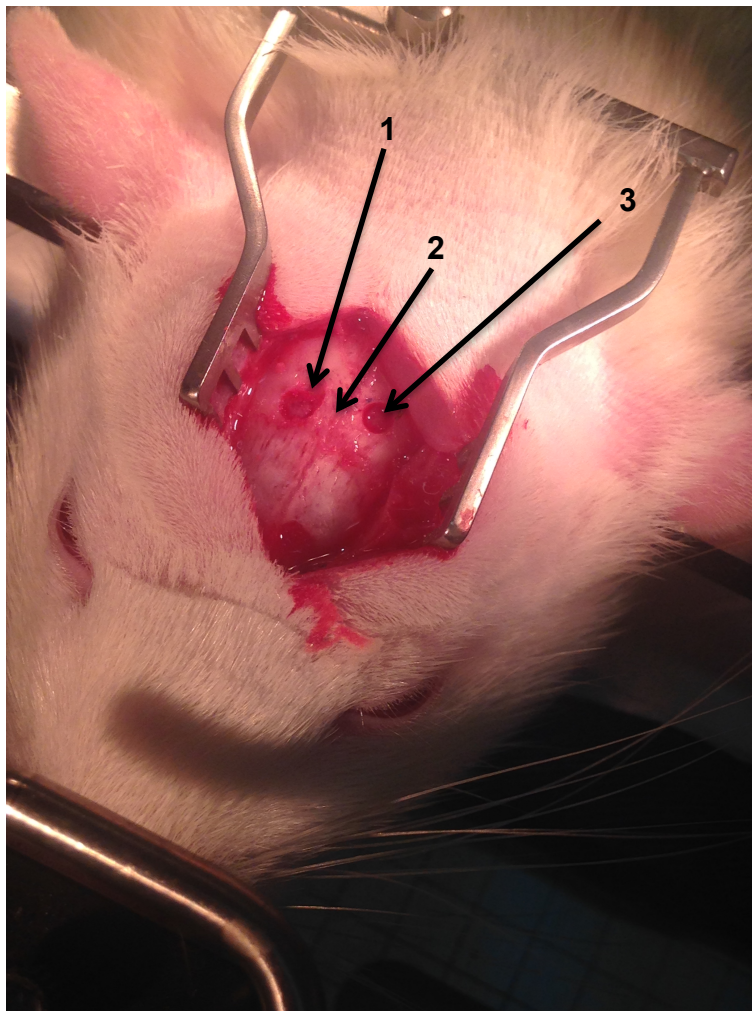


**Figure 8 – Bilateral Craniotomy Holes.** (1) CC1.R oxygen probe site (-1mmAP, -3mmML); (2) Bregma point; (3) CB.8 temperature probe site.

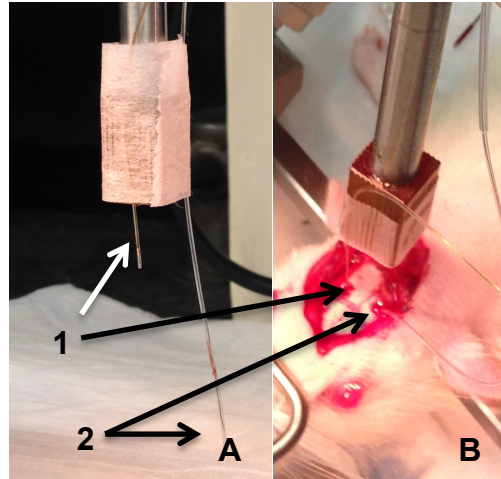


**Figure 9: Licox® PbtO<sub>2</sub> Electrode Preparation & Placement (A)**  
 Licox® electrodes taped to stereotaxic manipulator arm. PB) Electrodes after placement into brain parenchyma. (1) Licox® CC1.R probe; (2) Licox® C8.B temperature probe.

#### 2.4.4 Insult, Treatment, & Post-Treatment Monitoring

Following the 30-minute stabilization period, a 100 $\mu$ L arterial blood sample was aspirated from the arterial cannula and analyzed using the ABL 800 Flex® blood gas analyzer. The following parameters were analyzed during blood gas analysis: pH, pO<sub>2</sub>, pCO<sub>2</sub>, HCO<sub>3</sub><sup>-</sup>, ctHb, %COHB, and lactic acid concentration. The arterial line was then flushed with a volume of heparinized saline equal to the catheter volume in order to remove blood from the catheter lumen. Exposure procedure was then initiated. This time point was flagged in the AcqKnowledge software for later reference and is considered Time 0, as per Figure 4. Rats were exposed for 30 minutes to either 2500ppm CO balanced in medical air (insult) or medical air (sham exposure). PbtO<sub>2</sub> was recorded every 5 minutes beginning at Time 0. Respiration rate was also recorded every 5 minutes concurrently with PbtO<sub>2</sub> recordings by observing chest rise for 30 seconds and multiplying the observed rate by a factor of 2. Isoflurane was continuously



administered at 2% with the assigned exposure gas. At the end of exposure protocol, Time 30, another 100 $\mu$ L arterial blood sample was obtained and analyzed. This time point was marked in the AcqKnowledge software. All rats were immediately switched back to breathing medical air with 2% isoflurane and each rat was administered the assigned IP injection of B12r according to a weight-based dosing scheme given in or an equivalent volume of isotonic normal saline (Table 2).

Intraperitoneal administration was chosen to maintain consistency with methods used in previous studies conducted in our laboratory on B12r as a potential therapy for CO poisoning.

**Table 2 – B12r Dosing Protocol**

| <b>Dose: (100mg OHCbl + 100mg AA)/ kg</b> |                             |                         |
|---|-----------------------------|-------------------------|
| <b>Weight (g)</b>                         | <b>Dose OHCbl + AA (mg)</b> | <b>Dose Volume (mL)</b> |
| 300                                       | 30 + 30                     | 0.6                     |
| 325                                       | 32.5 + 32.5                 | 0.65                    |
| 350                                       | 35 + 35                     | 0.7                     |
| 375                                       | 37.5 + 37.5                 | 0.75                    |
| 400                                       | 40.0 + 40.0                 | 0.8                     |
| 425                                       | 42.5 + 42.5                 | 0.85                    |

A 1:1 mass ratio of 50mg/mL OHCbl and AA was used and administered at 100mg/kg intraperitoneally. Rats assigned to vehicle treatment received an equivalent intraperitoneal dose of normal saline.

PbtO<sub>2</sub> readings were recorded every 5 minutes for another 60 minutes. Additional arterial blood samples were obtained and analyzed at 20 and 60 minutes (Time 50 and Time 90, respectively) after treatment administration. The 20 minute post-administration time was chosen because we noted that rats receiving B12r were excreting purple urine 15-20 minutes following intraperitoneal injection, indicating that the treatment was not only in the vasculature but also being actively cleared by the animal's renal system. Monitoring was terminated 60 minutes after antidote administration (Time 90) and each animal was humanely euthanized via IP injection of a high-dose pentobarbital and phenytoin solution (Euthasol®, Virbac Animal Health™).

Upon completion of the procedure, mean arterial pressure data were obtained using the hemodynamic analysis algorithm within the AcqKnowledge software. A 30-second period of time was selected at 5 minute intervals to correspond with PbtO<sub>2</sub> measurements and the mean arterial pressure was recorded.

## **2.5 Statistical Analysis**

PbtO<sub>2</sub> and MAP data were analyzed using the SAS™ software Type 3 Tests of Fixed Effects analysis algorithm and paired Student's t-tests with corresponding  $p < .05$  considered significant. Arterial blood gas parameters and respiratory rate data were analyzed using StatPlus Pro™ two-way ANOVA. Fisher Least Square Difference tests and paired Student's t-tests were used for inter-group comparisons with corresponding  $p < 0.05$  considered significant.

## RESULTS

### 3.1 Brain Tissue Oxygen Tension Results

Mean PbtO<sub>2</sub> values and standard deviations were calculated for all measurements (Table 3) and plotted against respective time points (Figure 10A). Mean percent change and standard deviation from PbtO<sub>2</sub> baseline was calculated and plotted as well (Figure 10B). The individual PbtO<sub>2</sub> trajectories with calculated means for subjects in each test group are presented in Figures 11A-D.

Statistical data were performed using SAS™ Type 3 Test of Fixed Effect ANOVA, which was felt to be a more appropriate algorithm than standard two-way ANOVA in order to account for individual subject baseline differences. Inter-group significance calculations at relevant time points were carried out using paired Student's t-tests in order to avoid the inherent increased risk of falsely significant differences associated with use of population-derived means in variance analysis. Summary statistical data and relevant inter-group comparisons are given in Table 4. Reported F-Values indicate significant effect on PbtO<sub>2</sub> over time and between groups (F=248.94, p<.0001; F=56.14, p<.0001).

No statistical difference was noted between all groups prior to start of the exposure protocol (Table 3). All rats exposed to CO exhibited marked decreases in PbtO<sub>2</sub>; mean PbtO<sub>2</sub> decreased from 31.3±1.2 mmHg to 18.3±1.0 mmHg in CO-B12r rats and from 31.2±0.7 mmHg to 18.3±1.3 mmHg in CO-Vehicle rats (p<.0001 in comparison to baseline and sham-exposed groups). There were no statistical significances between the PbtO<sub>2</sub> values of the two CO-exposed groups after or during the 30-minute exposure (p>0.5, p=1.0 at end of exposure). Sham-B12r and Sham-Vehicle rats did show a small

PbtO<sub>2</sub> increase during exposure from 30.7±0.6 to 31.2±1.0 and 30.6±0.6 to 31.7±9, respectively (p<.05). There was no statistical difference between the PbtO<sub>2</sub> of the two sham-exposed groups (p>0.2).

Neither B12r nor Vehicle treatments had a significant effect on PbtO<sub>2</sub> in sham-exposed rats as compared between and within the two sham groups and (p>0.1). Poisoned rats treated with B12r demonstrated a rapid PbtO<sub>2</sub> increase with recovery to above the published murine mean PbtO<sub>2</sub> of 29.4mmHg within 55 minutes of administration (29.8±1.9 mmHg, p<.0001). There was no statistical significance between the CO-B12r group and Sham groups 35 minutes after treatment (p<.05). The recovery seen in the CO-Vehicle group was significantly slower in comparison to the CO-B12r group; PbtO<sub>2</sub> did not reach >25mmHg until 45 minutes post-treatment and did not return to baseline (p<.0001 compared to sham groups at all time points after treatment). Differences in PbtO<sub>2</sub> between CO-B12r and CO-Vehicle rats were statistically significant for all time points after administration (p<.0001).

**Table 3 - Mean PbtO<sub>2</sub> Values and Standard Deviations of the Mean**

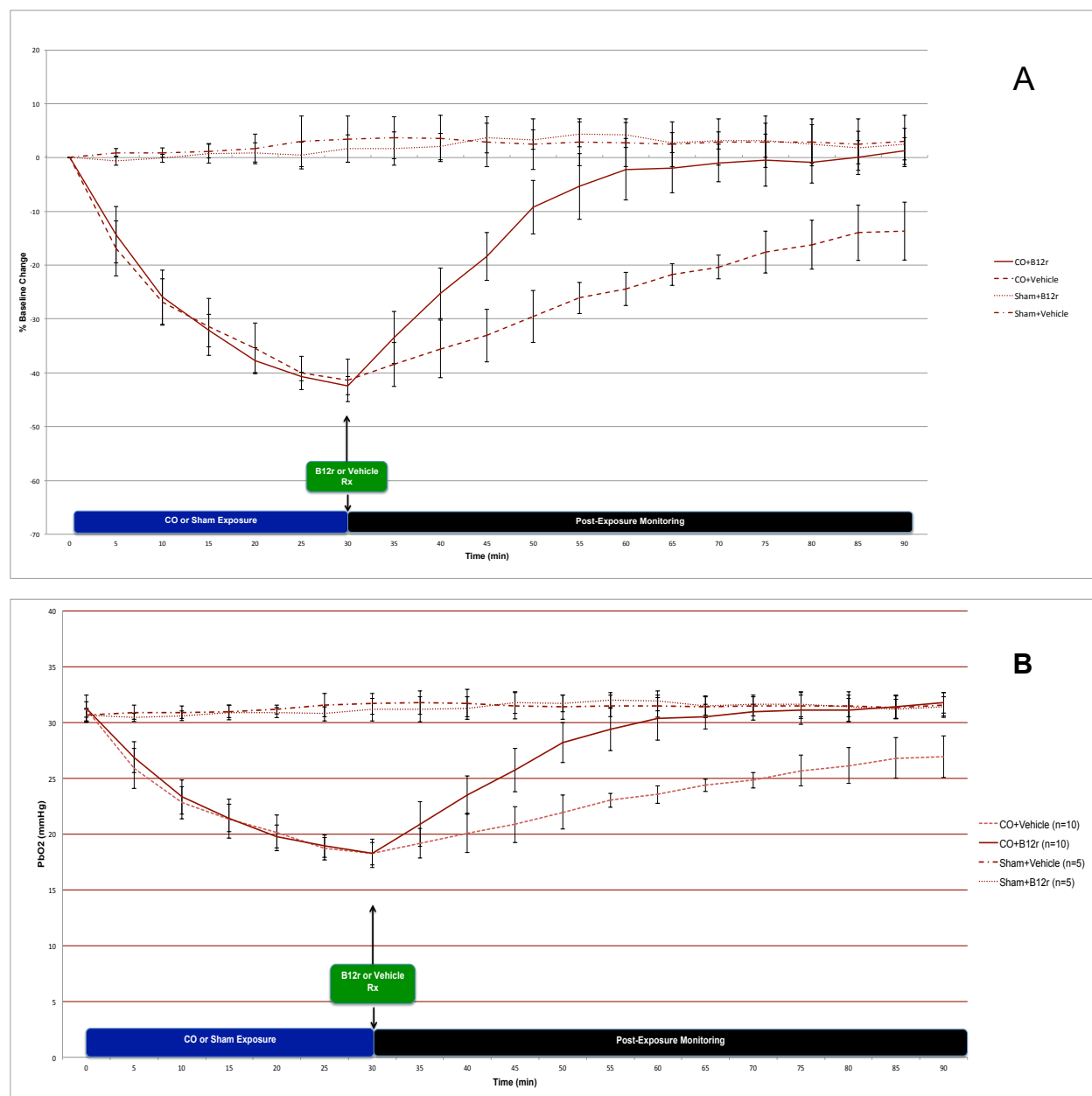
| Time | CO-B12r                 | CO-Vehicle            | Sham-B12r             | Sham-Vehicle          |
|------|-------------------------|-----------------------|-----------------------|-----------------------|
| 0    | 31.3±1.2 <sup>a</sup>   | 31.2±0.7 <sup>a</sup> | 30.7±0.6 <sup>a</sup> | 30.6±0.6 <sup>a</sup> |
| 5    | 26.9±1.4                | 25.9±1.8              | 30.5±0.4              | 30.9±0.6              |
| 10   | 23.3±1.5                | 22.8±1.4              | 30.6±0.4              | 30.9±0.5              |
| 15   | 21.4±1.2                | 21.4±1.7              | 30.9±0.7              | 31.0±0.6              |
| 20   | 19.8±1.0                | 20.1±1.6              | 30.9±0.5              | 31.2±0.4              |
| 25   | 18.9±1.0                | 18.7±1.0              | 30.8±0.7              | 31.5±1.1              |
| 30   | 18.2±1.0 <sup>b</sup>   | 18.2±1.3 <sup>b</sup> | 31.2±1.0 <sup>c</sup> | 31.7±0.9 <sup>c</sup> |
| 35   | 20.9±2.0 <sup>d</sup>   | 19.2±1.3              | 31.2±1.1              | 31.8±1.0              |
| 40   | 23.5±1.7 <sup>e</sup>   | 20.1±1.7              | 31.3±1.0              | 31.7±1.2              |
| 45   | 25.8±2.0                | 20.9±1.6              | 31.8±1.0              | 31.5±1.2              |
| 50   | 28.2±1.8                | 22.0±1.5              | 31.7±0.7              | 31.4±1.1              |
| 55   | 29.4±1.9                | 23.0±0.6              | 32.0±0.7              | 31.5±1.0              |
| 60   | 30.3±1.9                | 23.6±0.8              | 31.9±0.9              | 31.5±1.0              |
| 65   | 30.5±1.1                | 24.4±0.6              | 31.5±0.9              | 31.4±0.9              |
| 70   | 30.9±0.7                | 24.8±0.7              | 31.6±0.7              | 31.5±0.9              |
| 75   | 31.1±1.3                | 25.8±1.4              | 31.6±1.1              | 31.5±1.1              |
| 80   | 31.1±1.0                | 26.1±1.6              | 31.4±1.3              | 31.5±1.0              |
| 85   | 31.4±1.0                | 26.8±1.8              | 31.2±0.9              | 31.4±1.0              |
| 90   | 31.8±0.9 <sup>e,f</sup> | 26.9±1.9 <sup>g</sup> | 31.4±0.9              | 31.6±1.1              |

<sup>a</sup> No statistical difference between baseline PbtO<sub>2</sub> between all groups. <sup>b</sup> Both CO-exposed showed significant PbtO<sub>2</sub> decreases compared to sham groups (p<.0001). <sup>c</sup> No statistical difference between sham groups at Time 30. <sup>d</sup> B12r significantly increased PbtO<sub>2</sub> compared to CO-Vehicle (p<.01). <sup>e</sup> p<.0001 compared to CO-Vehicle <sup>f</sup> No significant difference between CO-B12r and sham groups. <sup>g</sup> p<.0001 compared to sham groups.

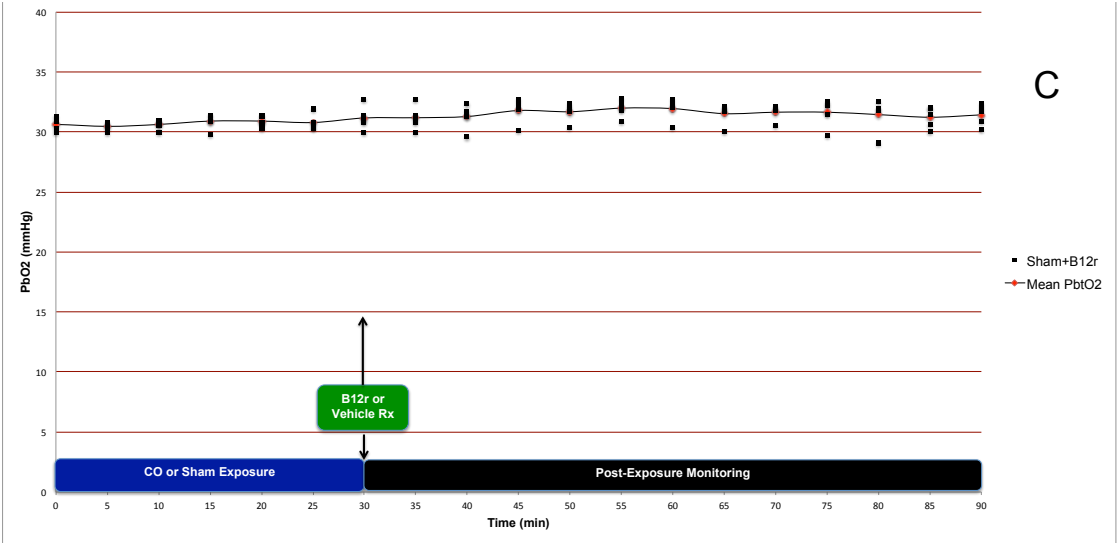
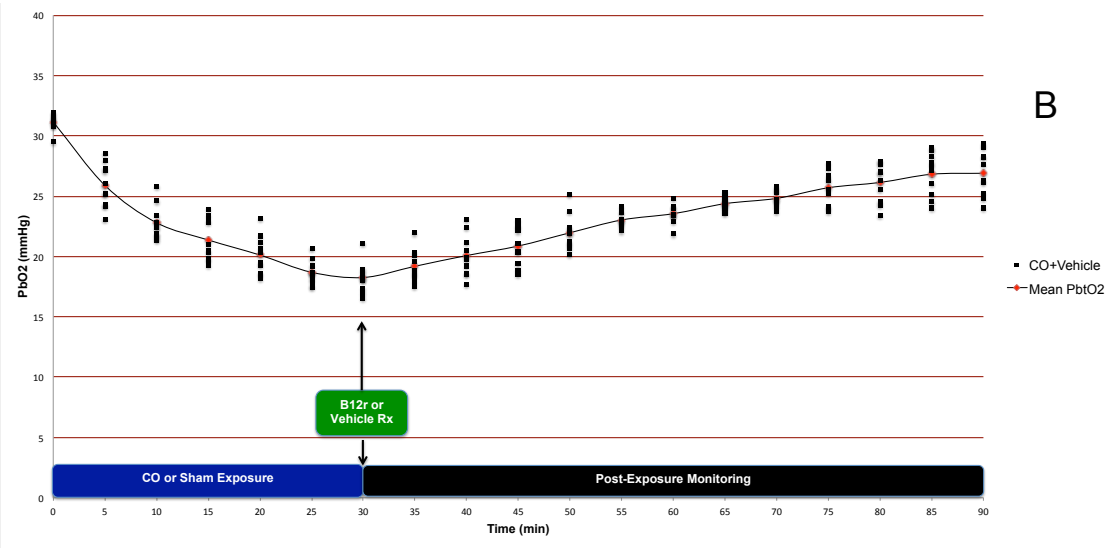
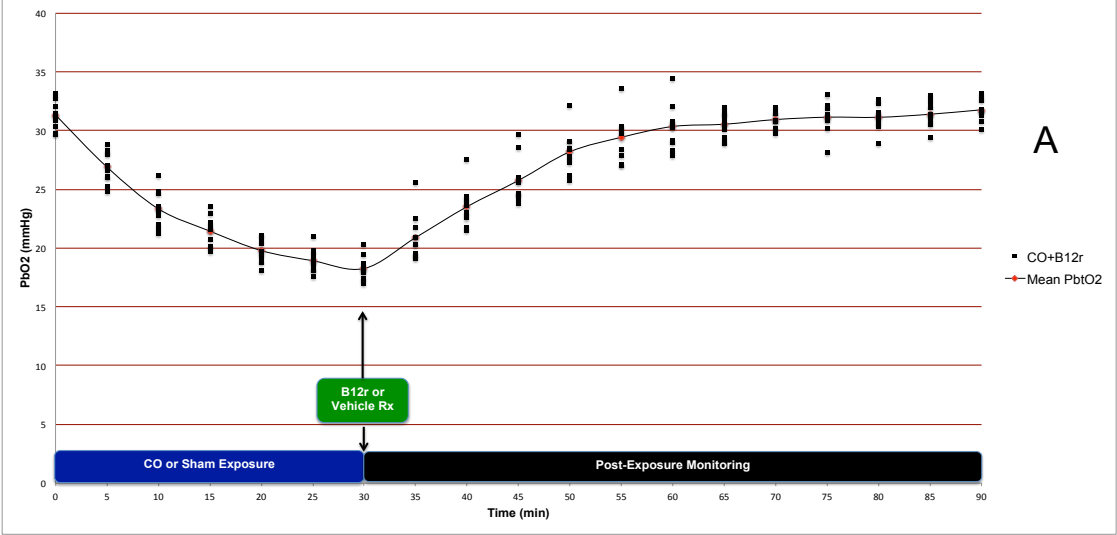
**Table 4 – Summary Statistical Data for PbtO<sub>2</sub> analysis.**

| Effect         | DF | Den DF | F-Value | Pr>F   |
|----------------|----|--------|---------|--------|
| Rx             | 3  | 15.8   | 248.94  | <.0001 |
| Time           | 18 | 431    | 56.14   | <.0002 |
| Treatment*Time | 54 | 374    | 22.56   | <.0003 |

F-Values calculated using SAS™ Type 3 Tests of Fixed Effects Analysis of Variance. Inter-group significance was calculated using paired Student's t-tests with p<.05 considered significant.



**Figure 10: Mean PbtO2 Values and Standard Deviations of the Mean Over Time.** (A) Mean PbtO2 values and standard deviations of the mean. Sham-exposed groups remained stable with no significant changes between Time 0 and Time 90 ( $p>0.1$ ). B12r rapidly rescued PbtO2 in CO-poisoned rats compared to Vehicle-treated rats within 5 minutes of treatment ( $p<.0001$ ). (B) Mean PbtO2 presented as percent change from baseline with standard deviations.



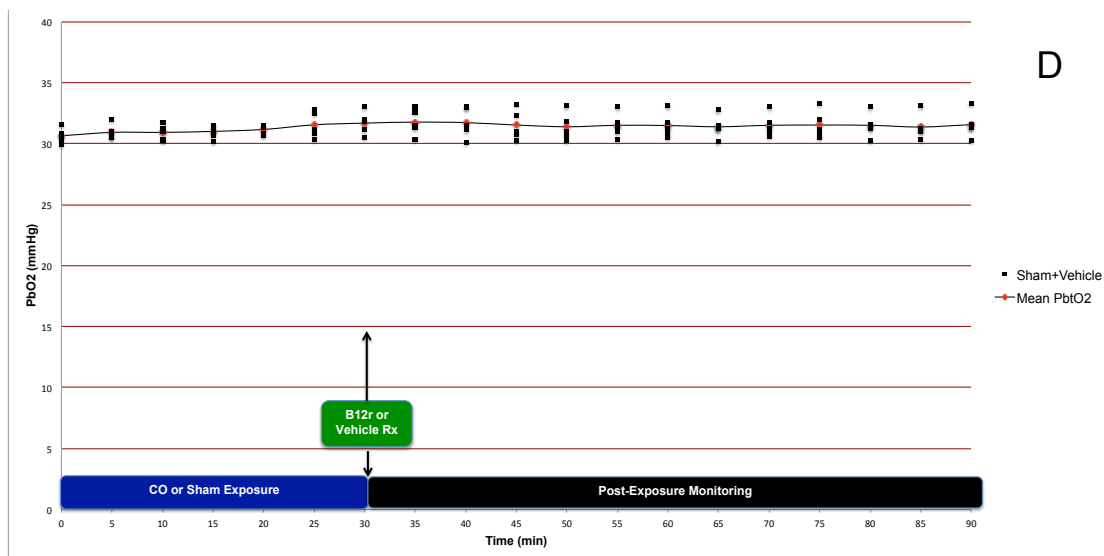


**Figure 11: Individual PbtO<sub>2</sub> Trajectories by Experimental Groups.** (A) CO-B12r, n=10 (on previous page); (B) CO-Vehicle, n=10 (on previous page); (C) Sham-B12r, n=5 (on previous page); (D) Sham-Vehicle, n=5.



### 3.2 Mean Arterial Pressure Results

Blood pressure was recorded continuously during the procedure. Mean arterial pressure for each subject was calculated from a 30-second sample of the continuous recording taken at five-minute intervals to correspond with PbtO<sub>2</sub> and respiration rate recordings. These data were then averaged with standard deviations calculated (Table 5) and plotted against time (Figure 12A). Subject data was again normalized for individual baselines and presented as percent change from baseline with standard deviations (Figure 12B). Because these data were manipulated multiple times to produce single mean values, individual subject trajectories by experimental group are presented in in Figures 13A-D.

Statistical analysis was again performed using SAS™ software Type 3 Tests of Fixed Effects ANOVA, which was felt to be more appropriate than standard two-way ANOVA. Inter-group significance calculations at relevant time points were carried out using paired Student's t-tests in order to avoid the inherent increased risk of falsely significant differences associated with use of population-derived means in variance analysis. Summary statistical data and relevant inter-group comparisons are given in Table 4. Reported F-Values indicate significant effect on PbtO<sub>2</sub> over time and between groups (F=248.94, p<.0001; F=56.14, p<.0001).

There was no difference in mean MAP between groups at the start of the procedure (p>0.7). Profound hypotension (46.2±1.9 and 45.4±2.0 mmHg) was seen at the end of CO exposure in CO-B12r and CO-Vehicle groups respectively (p<.0001 compared to shams, p>0.77 between CO-exposed groups). The individual MAP

trajectories during CO exposure varied widely, however there were noticeable patterns. Figures 12A and 12B demonstrate that some subjects demonstrated rapid decompensation within 15 minutes in an almost exponential-like fashion. Others were able to compensate adequately for 15 minutes before MAP dropped below 70mmHg. Sham-exposed rats did not demonstrate any changes during sham exposure ( $p>0.9$ ).

Cessation of CO exposure caused an immediate upward MAP trend in both CO-exposed groups. The CO-B12r group exhibited a small but significant increase in MAP 10 minutes after treatment that lasted for approximately 10 minutes ( $p<.05$  compared to CO-Vehicle). MAP recovery in vehicle-treated rats was significantly slower and remained significantly lower than both sham-exposed groups by end of monitoring ( $p<.001$ ). There was no significant difference between sham groups and CO-B12r rats at Time 90 ( $p>0.6$ ). Administration of B12r to Sham-exposed rats caused a significant transient MAP increase ( $89.6\pm3.4$  to  $98.5\pm2.3$  mmHg) that lasted for 25 minutes ( $p<.0001$ ). Vehicle administration did not affect MAP of Sham-exposed rats ( $p>0.2$  compared to baseline).

**Table 5: Mean MAP Values and Standard Deviations of the Mean**

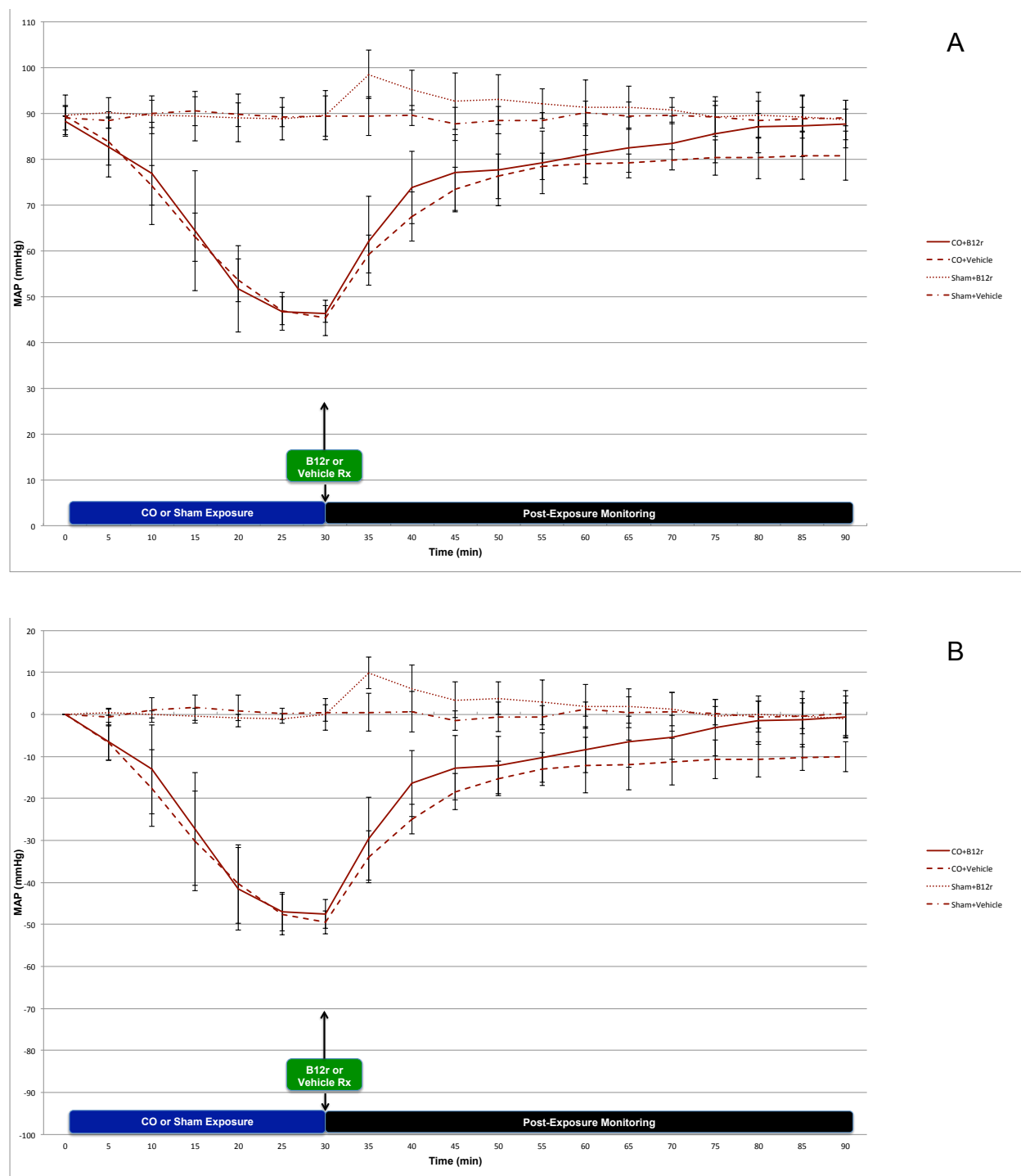
| Time | CO-B12r               | CO-Vehicle             | Sham-B12r             | Sham-Vehicle          |
|------|-----------------------|------------------------|-----------------------|-----------------------|
| 0    | 88.2±3.2 <sup>a</sup> | 89.3±3.5 <sup>a</sup>  | 89.6±2.5 <sup>a</sup> | 89.0±2.5 <sup>a</sup> |
| 5    | 82.7±6.6              | 83.8±4.9               | 90.1±3.1              | 88.5±1.9              |
| 10   | 76.9±11.2             | 74.2±9.7               | 89.7±2.5              | 89.9±1.6              |
| 15   | 64.4±13.1             | 63.0±12.0              | 89.3±2.3              | 90.5±1.3              |
| 20   | 51.7±9.5              | 53.6±8.8               | 88.9±2.1              | 89.7±1.7              |
| 25   | 46.8±4.2              | 47.0±4.0               | 88.7±2.2              | 89.2±1.5              |
| 30   | 46.2±1.9 <sup>b</sup> | 45.4±2.0 <sup>b</sup>  | 89.6±3.4 <sup>b</sup> | 89.4±2.4 <sup>b</sup> |
| 35   | 62.2±9.7              | 59.3±5.0               | 98.5±2.3 <sup>c</sup> | 89.4±1.5              |
| 40   | 73.8±7.9 <sup>d</sup> | 67.4±3.8 <sup>d</sup>  | 95.1±3.4              | 89.5±2.2              |
| 45   | 77.1±8.3              | 73.4±5.2               | 92.7±2.3              | 87.7±1.3              |
| 50   | 77.7±7.9              | 76.2±6.2               | 93.0±2.7 <sup>e</sup> | 88.5±2.0 <sup>e</sup> |
| 55   | 79.2±2                | 78.41±7.0              | 92.1±4.5              | 88.4±3.4              |
| 60   | 80.9±6.4              | 79.1±7.9               | 91.3±3.9              | 90.1±1.8              |
| 65   | 82.5±6.6              | 79.1±6.9               | 91.3±2.6              | 89.4±1.3              |
| 70   | 83.4±5.9              | 79.8±6.7               | 90.8±2.6              | 89.5±1.7              |
| 75   | 85.4±6.3              | 80.4±6.6               | 89.3±1.4              | 89.2±0.6              |
| 80   | 87.0±5.6              | 80.3±5.7               | 89.5±2.5              | 88.5±1.1              |
| 85   | 87.2±6.7              | 80.7±5.0               | 89.2±3.2              | 88.7±1.5              |
| 90   | 87.7±5.3 <sup>e</sup> | 80.8±4.15 <sup>e</sup> | 88.6±2.7              | 89.0±2.4              |

<sup>a</sup> No significant difference between groups at Time 0. <sup>b</sup> No significant difference between CO-exposed groups or between sham-exposed groups.  $p < .0001$  CO-exposed to sham-exposed. <sup>c</sup> Significant MAP increase after B12r administration.  $p < .0001$  compared to CO-Vehicle. <sup>d</sup> B12r administration significantly increased MAP.  $p < .05$  compared to CO-Vehicle. <sup>e</sup> Indicates  $p < .05$  between marked group at corresponding time points.

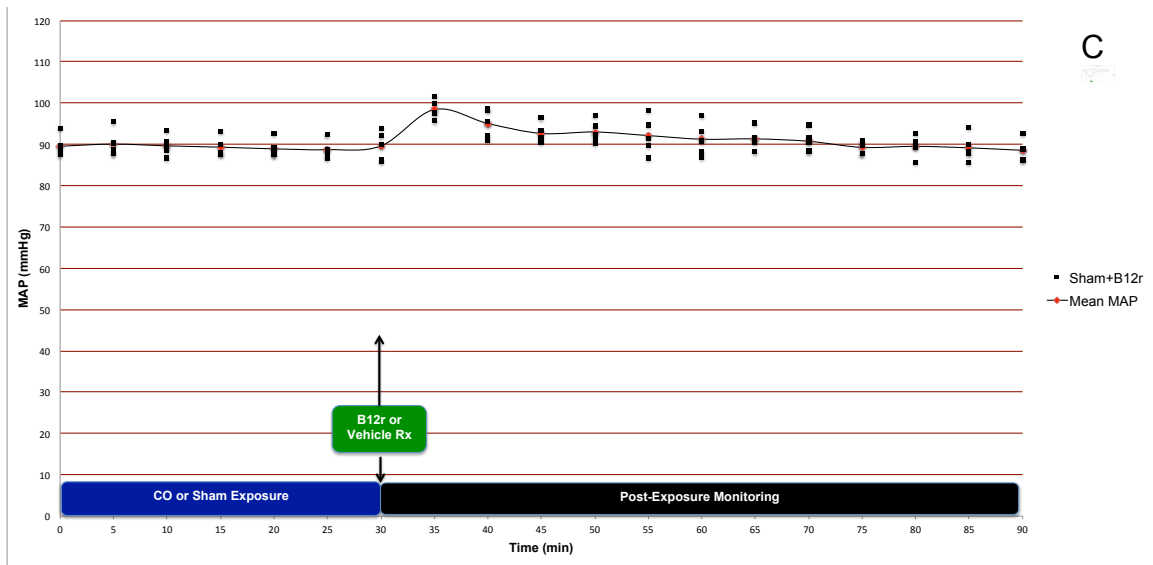
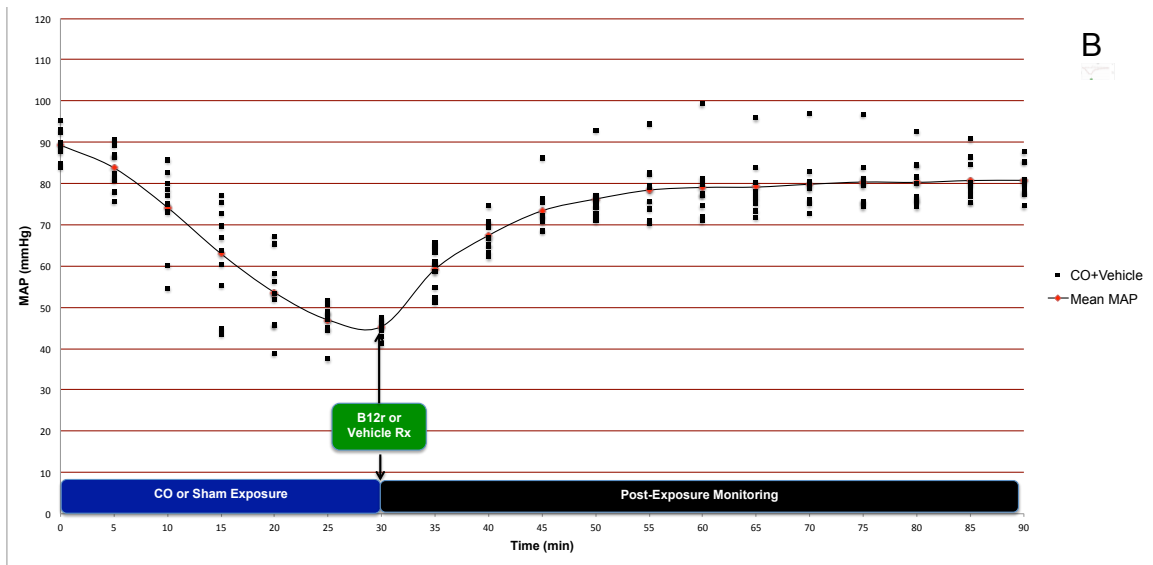
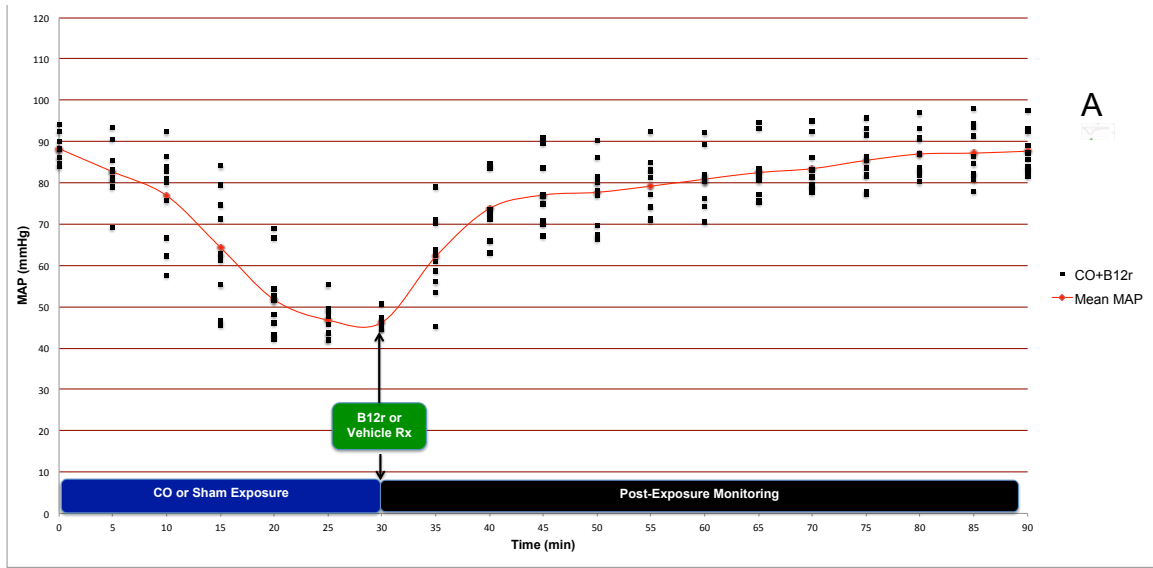
**Table 6 – Summary Statistical Data for MAP Analysis.**

| Effect         | DF | Den DF | F-Value | Pr>F   |
|----------------|----|--------|---------|--------|
| Rx             | 3  | 22.8   | 116.2   | <.0001 |
| Time           | 18 | 433    | 38.01   | <.0001 |
| Treatment*Time | 54 | 359    | 13.16   | <.0001 |

F-Values calculated using SAS™ Type 3 Tests of Fixed Effects Analysis of Variance. Inter-group significance was calculated using paired Student's t-tests with  $p < .05$  considered significant.



**Figure 12: Mean MAP and Standard Deviations of the Mean Over Time.** (A) Mean map and standard deviations of the mean. CO exposure caused similar profound hypotension in CO-B12r and CO-Vehicle rats ( $p>0.7$ ). MAP of sham-exposed groups did not change ( $p>0.9$ ). B12r caused significant transient MAP increases in both treatment groups ( $p<0.05$ ). CO-B12r rats demonstrated significantly higher MAP 60 minutes after treatment that did not differ from sham-exposed groups ( $p<.001$ ,  $p>0.6$ ). (B) Mean MAP and standard deviations presented as % change from baseline.



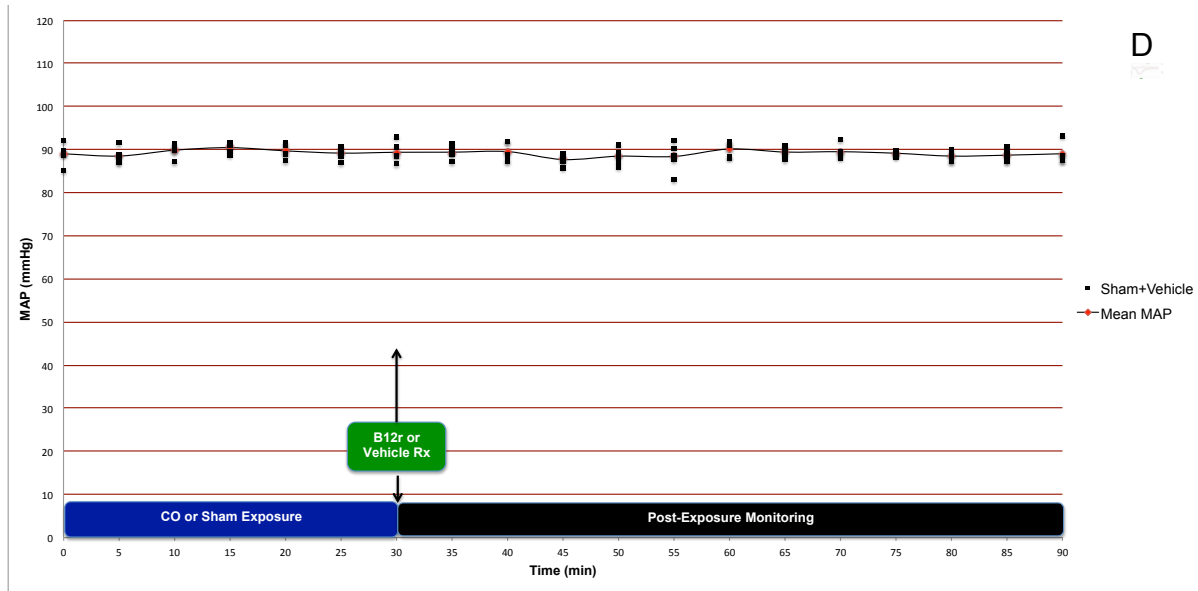


**Figure 13: Individual MAP Trajectories by Experimental Group.** CO-exposed rats displayed marked hypotension with unique patterns of compensation. Treatment with B12r caused a transient significant MAP increase in both groups in comparison to their respective vehicle control ( $p < .05$ ). (A) CO-B12r,  $n=10$  (on previous page); (B) CO-Vehicle,  $n=10$  (on previous page); (C) Sham-B12r,  $n=5$  (on previous page); (D) Sham-Vehicle,  $n=5$ .

### 3.3 Arterial Blood Gas Results

Arterial blood samples were taken at the following experimental time points marked in Figure 4: Time 0 (baseline), Time 30 (post-exposure), Time 50 (20 minutes post-treatment) and Time 90 (final). Parameters analyzed included pH, pO<sub>2</sub>, PCO<sub>2</sub>, HCO<sub>3</sub><sup>-</sup>, ctHb, %COHb, and lactic acid. Values of %COHb were not recorded for rats receiving B12r, as hydroxocobalamin interferes with absorbance spectroscopy and provides unreliable data.<sup>203,204</sup> Means of each parameter and standard deviations were calculated (Table 7) and each parameter was analyzed using two-way ANOVA. Statistical significance was calculated using the Fisher Least Square Difference test and paired Student's t-tests with p<.05 considered significant. Summary statistical data for ANOVA of each parameter are presented in Table 8.

There were no differences in baseline (Time 0) arterial blood chemistry between groups and all parameters were within normal published limits for anesthetized rats.<sup>205</sup> Mean post-exposure %COHb in CO-B12r and CO-Vehicle groups was 58.4±5.6% and 60.1±3.6% (p<.0001 compared to shams). A significant increase in pO<sub>2</sub> and decrease in pCO<sub>2</sub> was noted in both CO-exposed groups at Time 30 due to the compensatory hyperventilation response to CO (p<.05 compared to baseline and shams). Lactate levels increased in CO-B12r (1.0±0.2mM to 3.4±0.9mM, p<.0001) and CO-Vehicle groups (1.0±0.2mM to 3.6±0.4mM, p<.0001) and a significant compensatory decrease in HCO<sub>3</sub><sup>-</sup> was seen in each group, indicating a compensated acidosis (p<.05). Although some individual rats did demonstrate pH changes after exposure to CO, no statistically

significant changes in pH were noted at any time in any of the 4 groups. There were no significant changes in  $\text{HCO}_3^-$  or lactate in sham-exposed groups at any point.

At Time 50,  $\text{pCO}_2$  remained significantly lower in CO-B12r and  $\text{HCO}_3^-$  remained significantly lower in both CO-exposed groups compared to shams ( $p < .05$ ). Lactate levels in CO-B12r and CO-Vehicle decreased; there were no differences between the two groups. By Time 90, all parameters except lactate and %COHb showed no statistical difference between groups. Again, no difference was seen in the rate of lactate decrease between CO-B12r and CO-Vehicle rats. The %COHb decrease from  $60.1 \pm 3.6$  to  $29.9 \pm 5.7$  indicates an approximate COHb half-life of 60 minutes. Although the analysis of Hb concentration (ctHb) was statistically significant over time and between groups ( $F=5.96$ ,  $F=34.79$ ), all rats remained within normal ranges of ctHb and this was attributed to minor surgical blood loss and individual ctHb between subjects among the groups.



**Table 7: Mean ABG Parameter Values and Standard Deviations of the Mean**

| Time 0                                  |                       |                       |           |              |
|---|-----------------------|-----------------------|-----------|--------------|
|   | CO-B12r               | CO-Vehicle            | Sham-B12r | Sham-Vehicle |
| pH (7.40±0.05)                          | 7.43±0.01             | 7.43±0.02             | 7.43±0.02 | 7.42±0.01    |
| pO <sub>2</sub> (95±14 mmHg)            | 89.9±3.3              | 91.2±6.5              | 89.2±6.6  | 91.8±3.8     |
| pCO <sub>2</sub> (45±10mmHg)            | 40.5±4.4              | 41.0±1.4              | 41.6±2.7  | 40.2±3.4     |
| HCO <sub>3</sub> <sup>-</sup> (25±3mEq) | 27.3±1.8              | 26.5±1.3              | 27.5±0.9  | 25.9±1.5     |
| Hb (11.5-16 mg/dL)                      | 13.4±0.3              | 13.5±0.6              | 13.8±0.6  | 14.2±0.4     |
| %COHb (1-3%)                            | 2.4±0.2               | 2.4±0.2               | 2.4±0.2   | 2.4±0.1      |
| Lactate (<1.5mM)                        | 1.0±0.2               | 1.0±0.2               | 0.9±0.2   | 1.0±0.1      |
| Time 30                                 |                       |                       |           |              |
|   | CO-B12r               | CO-Vehicle            | Sham-B12r | Sham-Vehicle |
| pH (7.40±0.05)                          | 7.42±0.04             | 7.38±0.06             | 7.43±0.10 | 7.42±0.01    |
| pO <sub>2</sub> (95±14 mmHg)            | 99.9±4.9 <sup>a</sup> | 99.9±7.2 <sup>a</sup> | 90.4±7.3  | 90.6±3.1     |
| pCO <sub>2</sub> (45±10mmHg)            | 37.4±2.3 <sup>b</sup> | 36.6±3.8 <sup>a</sup> | 41.4±2.5  | 41.1±2.9     |
| HCO <sub>3</sub> <sup>-</sup> (25±3mEq) | 24.6±2.0 <sup>c</sup> | 22.6±2.3 <sup>a</sup> | 27.2±1.0  | 24.9±2.2     |
| Hb (11.5-16 mg/dL)                      | 13.3±0.4              | 13.5±0.5              | 13.7±1.0  | 14.0±0.4     |
| %COHb (1-3%)                            | 58.4±5.6 <sup>d</sup> | 60.1±3.6 <sup>d</sup> | 2.4±0.3   | 2.2±0.2      |
| Lactate (<1.5mM)                        | 3.4±0.9 <sup>d</sup>  | 3.6±0.4 <sup>d</sup>  | 1.1±0.2   | 1.0±0.1      |
| Time 50                                 |                       |                       |           |              |
|   | CO-B12r               | CO-Vehicle            | Sham-B12r | Sham-Vehicle |
| pH (7.40±0.05)                          | 7.42±0.03             | 7.40±0.08             | 7.42±0.02 | 7.42±0.02    |
| pO <sub>2</sub> (95±14 mmHg)            | 86.8±3.6              | 85.7±3.9              | 89.4±4.0  | 88.7±1.6     |
| pCO <sub>2</sub> (45±10mmHg)            | 38.8±2.4 <sup>a</sup> | 39.8±4.9              | 42.1±2.1  | 40.9±1.9     |
| HCO <sub>3</sub> <sup>-</sup> (25±3mEq) | 23.8±2.6 <sup>a</sup> | 23.4±2.8 <sup>a</sup> | 26.6±1.1  | 26.5±1.6     |
| Hb (11.5-16 mg/dL)                      | 13.2±0.3              | 13.2±0.5              | 13.8±0.7  | 13.8±0.2     |
| %COHb (1-3%)                            | -----                 | 42.9±4.7 <sup>d</sup> | -----     | 2.4±0.2      |
| Lactate (<1.5mM)                        | 3.0±1.0 <sup>c</sup>  | 2.9±0.9 <sup>c</sup>  | 1.1±0.2   | 1.0±0.1      |
| Time 90                                 |                       |                       |           |              |
|   | CO-B12r               | CO-Vehicle            | Sham-B12r | Sham-Vehicle |
| pH (7.40±0.05)                          | 7.41±0.03             | 7.43±0.3              | 7.42±0.03 | 7.42±0.01    |
| pO <sub>2</sub> (95±14 mmHg)            | 88.8±3.9              | 88.2±2.4              | 88.1±6.8  | 89.3±4.2     |
| pCO <sub>2</sub> (45±10mmHg)            | 39.6±1.5              | 40.6±3.6              | 40.6±3.5  | 39.5±2.8     |
| HCO <sub>3</sub> <sup>-</sup> (25±3mEq) | 25.9±2.3              | 26.3±1.4              | 26.0±1.1  | 26.4±1.4     |
| Hb (11.5-16 mg/dL)                      | 13.2±0.4              | 13.2±0.4              | 13.9±0.6  | 13.9±0.2     |
| %COHb (1-3%)                            | -----                 | 29.9±5.7 <sup>d</sup> | -----     | 2.4±0.3      |
| Lactate (<1.5mM)                        | 1.9±0.7 <sup>a</sup>  | 1.8±0.6 <sup>a</sup>  | 1.2±0.3   | 1.0±0.1      |

Normal murine reference ranges are given as well. Note the evidence of compensatory hyperventilation (increased pO<sub>2</sub> and decreased pCO<sub>2</sub>) and compensated lactic acidosis in CO-exposed groups.

<sup>a</sup> (p<.05), <sup>b</sup> (p<.01), <sup>c</sup> (p<.001), <sup>d</sup> (p<.0001) in comparison to sham groups.

**Table 8: Summary Statistical Data for ABG Parameter Analysis.**

| Parameter                     | Variable | F-Value | p       |
|-------------------------------|----------|---------|---------|
| pH                            | Time     | 15.8    | 0.35    |
|                               | Group    | 431     | 0.63    |
| pO <sub>2</sub>               | Time     | 8.01    | 0.01*   |
|                               | Group    | 0.4     | 0.39    |
| pCO <sub>2</sub>              | Time     | 2.91    | 0.09    |
|                               | Group    | 2.72    | 0.11    |
| HCO <sub>3</sub> <sup>-</sup> | Time     | 5.68    | 0.02*   |
|                               | Group    | 2.58    | 0.12    |
| Hb                            | Time     | 5.82    | 0.02*   |
|                               | Group    | 34.79   | <.0001* |
| COHb                          | Time     | 5.96    | 0.02*   |
|                               | Group    | 6.57    | 0.01*   |
| Lac                           | Time     | 6.64    | 0.01*   |
|                               | Group    | 5.69    | 0.02*   |

Calculated for  $\alpha=0.05$ , degrees of freedom (Time) = 18, degrees of freedom (Group) = 3. Critical F-Value = 3.17. \* denotes statistical significance of  $p<0.05$ .

### 3.4 Respiratory Rate Results

Respiratory rate (RR) for each subject was measured every 5 minutes starting at Time 0 by observing chest rise for 30 seconds and doubling the observed rate to obtain respiration rate per minute. Means and standard deviations were then calculated (Table 11) and plotted against respective time points (Figure 14). Data were analyzed using StaPlus Pro® two-way ANOVA (Table 10). Significance was calculated using the Fisher Least Square Difference test and paired Student's t-tests with  $p < .05$  considered significant.

Neither sham-exposed groups demonstrated any significant changes in respiratory rate over time or between groups for the duration of the procedure. Both groups exposed to CO demonstrated a significant exponential-like decrease in RR during exposure compared to sham groups ( $p < .0001$  at Time 30). This decrease in RR was associated with an observed increase in tidal volume (TV) and appearance of a Kussmaul-like respiration pattern. This could not be quantified, as TV was not measured. However, the increase in  $pO_2$  and decrease in  $pCO_2$  indicate an overall increase in minute volume (MV), which confirms that TV must have increased.

Cessation of CO exposure resulted in recovery to baseline RR and observed decrease in TV to baseline within 40 minutes in both CO-B12r and CO-Vehicle groups. The CO-B12r remained significantly lower than sham groups until Time 60; CO-Vehicle groups showed no significant difference from sham groups by Time 40. No significant difference in RR was noted between CO-B12r and CO-Vehicle groups after treatment, however the CO-Vehicle group did exhibit an insignificant change of approximately 2

resp/min compared to CO-B12r. There were no significant differences between the 4 groups from Time 60 to procedural end.

**Table 9 – Mean Respiratory Rate and Standard Deviations of the Mean**

| Time | CO-B12r           | CO-Vehicle        | Sham-B12r | Sham-Vehicle |
|------|-------------------|-------------------|-----------|--------------|
| 0    | 57±3              | 57±2              | 58±4      | 57±3         |
| 5    | 53±4              | 54±3              | 58±3      | 57±2         |
| 10   | 49±5 <sup>a</sup> | 50±2 <sup>a</sup> | 60±4      | 57±3         |
| 15   | 48±4 <sup>b</sup> | 48±3 <sup>b</sup> | 57±5      | 58±3         |
| 20   | 46±4 <sup>b</sup> | 47±3 <sup>b</sup> | 58±5      | 56±3         |
| 25   | 45±3 <sup>c</sup> | 45±3 <sup>c</sup> | 57±5      | 58±2         |
| 30   | 45±3 <sup>c</sup> | 46±4 <sup>c</sup> | 59±5      | 57±4         |
| 35   | 49±3 <sup>b</sup> | 50±4 <sup>a</sup> | 56±5      | 56±4         |
| 40   | 50±4 <sup>a</sup> | 52±5              | 56±5      | 56±2         |
| 45   | 52±3 <sup>a</sup> | 54±3              | 58±6      | 57±4         |
| 50   | 53±2 <sup>a</sup> | 53±3 <sup>a</sup> | 58±5      | 57±3         |
| 55   | 52±3 <sup>a</sup> | 54±4              | 56±3      | 56±2         |
| 60   | 55±3              | 54±4              | 57±6      | 56±2         |
| 65   | 55±3              | 54±3              | 60±5      | 56±3         |
| 70   | 55±3              | 55±3              | 59±3      | 55±2         |
| 75   | 55±3              | 56±3              | 56±4      | 56±4         |
| 80   | 57±3              | 56±3              | 56±5      | 56±1         |
| 85   | 55±2              | 56±2              | 57±4      | 57±3         |
| 90   | 56±2              | 57±3              | 56±4      | 57±2         |

Rate decreased significantly in CO-exposed rats and returned to baseline within 40 minutes.<sup>a</sup> (p<.05), <sup>b</sup> (p<.01), <sup>c</sup> (p<.001), in comparison to sham groups.

**Table 10 – Summary Statistical Data for Respiratory Rate Analysis**

| Variable | F-Value | p       |
|----------|---------|---------|
| Time     | 4.51    | <.0001* |
| Group    | 23.98   | *<.0001 |

Calculated for  $\alpha=0.05$ , degrees of freedom (Time) = 18, degrees of freedom (Group) = 3. Critical F-Value = 3.17. Asterisk denotes statistical significance of p<.05.

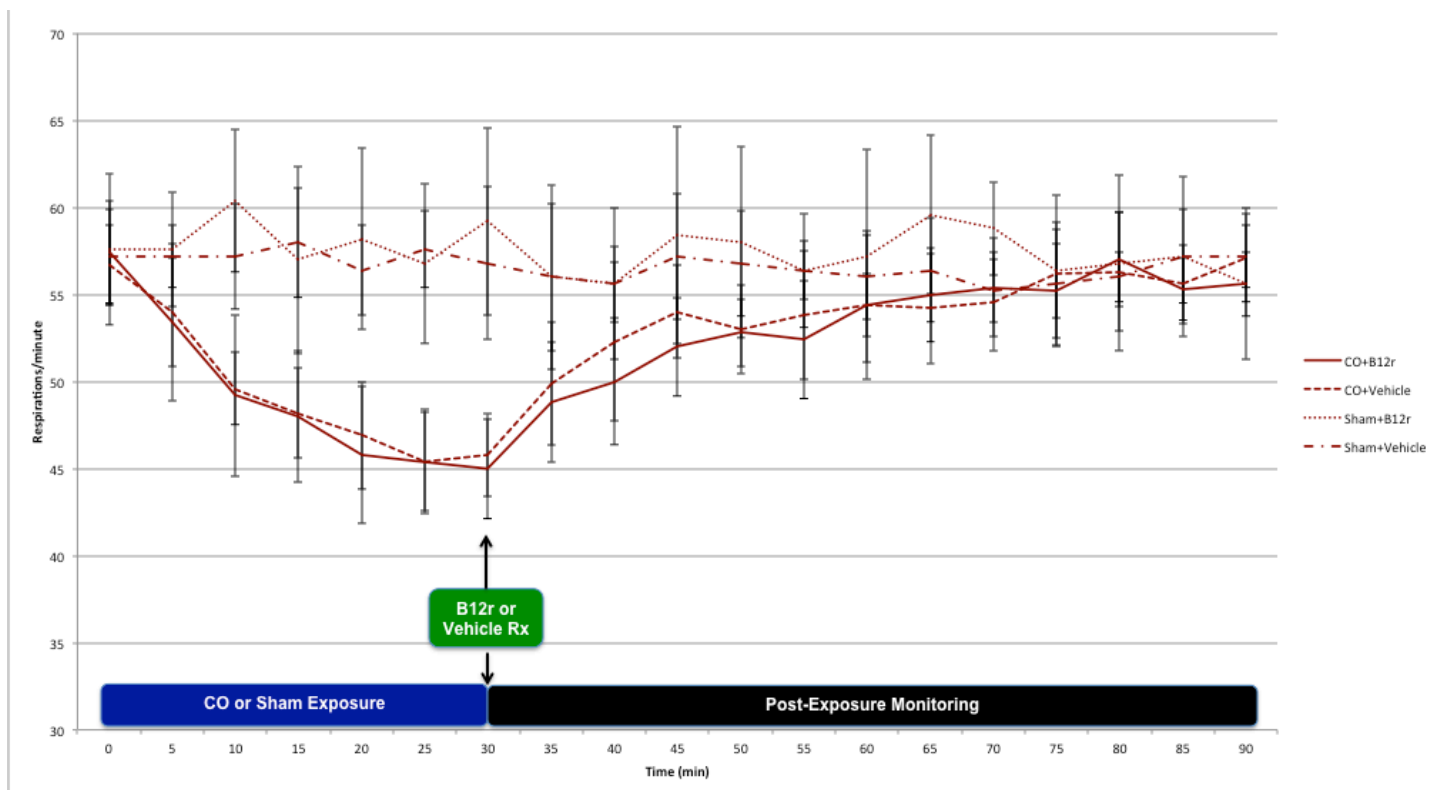


**Figure 14 – Mean Respiratory Rate and Standard Deviations of the Mean Over Time.** Sham-exposed groups did not demonstrate significant RR changes. CO exposure caused marked RR decreases in both CO-exposed groups.. There were no significant differences in the rates of RR recovery between the two CO-exposed groups.

## DISCUSSION

### 4.1 CO Poisoning, Perfusion, & Oxygenation

The most significant and novel observation from this study was that exposure to CO caused marked decreases in PbtO<sub>2</sub> that were rapidly rescued by B12r treatment (Figure 10,  $p < .0001$ ). To the best of our knowledge, this is the first time that PbtO<sub>2</sub> has ever been evaluated in the context of CO exposure. Implicit to the pathology of CO poisoning and the hypothesis of this study is the idea that PbtO<sub>2</sub> values are indicative of cerebral cellular oxygenation. That is, low values indicate hypoxia and high values indicate adequate brain oxygenation. While the temptation exists to interpret the decrease in PbtO<sub>2</sub> as evidence of CO-mediated hypoxia, much of the current literature argues against the hypoxic theory of CO poisoning.<sup>46,51,89,95,98</sup> Extreme caution must therefore be taken in interpretation of these data. Given the complicated, poorly understood pathophysiology of CO poisoning and the limited number of physiological parameters measured, elucidating the exact physiological mechanisms responsible for all changes seen is not possible. The physiological basis of PbtO<sub>2</sub>, determinants of PbtO<sub>2</sub> changes, and the correlation to other physiological parameters must be first considered in the context of published data on the complex pathophysiological mechanisms of CO poisoning.

PbtO<sub>2</sub> is a measurement of extracellular dissolved O<sub>2</sub>, and is believed to represent the balance between oxygen supply and metabolic needs, although the exact relation of PbtO<sub>2</sub> to cerebral oxygen supply/demand and other physiological parameters is still under discussion in the literature.<sup>199,206</sup> Determination of PbtO<sub>2</sub> depends on the complex interactions of factors that determine O<sub>2</sub> delivery such as CBF, MAP, O<sub>2</sub>

content of the blood, proper dissociation of O<sub>2</sub> from Hb, ventilation, and the fraction of inhaled oxygen (FiO<sub>2</sub>) as well as cerebral metabolic demands.<sup>200,207</sup> The amount of oxygen delivered to the brain can be derived from the Fick equation and is the product of CBF and arterial oxygen content (CaO<sub>2</sub>):  $DO_2 = CBF \times C_aO_2$ , where CaO<sub>2</sub> is equal to:  $ctHb \left( \frac{g}{dL} \right) \times 1.36 \frac{mLO_2}{gHb} \times S_aO_2\% + 0.0032kPa \times PaO_2$  ( $S_aO_2\% = \%O_2Hb$ ,  $PaO_2$ =arterial pO<sub>2</sub>).

The formation of COHb and subsequent left-shift of the O<sub>2</sub>-Hb dissociation curve creates a functional anemia and significantly reduces C<sub>a</sub>O<sub>2</sub>, which is the foundation of the hypoxic theory of CO poisoning.<sup>41,46,62,76,89,150</sup> A decrease in C<sub>a</sub>O<sub>2</sub> should theoretically lead to a corresponding decrease in PbtO<sub>2</sub>, however the brain exhibits an exquisite ability to autoregulate CBF in order to meet metabolic demands.<sup>201,208,209</sup> It has been established that CO poisoning causes an immediate NO-mediated compensatory CBF increase in both animals and humans that is capable of maintaining DO<sub>2</sub> even as %COHb approaches 30-50% or higher, depending on the study.<sup>76,89,97,105-111</sup>

Additionally, Rostenthal and colleagues examined PbtO<sub>2</sub> changes in traumatic brain injury patients and reported that PbtO<sub>2</sub> primarily reflects diffusion of dissolved oxygen, and is therefore not an ischemia monitor *per se*.<sup>150</sup> However, Rosenthal's study was performed on patients with normal O<sub>2</sub>Hb saturation and a similar analysis on CO-poisoned blood has yet to be performed in humans, which could yield conflicting results as COHb formation drastically reduces C<sub>a</sub>O<sub>2</sub>. Based on this, we cannot conclude that the PbtO<sub>2</sub> decrease was related to COHb formation alone despite %COHb in CO-B12r (58.4±5.6) and CO-Vehicle (60.1±3.6) groups being above 50%. Indeed, we can conclude that brain tissue oxygen tension is not directly related to %COHb *per se*.

The ability of the brain to autoregulate CBF is MAP-dependent. In humans and rodents, autoregulatory capacity is lost when MAP is <60mmHg, at which point CBF begins to vary linearly with MAP.<sup>207,209</sup> In the rat, CBF decreases from 100mL/min/100g tissue to 60mL/min/100g tissue when MAP decreases from 90mmHg to 50mmHg.<sup>209,210</sup> In our study, CO-B12r and CO-Vehicle groups demonstrated significant decreases in MAP from  $88.2 \pm 3.2$  to  $46.2 \pm 1.9$  mmHg and  $89.3 \pm 3.5$  to  $45.4 \pm$  mmHg, respectively ( $p < .0001$  compared to controls). An examination of the correlation between mean PbtO<sub>2</sub> and MAP in the CO-B12r and CO-Vehicle groups during exposure shows a tight nonlinear correlation. A sigmoidal relationship is seen between the two variables, and a linear trend between MAP and PbtO<sub>2</sub> was noted with MAP <80mmHg, which could indicate that autoregulation of CBF was compromised during CO exposure when MAP dropped below 80mmHg and that subsequent PbtO<sub>2</sub> changes were MAP-dependent. Although we did not measure CBF during this study and therefore cannot determine if autoregulation of CBF was indeed compromised, PbtO<sub>2</sub> shares a sigmoidal relationship with regional CBF when normal autoregulatory mechanisms are present that becomes linear when compromised in traumatic brain injury studies ( $r=0.74$ ,  $r=0.66$ ).<sup>199,211</sup> A recently published computational study modeled PbtO<sub>2</sub> changes in relation to changes in MAP and S<sub>a</sub>O<sub>2</sub> states that manipulation of a single physiological variable is often incapable of causing significant PbtO<sub>2</sub> changes due to the ability of the brain to autoregulate, however ischemia is predicted when two or more physiological derangements are present.<sup>207</sup> In our study, both MAP and S<sub>a</sub>O<sub>2</sub> were markedly altered, and could therefore result in ischemia.



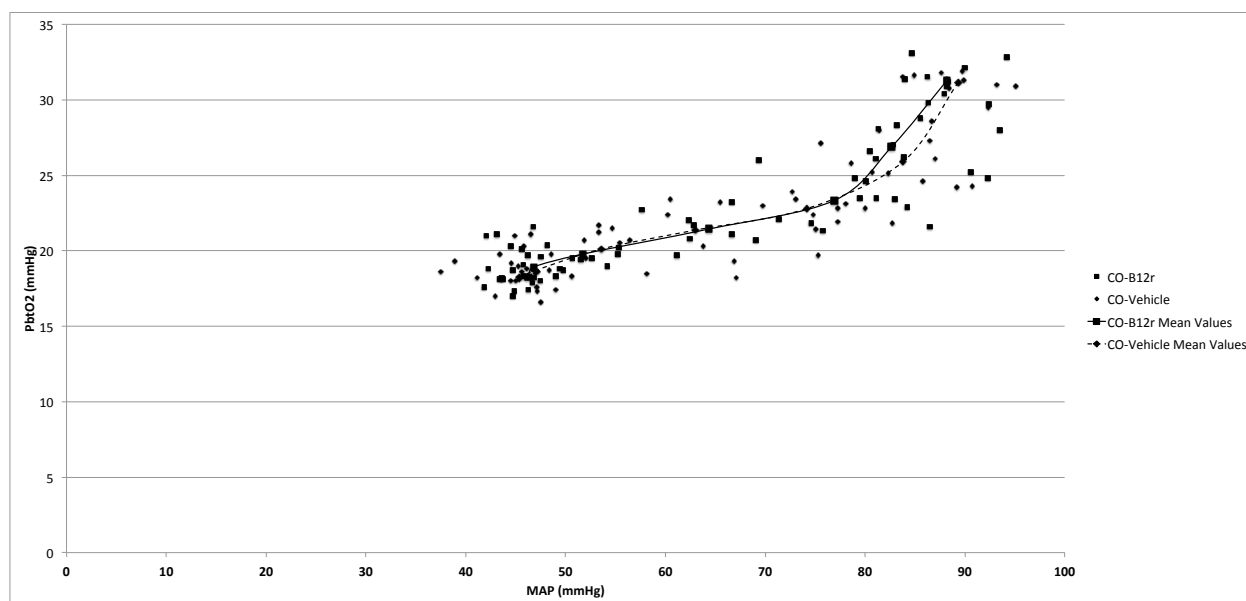


**Figure 15: Correlation of PbtO<sub>2</sub> and MAP During CO exposure.** Sigmoidal correlation of mean PbtO<sub>2</sub>/MAP during 30-minute CO exposure. Data presented as as mean PbtO<sub>2</sub>/MAP for each group (trend lines) with paired individual subject observations.

A swine study by Hemphill et al. evaluating  $P_{btO_2}$  changes associated with varying hemodynamic parameters corroborates our hypothesis that the decrease in MAP is at least partly responsible for the noted  $P_{btO_2}$  in this study. They reported a strong sigmoidal correlation ( $r^2=0.72$ ) of  $P_{btO_2}$  with MAP when MAP is between 60mmHg and 150mmHg (Figure 16). According to his data, MAP values of 50 correlated to  $P_{btO_2}$  values between 10-20mmHg, which is concurrent with our  $P_{btO_2}$  data set.<sup>212</sup> Given the striking similarities in data and the linear variability of  $P_{btO_2}$  with MAP, it can be reasonably hypothesized that autoregulatory capacity was lost and that hypotension was the significant contributing factor to our data.

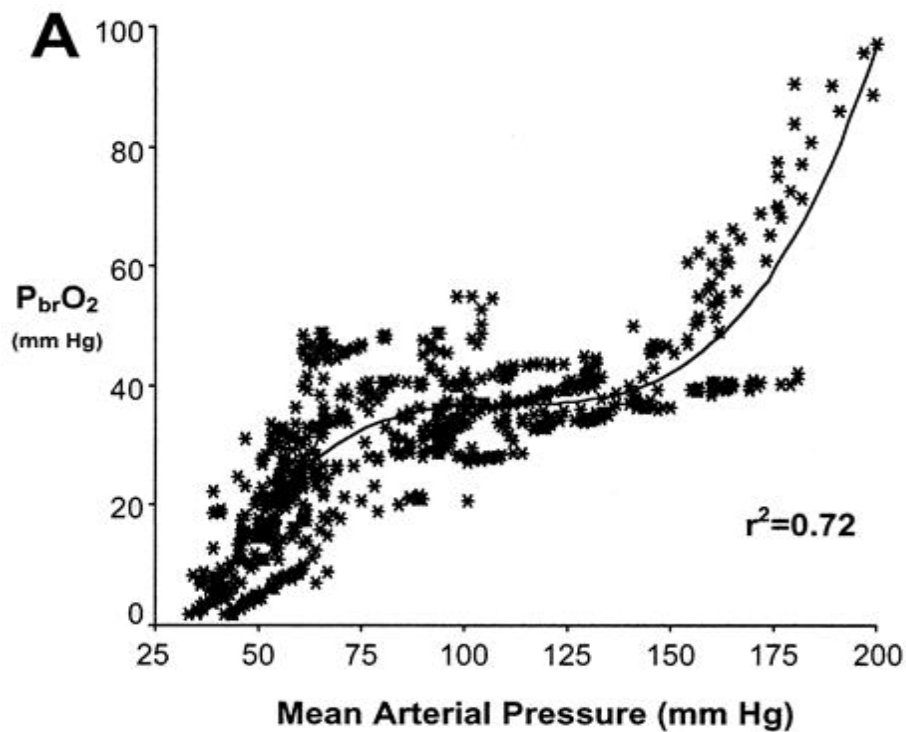


**Figure 16: Correlation of  $P_{btO_2}$  with MAP - Hemphill et al.** Adapted from “Carbon Dioxide Reactivity and Pressure Autoregulation of Brain Tissue” by Hemphill et al. *Neurosurgery* (2001). 48(2):377-383. Copyright Wolters Kluwer. Used with permission.

However, hypotension was not the only pathological variable and our PbtO<sub>2</sub> data demonstrated the greatest rate of decrease within the first 10 minutes of exposure when MAP appeared high enough to maintain autoregulation. Interpretation of this variance from published data requires consideration of the relationship between PbtO<sub>2</sub> to other physiological parameters. Multiple studies have demonstrated that PbtO<sub>2</sub> correlates highly with S<sub>ijv</sub>O<sub>2</sub> values ( $r^2=0.71, r^2=0.69$ ), which is a well-studied and understood indicator of cerebral oxygen delivery and consumption.<sup>199,213,214</sup> Decreases in S<sub>ijv</sub>O<sub>2</sub> correspond to an increase in oxygen uptake from capillaries, via an increase in cerebral metabolism or decrease in DO<sub>2</sub>, both of which result in a subsequent increase in OER, therefore causing decreased S<sub>ijv</sub>O<sub>2</sub>.<sup>215–217</sup> Multiple animal studies have reported decreased S<sub>ijv</sub>O<sub>2</sub> during CO poisoning, which was believed to be the result of a compensatory increase in OER.<sup>62,76,89</sup> It is therefore possible that the initial rate of PbtO<sub>2</sub> decrease seen in our data could reflect an increase in OER as a compensatory mechanism to CO. Our PbtO<sub>2</sub> data appear to decrease in an exponential fashion, and a simple exponential regression line gives  $r^2=0.87$  and  $r^2=0.83$  for CO-B12r and CO-Vehicle groups respectively. This exponential rate of decay could indicate approaching a steady-state equilibrium between O<sub>2</sub> delivery from poisoned blood and CMRO<sub>2</sub>. Even in the presence of a decrease in cerebral metabolism and increase in CBF, a 60% reduction in C<sub>a</sub>O<sub>2</sub> (approximately 60% COHb) could still require a compensatory OER increase, which would be recorded as a decrease in PbtO<sub>2</sub> as long as autoregulation is maintained. In order to confirm this, a detailed study on the cerebrovascular and PbtO<sub>2</sub> responses to CO poisoning would be required.

We must also take into account this study's greatest limitation and confounding variable: anesthesia. This procedure required general anesthesia, however measures were taken to ensure that minimal anesthesia was used while maintaining experimental consistency. All rats received 2.0% isoflurane balanced in 2500ppm CO in medical air or medical air during exposure and monitoring. This is approximately equivalent to 1.3 MAC.<sup>218</sup> Although widely used in our laboratory and in myriad veterinary practices, isoflurane is not without adverse effects. Isoflurane is vasoactive, and dose-dependent decreases in MAP are well documented with its use.<sup>219,220</sup> When given at 2.0 MAC it is known to cause autoregulation dysfunction.<sup>221,222</sup> Hoffman et al. reported that isoflurane does not affect autoregulation at 1.0 MAC.<sup>222</sup> Strebel et al. reported delayed autoregulatory function at 1.0 MAC and ablation of autoregulation at 1.5 MAC.<sup>221</sup> A study on canine hemodynamics under anesthesia reported a 20% decrease in Q at 1.1MAC (1.7%) and that this was dose dependent.<sup>223</sup> Recent anesthesia studies on rabbits and rats have both demonstrated that 2% isoflurane can also cause loss of autoregulation and decreases in PbtO<sub>2</sub>.<sup>224,225</sup> It was recognized in designing this experiment that using baseline anesthesia as a control to evaluate the additive effects of anesthesia and CO was an unavoidable necessity. We must then consider the potential additive effects of combining CO and isoflurane. Very little literature exists on the interactions between the two; the only relevant publishing found during a literature search was a case study on a perioperative CO poisoning case that did not provide any hemodynamic parameters.<sup>226</sup> Isoflurane is a substrate of sGC and can competitively inhibit CO at the active site, but the extent to which this happens is not known. But despite the lack of literature on clinical interactions of CO and isoflurane, it can be

reasonably inferred that exposing an isoflurane-anesthetized animal with potentially unstable cerebral hemodynamics to 2500ppm CO could cause rapid decompensation and total loss of autoregulation that would be reflected by a drop in PbtO<sub>2</sub>.

The possible impact of mitochondrial inhibition must also be considered. *In vitro* studies and *in vivo* studies on humans and rats have demonstrated significant reductions in CcO activity following acute CO poisoning.<sup>65,99,102,126</sup> The ability of O<sub>2</sub> to dissociate from hemoglobin and diffuse into tissue depends on the presence of an oxygen gradient between the capillary and surrounding tissue. The main driving force behind this gradient continuous reduction of O<sub>2</sub> to create ATP by mitochondria during oxidative phosphorylation.<sup>200</sup> If oxidative phosphorylation is uncoupled, the driving force for oxygen diffusion is reduced, resulting in an increase of PbtO<sub>2</sub>. This was recently demonstrated by Nielsen and colleagues using a swine model of cyanide poisoning, which is an inhibitor of oxidative phosphorylation.<sup>227</sup>

Regardless of the mechanisms, our data do indicate signs of global ischemia without the presence of hypoxia in CO-exposed rats. Lactic acid levels were significantly elevated in both CO-exposed groups after exposure, although pH remained unchanged (p<.0001). Normal blood pH during and following CO poisoning is well documented.<sup>76,80</sup> All CO-exposed rats demonstrated a hyperventilation response during CO poisoning that was noted by a significantly decreased RR and observed increase in TV (p<.001). Arterial blood gas analysis confirms that although RR decreased, MV must have increased substantially as pO<sub>2</sub> increased and pCO<sub>2</sub> decreased significantly (p<.05, p<.01, respectively). Significant decreases in HCO<sub>3</sub><sup>-</sup> were also seen (p<.001). Hyperventilation is a well known compensatory mechanism demonstrated during CO

poisoning.<sup>76,77,82</sup> Increases in MV via an increase in TV are characteristic of a central chemoreceptor-mediated response to cerebral acidosis. Although arterial pH was adequately compensated for by the hyperventilatory response-induced decrease in pCO<sub>2</sub> and HCO<sub>3</sub><sup>-</sup>, CSF pH was not measured and can differ widely from blood pH.<sup>76</sup>

## 4.2 Post-Exposure & Treatment

The most profound finding of this study is the significant rescuing effect of B12r on the noted decreases in PbtO<sub>2</sub> ( $p < .0001$  in comparison to CO-Vehicle rats). Previous *in vitro* studies by Roderique et al. and Somera et al. indicated that B12r was capable of reacting with Hb-bound CO and oxidizing it to CO<sub>2</sub>.<sup>191,193</sup> Unfortunately, the analytical methods available to our laboratory could not accurately quantify COHb in the presence of B12r. The Radiometer® ABL 800 blood analyzer used for ABG analyses determines %COHb using spectrophotoscopic methods, and the absorbance spectrum of hydroxocobalamin interferes with this analysis, therefore post-treatment %COHb readings were not deemed to be accurate.<sup>203,204</sup> However, the respiratory rate data does suggest that this mechanism might also be conserved *in vivo*.

The CO-B12r group exhibited a significantly decreased respiratory rate and Kussmaul-like pattern of TV for 25 minutes after treatment in comparison to sham-exposed groups, whereas the CO-Vehicle group was not statistically different from sham-exposed groups within 10 minutes of treatment, except for the noted difference at Time 50 ( $p < .05$ ). If B12r is truly oxidizing CO to CO<sub>2</sub>, this retained respiratory pattern could be a compensatory mechanism to offgas the produced CO<sub>2</sub>. However, no related increase in pCO<sub>2</sub> or other blood chemistry changes were noted in CO-B12r rats after treatment. The lack of significant differences in ABG parameters is clinically significant

as it highlights the safety of OHCbl and AA in high doses. It also indicates that B12r does not cause any substantial increases in  $p\text{CO}_2$  that could result in acidosis.

Both B12-r treated rats demonstrated significant MAP increases within 5-10 minutes after treatment ( $p<.0001$ , CO-Vehicle;  $p<.05$ , CO-B12r). Hydroxocobalamin is a powerful scavenger of the vasodilatory NO molecule and NOS inhibitor.<sup>183,184</sup> Removal of free NO from circulation and decreased NO production by NOS inhibition causes vasoconstriction, thus increasing blood pressure. This vasopressor response to OHCbl is well documented across species.<sup>185,187</sup> While the NO-scavenging mechanisms of B12r explain the transient MAP increase after treatment, our data indicate that this is not the mechanism behind the PbtO2 rescue.

Reanalysis of the correlation between PbtO2 and MAP post-treatment (Figure 17) yield two distinct patterns of recovery between the CO-B12r and CO-Vehicle groups. Ratio plots of both CO-exposed groups show long linear tails that correlate with published findings that PbtO2 varies directly with CBF, and therefore MAP, when autoregulation is compromised.<sup>212</sup> However, the opposing increases and decreases of the treatment group PbtO2/MAP ratios away from the original CO exposure trend line cannot be explained by blood pressure changes alone, given that PbtO2 varies in a sigmoidal fashion with MAP. Post-treatment CO-B12r PbtO2/MAP is shifted left from the exposure trend line and demonstrates a clear sigmoidal pattern of PbtO2 recovery in relation to MAP when  $\text{MAP}>70\text{mmHg}$ . CO-Vehicle post-treatment data shifted horizontally to the right from the exposure trend line and also showed a sharp  $\Delta\text{PbtO}_2/\Delta\text{MAP}$  increase with  $\text{MAP}>70\text{mmHg}$ . Based on the  $\Delta\text{PbtO}_2/\Delta\text{MAP}$  increase seen in both groups at  $\text{MAP}>70\text{mmHg}$  and published data on rat autoregulation, this

very likely indicates recovery of CBF autoregulation in both groups when MAP >70mmHg. Recovery of autoregulation would rapidly increase DO<sub>2</sub> and therefore theoretically associate with marked increases in the PbtO<sub>2</sub>/MAP ratio as PbtO<sub>2</sub> rises in relation to MAP before reaching a steady state plateau. Although CO-Vehicle group mean MAP at Time 50 was 76.2±6.2mmHg, a resurgent increase in PbtO<sub>2</sub> back to baseline levels was not seen. This, along with the shifts of the post-treatment PbtO<sub>2</sub>/MAP ratios are evidence that there are latent determinants of PbtO<sub>2</sub> that cannot be accounted for given the limited parameters measured during this study.

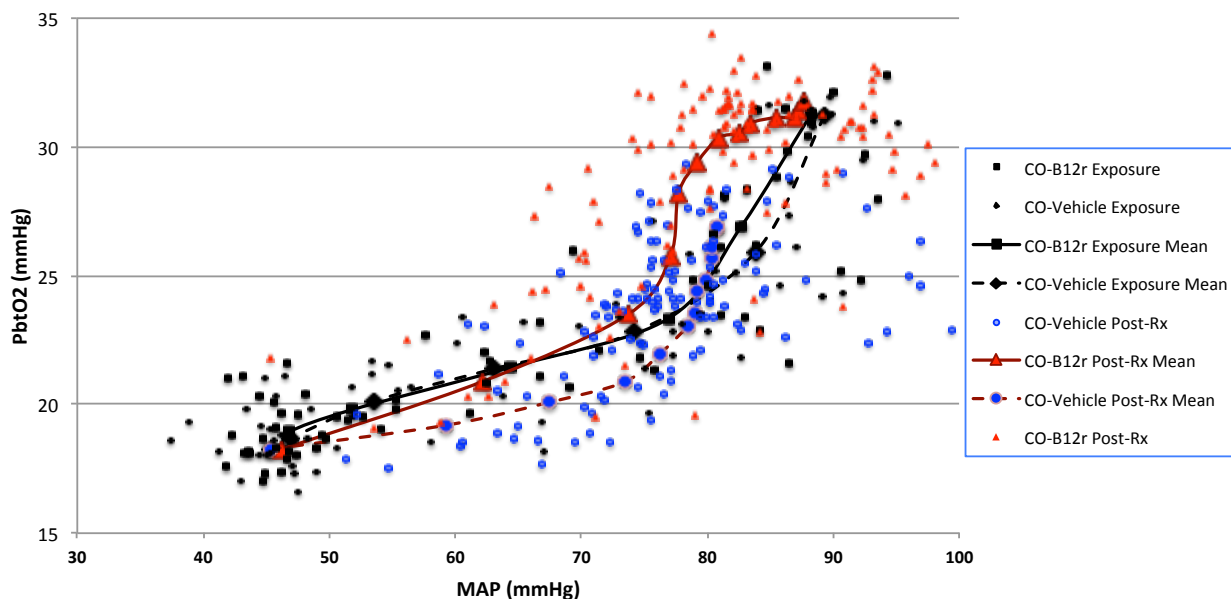


**Figure 17: Overlay of Pre- & Post-Treatment PbtO<sub>2</sub>/MAP.** CO-B12r (red) shifted to the left of the previous sigmoidal relation. CO-Vehicle (blue) PbtO<sub>2</sub>/MAP recovery was marked by a right shift of PbtO<sub>2</sub>/MAP and increased ratio at MAP >80mmHg.



Addition of PbtO<sub>2</sub>/MAP ratios from sham groups to the PbtO<sub>2</sub>/MAP ratio plot yields a more complete understanding of the overall of the relation between these two variables (Figure 18).

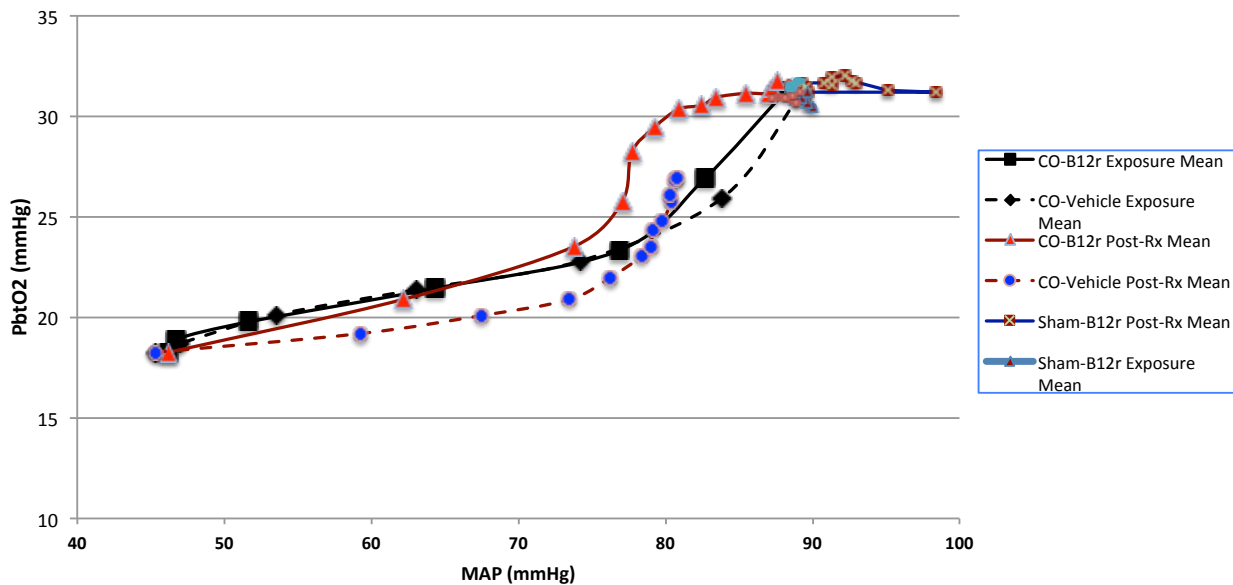


**Figure 18: Mean PbtO<sub>2</sub>/MAP for all Groups and Times.** The sigmoidal relationship between MAP and PbtO<sub>2</sub> is clearly demonstrated by junction of the Sham-B12r and CO-B12r ratio.

The junction of the Sham-B12r and CO-B12r PbtO<sub>2</sub>/MAP clearly, albeit somewhat unorthodoxly, shows the lower end of the sigmoidal PbtO<sub>2</sub>/MAP relationship. Despite the presence of a MAP great enough to sustain normal autoregulation, PbtO<sub>2</sub> remained decreased after CO exposure in CO-Vehicle rats.

Our data can only account for changes in PbtO<sub>2</sub> and MAP, and we cannot draw conclusions as to the states of other variables based on these. However, mechanistic inferences can be made based on basic physiological concepts. The decrease of the

CO-Vehicle PbtO<sub>2</sub>/MAP ratio may signify impaired cerebral oxygen delivery based on the simplified Fick principle  $DO_2 = CBF \times C_aO_2$ , where CBF is equal to the difference between MAP and intracranial pressure. If PbtO<sub>2</sub> is an indicator of cerebral perfusion, then we can alter that equation to  $PbtO_2 \sim MAP \times C_aO_2 = \frac{PbtO_2}{MAP} \sim C_aO_2$  and infer that the right shift and decrease in PbtO<sub>2</sub>/MAP ratio seen after CO exposure corresponds to decreased CaO<sub>2</sub>, possibly due to COHb hypoxia or continued cerebrovascular dysfunction. Decreases in CMRO<sub>2</sub> have also been described in multiple CO studies, which could also correlate to a sustained decrease in PbtO<sub>2</sub>.<sup>97</sup>

We could also boldly make the reverse assumption regarding the CO-B12r group. That is, a leftward shift of the PbtO<sub>2</sub>/MAP ratio could indicate increased CaO<sub>2</sub>. Assuming that the *in vitro* reactivity of B12r with COHb is conserved *in vivo*, we cannot rule out that B12r may have reacted with COHb without further animal studies. However, these inference are simple and do not take any other physiological parameters or the myriad pathological mechanisms of CO into account.

#### 4.3 Limitations & Sources of Error

The biggest confounding variable in this stud was the previously discussed and unavoidable anesthetic requirement and use of isoflurane. Given the current data on the cerebrovascular actions of 2% isoflurane and the compensatory CBF increase in CO poisoning that is capable of maintaining DO<sub>2</sub>, it is likely that the loss of autoregulated CBF indicated by was a product of the combined actions of the two gases and these data may prove difficult to replicate in awake subjects during future studies. The Licox® system itself is another possible source of human error. The sensitive tip on the CC1.R probe is 1mm long and is prone to fluctuations if moved a fraction of a millimeter after

equilibrating. Literature from Integra Neuroscience states that the Licox® system can deliver accurate readings within 2 minutes, however we opted for a 30-minute equilibration time to avoid artifact from any microtrauma caused during placement; it is possible that some of the PbtO<sub>2</sub> data was influenced by catheter insertion-related microtrauma despite careful surgical technique. The arterial blood gas analysis data from this study show stable lactate and pO<sub>2</sub> levels through the duration of the procedures and gives evidence of high quality surgical work. We were additionally limited in our inability to analyze blood for %COHb after B12r exposure.

#### **4.4 Future Directions**

The results of this study desperately warrant repetition, as this is the first documented evaluation of PbtO<sub>2</sub> in carbon monoxide poisoning and the first glimpse into the physiology of the potential antidote designed by Roderique et al.<sup>191</sup> The effects of CO poisoning are myriad, complex, and still poorly understood.<sup>11,46,48,62,89,97,99,101,125</sup> Future work with respect to this study should probe the interactions between PbtO<sub>2</sub>, cerebral hemodynamics, and cerebral blood flow that occur during acute CO exposure and following B12r administration using PbtO<sub>2</sub> electrodes in combination with S<sub>jv</sub>O<sub>2</sub> and arterial oximetry. An experimental design not confounded by anesthesia would be preferable, as isoflurane and other volatile inhaled anesthetics disrupt normal cerebrovascular coupling even at 1.0 MAC or below.<sup>220–222,225</sup> It would also be poignant to determine how PbtO<sub>2</sub> changes with varying concentrations and exposure times to CO. Given that there is no correlation between %COHb and prognosis, PbtO<sub>2</sub> could become a potential prognostic indicator for severe CO poisoning or serve as the

foundation for a standard set of criteria to determine severity of CO exposure based on correlated changes in PbtO<sub>2</sub>.<sup>35,46,48,129,131</sup>

One of the most pressing questions with respect to B12r is whether or not is truly is capable of reacting with COHb, which is deceptively simple to answer as typical spectrophotometric analytical techniques are invalidated by the presence of OHCbl.<sup>203,204</sup> Blood analysis via GC-MS is capable of analyzing %COHb in the presence of OHCbl.<sup>228–230</sup> If given access to suitable equipment, analysis of %COHb changes with or without B12r treatment in a small animal model would be a simple to perform.

#### **4.5 Summary**

Previous studies by Roderique et al. and Somera et al. have implicated a reduced form of hydroxocobalamin (B12r) as a potential therapy for acute CO poisoning. Based on their data, we aimed to characterize the acute effects of CO poisoning on brain tissue oxygen tension (PbtO<sub>2</sub>), mean arterial pressure (MAP), respiratory rate (RR), and arterial blood gas (ABG) chemistry. MAP was recorded continuously, PbtO<sub>2</sub> and RR recorded every 5 minutes, and ABG samples taken at baseline, post-exposure, and at two time points 20 and 60 minutes after treatment. PbtO<sub>2</sub> was monitored via an oxygen- sensitive Licox® Clark-type electrode placed into the primary somatosensory cortex of anesthetized rats using stereotaxic technique and exposed them to 2500ppm CO in medical air or medical air, both mixed with 2% isoflurane to maintain sedation. Additional parameters measured included MAP, respiratory rate, and serial blood gas analyses. Mean PbtO<sub>2</sub> decreased from 31.3±1.2mmHg to 18.3±1.0mmHg in the CO-B12r group (n=10) and from 31.2±0.7mmHg to 18.2±1.3mmHg in the CO-Vehicle group (n=10)(p<.0001). MAP

decreased significantly in both CO-exposed groups as well, from  $88.2 \pm 3.2$  mmHg to  $46.2 \pm 1.9$  mmHg in CO-B12r and from  $89.3 \pm 3.5$  mmHg to  $45.4 \pm 2.0$  mmHg in CO-Vehicle ( $p < .0001$ ). Exposure to CO was associated with a significant decrease in respiratory rate and observed increase in tidal volume. Significant compensated lactic acidosis was seen after CO exposure with mean lactate  $> 3$  mM in both CO-exposed groups ( $p < .001$ ). Both sham-exposed groups ( $n = 5$ ) did not demonstrate any significant parameter differences with any of the groups at baseline or during sham exposure to medical air.

Following 30 minute exposure protocol, rats were administered a randomly assigned treatment of 100mg/kg B12r (50mg OHCbl + 50mg AA/mL) or equivalent volume of normal saline and monitored for 60 minutes. Rats were then humanely euthanized.

Administration of B12r to CO-poisoned rats had a profound rescuing effect on the decrease in PbtO<sub>2</sub>; mean CO-B12r was significantly higher than the CO-Vehicle group within 5 minutes ( $p < .01$ ). A correlating and significant increase in MAP was seen as well ( $p < .05$ ). CO-B12r RR remained significantly below CO-Vehicle RR for 15 minutes after treatment ( $p < .05$ ). No significant differences were noted in ABG analysis between the two CO-exposed groups. Administration of B12r to sham-exposed rats caused a significant transient MAP increase as well.

#### **4.6 Conclusions**

We were able to successfully demonstrate and reproduce decreased PbtO<sub>2</sub> in the rat brain during exposure to CO. It is widely accepted that CO poisoning causes an immediate, NO-mediated increase in CBF, and that this is capable of maintaining DO<sub>2</sub> to the brain.<sup>89,95,98,104–107</sup> Our PbtO<sub>2</sub> data correlated highly to MAP in a sigmoidal

manner above 70mmHg and linearly below 70mmHg, which is consistent with the published relationship between PbtO<sub>2</sub> and MAP.<sup>212</sup> This relationship became linear when MAP dropped below 70mm, which is the approximate lower MAP limit of rat cerebral autoregulation, and is consistent with loss of cerebrovascular coupling.<sup>209,212</sup> Our findings suggest that the decrease in PbtO<sub>2</sub> seen during CO poisoning was mediated by loss of cerebral vasomotor tone and autoregulation. Isoflurane may have played a role in destabilizing CBF that was exacerbated by the NO/cGMP-mediated vasodilation of CO and resulted in vascular collapse.<sup>221,222,225</sup> However, the complex pathology of CO must also be considered, making it difficult to draw conclusions based on this one study. Our data warrant repetition in a more hemodynamically stable animal model.

Recovery of PbtO<sub>2</sub> showed two very unique trends between CO-B12r and CO-Vehicle groups characterized by rapid PbtO<sub>2</sub> recovery and respective increases and decreases of the PbtO<sub>2</sub>/MAP ratio. We believe that the NO-scavenging and inhibitory effects on NOS by B12r are partially responsible for this effect. However, blood pressure alone cannot explain the difference in PbtO<sub>2</sub> recovery trends as the CO-Vehicle MAP means were high enough to sustain autoregulation. It is possible that the difference in PbtO<sub>2</sub>/MAP ratio seen in the CO-Vehicle group was indicative of continued vascular dysfunction and/or COHb hypoxia. Although bold, we also postulate that the PbtO<sub>2</sub>/MAP increase associated with B12r administration could be the result of an increased arterial oxygen capacity as a result of B12r treatment and reaction with COHb. The only concrete conclusions that this author feels comfortable drawing are

that this study absolutely warrants further related work, and that like with any exciting study we are left with more questions than answers.

## Bibliography

1. Blumenthal, I. Carbon monoxide poisoning. *J. R. Soc. Med.* **94**, 270 (2001).
2. Sampling and Analytical Methods: Carbon Monoxide In Workplace Atmospheres (Direct-Reading Monitor), ID209. at  
<<https://www.osha.gov/dts/sltc/methods/inorganic/id209/id209.html>>
3. Man dies, dozens hospitalized after carbon monoxide leak at New York mall. *CNN* at  
<<http://www.cnn.com/2014/02/23/justice/new-york-carbon-monoxide-poisoning/index.html>>
4. Carbon monoxide--related deaths--United States, 1999-2004. *MMWR Morb. Mortal. Wkly. Rep.* **56**, 1309–1312 (2007).
5. Carbon Monoxide Exposures --- United States, 2000--2009. at  
<<http://www.cdc.gov/mmwr/preview/mmwrhtml/mm6030a2.htm>>
6. MMWR. Unintentional Non-Fire Related Carbon Monoxide Exposures - United States 2001-2003. at <<http://www.cdc.gov/mmwr/preview/mmwrhtml/mm5402a2.htm>>
7. Braubach, M. *et al.* Mortality associated with exposure to carbon monoxide in WHO European Member States. *Indoor Air* **23**, 115–125 (2013).
8. Hall, J. Fatal Effects of Fire. (2011). at  
<<http://www.nfpa.org/~media/Files/Research/NFPA%20reports/Overall%20Fire%20Statistics/osfataleffects.pdf>>
9. Alarie, Y. Toxicity of Fire Smoke. *Crit. Rev. Toxicol.* **32**, 259 (2002).
10. Raub, J. A., Mathieu-Nolf, M., Hampson, N. B. & Thom, S. R. Carbon monoxide poisoning — a public health perspective. *Toxicology* **145**, 1–14 (2000).
11. Omaye, S. T. Metabolic modulation of carbon monoxide toxicity. *Toxicology* **180**, 139–150 (2002).
12. Iqbal, S., Clower, J. H., Hernandez, S. A., Damon, S. A. & Yip, F. Y. A review of disaster-related carbon monoxide poisoning: surveillance, epidemiology, and opportunities for prevention. *Am. J. Public Health* **102**, 1957–1963 (2012).
13. Chen, B. C. *et al.* Carbon monoxide exposures in New York City following Hurricane Sandy in 2012. *Clin. Toxicol. Phila. Pa* **51**, 879–885 (2013).
14. Johnson-Arbor, K. K., Quental, A. S. & Li, D. A Comparison of Carbon Monoxide Exposures After Snowstorms and Power Outages. *Am. J. Prev. Med.* **46**, 481–486 (2014).
15. Goldman, A., Eggen, B., Golding, B. & Murray, V. The health impacts of windstorms: a systematic literature review. *Public Health* **128**, 3–28 (2014).
16. Scott, T. & Theresa, F. Assessing carbon monoxide poisoning. *Emerg. Nurse J. RCN Accid. Emerg. Nurs. Assoc.* **20**, 14–19 (2013).
17. Zhang, J. *et al.* Carbon monoxide from cookstoves in developing countries: 1. Emission factors. *Chemosphere - Glob. Change Sci.* **1**, 353–366 (1999).
18. Mohankumar, T. S. *et al.* Gas geyser – A cause of fatal domestic carbon monoxide poisoning. *J. Forensic Leg. Med.* **19**, 490–493 (2012).
19. Sharma, S., Gupta, R., Paul, B. S., Puri, S. & Garg, S. Accidental carbon monoxide poisoning in our homes. *Indian J. Crit. Care Med. Peer-Rev. Off. Publ. Indian Soc. Crit. Care Med.* **13**, 169–170 (2009).
20. Hampson, N. B. & Bodwin, D. Toxic CO-ingestions in Intentional Carbon Monoxide Poisoning. *J. Emerg. Med.* **44**, 625–630 (2013).



21. Peiris-John, R., Kool, B. & Ameratunga, S. Fatalities and hospitalisations due to acute poisoning among New Zealand adults. *Intern. Med. J.* **44**, 273–281 (2014).
22. Prahlow, J. A. & Doyle, B. W. A suicide using a homemade carbon monoxide 'death machine'. *Am. J. Forensic Med. Pathol.* **26**, 177–180 (2005).
23. Patel, F. Carbon copy deaths: Carbon monoxide gas chamber. *J. Forensic Leg. Med.* **15**, 398–401 (2008).
24. Salameh, S., Amitai, Y., Antopolsky, M., Rott, D. & Stalnicowicz, R. Carbon monoxide poisoning in Jerusalem: epidemiology and risk factors. *Clin. Toxicol. Phila. Pa* **47**, 137–141 (2009).
25. Chung, W. S. D. & Leung, C. M. Carbon Monoxide Poisoning as a New Method of Suicide in Hong Kong. *Psychiatr. Serv.* **52**, 836–837 (2001).
26. Oström, M., Thorson, J. & Eriksson, A. Carbon monoxide suicide from car exhausts. *Soc. Sci. Med.* **1982** **42**, 447–451 (1996).
27. Chou, C.-H., Lai, C.-H., Liou, S.-H. & Loh, C.-H. Carbon monoxide: An old poison with a new way of poisoning. *J. Formos. Med. Assoc.* **111**, 452–455 (2012).
28. Lee, D. T. S., Chan, K. P. M. & Yip, P. S. F. Charcoal burning is also popular for suicide pacts made on the internet. *BMJ* **330**, 602 (2005).
29. Skopek, M. A. & Perkins, R. Deliberate exposure to motor vehicle exhaust gas: the psychosocial profile of attempted suicide. *Aust. N. Z. J. Psychiatry* **32**, 830–838 (1998).
30. Thomsen, A. H. & Gregersen, M. Suicide by carbon monoxide from car exhaust-gas in Denmark 1995-1999. *Forensic Sci. Int.* **161**, 41–46 (2006).
31. Pan, Y.-J., Liao, S.-C. & Lee, M.-B. Suicide by charcoal burning in Taiwan, 1995–2006. *J. Affect. Disord.* **120**, 254–257 (2010).
32. Wirth, I. & Strauch, H. [Suicides in East Berlin from 1980 to 1989]. *Arch. Für Kriminol.* **219**, 73–88 (2007).
33. Chen, Y.-Y., Yip, P. S., Lee, C. K., Gunnell, D. & Wu, K. C.-C. The diffusion of a new method of suicide: charcoal-burning suicide in Hong Kong and Taiwan. *Soc. Psychiatry Psychiatr. Epidemiol.* 1–10 (2014). doi:10.1007/s00127-014-0910-4
34. Vossberg, B. & Skolnick, J. The role of catalytic converters in automobile carbon monoxide poisoning\*: A case report. *CHEST J.* **115**, 580–581 (1999).
35. Hampson, N. B. INTentional carbon monoxide poisoning. *CHEST J.* **116**, 586–587 (1999).
36. Hunt, J. How to Kill Yourself Using the Inhalation of Carbon Monoxide Gas. at <<http://www.jerryhunt.org/kill.htm>>
37. Ideas On Easiest & Most Reliably Successful Methods Of Suicide? - Find Answers to this Question. *Exp. Proj.* at <<http://www.experienceproject.com/question-answer/Ideas-On-Easiest--Most-Reliably-Successful-Methods-Of-Suicide/671842>>
38. Leung, C. M., Chung, W. S. D. & So, E. P. M. Burning charcoal: an indigenous method of committing suicide in Hong Kong. *J. Clin. Psychiatry* **63**, 447–450 (2002).
39. Naito, A. Internet suicide in Japan: implications for child and adolescent mental health. *Clin. Child Psychol. Psychiatry* **12**, 583–597 (2007).
40. Douglas, C. G., Haldane, J. S. & Haldane, J. B. The laws of combination of haemoglobin with carbon monoxide and oxygen. *J. Physiol.* **44**, 275–304 (1912).
41. Haldane, J. The Action of Carbonic Oxide on Man. *J. Physiol.* **18**, 430–462 (1895).

42. Lippi, G., Rastelli, G., Meschi, T., Borghi, L. & Cervellin, G. Pathophysiology, clinics, diagnosis and treatment of heart involvement in carbon monoxide poisoning. *Clin. Biochem.* **45**, 1278–1285 (2012).
43. Fisher, J. A., Iscoe, S., Fedorko, L. & Duffin, J. Rapid elimination of CO through the lungs: coming full circle 100 years on. *Exp. Physiol.* **96**, 1262–1269 (2011).
44. Prockop, L. D. & Chichkova, R. I. Carbon monoxide intoxication: an updated review. *J. Neurol. Sci.* **262**, 122–130 (2007).
45. Goldstein, M. Carbon Monoxide Poisoning. *J. Emerg. Nurs.* **34**, 538–542 (2008).
46. Gorman, D., Drewry, A., Huang, Y. L. & Sames, C. The clinical toxicology of carbon monoxide. *Toxicology* **187**, 25–38 (2003).
47. Ernst, A. & Zibrak, J. D. Carbon monoxide poisoning. *N. Engl. J. Med.* **339**, 1603–1608 (1998).
48. Guzman, J. A. Carbon Monoxide Poisoning. *Crit. Care Clin.* **28**, 537–548 (2012).
49. Jeong Mi, M., Min Ho, S. & Byeong Jo, C. The value of initial lactate in patients with carbon monoxide intoxication: in the emergency department. *Hum. Exp. Toxicol.* **30**, 836–843 (2011).
50. Hampson, N. B., Dunn, S. L. & UHMCS/CDC CO Poisoning Surveillance Group. Symptoms of carbon monoxide poisoning do not correlate with the initial carboxyhemoglobin level. *Undersea Hyperb. Med. J. Undersea Hyperb. Med. Soc. Inc* **39**, 657–665 (2012).
51. Haldane, J. B. S. Carbon Monoxide as a Tissue Poison. *Biochem. J.* **21**, 1068–1075 (1927).
52. Satran, D. *et al.* Cardiovascular manifestations of moderate to severe carbon monoxide poisoning. *J. Am. Coll. Cardiol.* **45**, 1513–1516 (2005).
53. Rochette, L., Cottin, Y., Zeller, M. & Vergely, C. Carbon monoxide: Mechanisms of action and potential clinical implications. *Pharmacol. Ther.* **137**, 133–152 (2013).
54. Leffler, C. W., Parfenova, H. & Jaggar, J. H. Carbon monoxide as an endogenous vascular modulator. *Am. J. Physiol. - Heart Circ. Physiol.* **301**, H1–H11 (2011).
55. Alshehri, A. *et al.* Mechanisms of the vasorelaxing effects of CORM-3, a water-soluble carbon monoxide-releasing molecule: interactions with eNOS. *Naunyn. Schmiedeberg's Arch. Pharmacol.* **386**, 185–196 (2013).
56. Dubuis, E., Potier, M., Wang, R. & Vandier, C. Continuous inhalation of carbon monoxide attenuates hypoxic pulmonary hypertension development presumably through activation of BKCa channels. *Cardiovasc. Res.* **65**, 751–761 (2005).
57. Hou, S., Heinemann, S. H. & Hoshi, T. Modulation of BKCa Channel Gating by Endogenous Signaling Molecules. *Physiology* **24**, 26–35 (2009).
58. Garg, J. *et al.* Cardiovascular Abnormalities in Carbon Monoxide Poisoning. *Am. J. Ther.* (2014). doi:10.1097/MJT.0000000000000016
59. Gandini, C. *et al.* Carbon Monoxide Cardiotoxicity. *Clin. Toxicol.* **39**, 35–44 (2001).
60. Henry, T. D., Lesser, J. R. & Satran, D. Myocardial Fibrosis From Severe Carbon Monoxide Poisoning Detected by Cardiac Magnetic Resonance Imaging. *Circulation* **118**, 792–792 (2008).

61. Fracasso, T. *et al.* Immunohistochemical expression of fibronectin and C5b-9 in the myocardium in cases of carbon monoxide poisoning. *Int. J. Legal Med.* **125**, 377–384 (2011).
62. Smithline, H. A., Ward, K. R., Chiulli, D. A., Blake, H. C. & Rivers, E. P. Whole body oxygen consumption and critical oxygen delivery in response to prolonged and severe carbon monoxide poisoning. *Resuscitation* **56**, 97–104 (2003).
63. Kleinert, H. D., Scales, J. L. & Weiss, H. R. Effects of carbon monoxide or low oxygen gas mixture inhalation on regional oxygenation, blood flow, and small vessel blood content of the rabbit heart. *Pflüg. Arch.* **383**, 105–111 (1980).
64. Stearns, W. H., Drinker, C. K. & Shaughnessy, T. J. The electrocardiographic changes found in 22 cases of carbon monoxide (illuminating gas) poisoning. *Am. Heart J.* **15**, 434–447 (1938).
65. Alonso, J.-R., Cardellach, F., López, S., Casademont, J. & Miró, Ò. Carbon Monoxide Specifically Inhibits Cytochrome C Oxidase of Human Mitochondrial Respiratory Chain. *Pharmacol. Toxicol.* **93**, 142–146 (2003).
66. Brown, S. D. & Piantadosi, C. A. In vivo binding of carbon monoxide to cytochrome c oxidase in rat brain. *J. Appl. Physiol.* **68**, 604–610 (1990).
67. Patel, A. P., John Moody, A., Handy, R. D. & Robert Sneyd, J. Carbon monoxide exposure in rat heart: glutathione depletion is prevented by antioxidants. *Biochem. Biophys. Res. Commun.* **302**, 392–396 (2003).
68. Thom, S. R., Kang, M., Fisher, D. & Ischiropoulos, H. Release of glutathione from erythrocytes and other markers of oxidative stress in carbon monoxide poisoning. *J. Appl. Physiol. Bethesda Md 1985* **82**, 1424–1432 (1997).
69. Thom, S. R., Fisher, D., Xu, Y. A., Notarfrancesco, K. & Ischiropoulos, H. Adaptive responses and apoptosis in endothelial cells exposed to carbon monoxide. *Proc. Natl. Acad. Sci. U. S. A.* **97**, 1305–1310 (2000).
70. Peers, C. & Steele, D. S. Carbon monoxide: A vital signalling molecule and potent toxin in the myocardium. *J. Mol. Cell. Cardiol.* **52**, 359–365 (2012).
71. André, L. *et al.* Carbon monoxide exposure enhances arrhythmia after cardiac stress: involvement of oxidative stress. *Basic Res. Cardiol.* **106**, 1235–1246 (2011).
72. Cetin, M. *et al.* A case of carbon monoxide poisoning presenting with supraventricular tachycardia. *Intern. Med. Tokyo Jpn.* **50**, 2607–2609 (2011).
73. Gürkan, Y., Canatay, H., Toprak, A., Ural, E. & Toker, K. Carbon monoxide poisoning - a cause of increased QT dispersion. *Acta Anaesthesiol. Scand.* **46**, 180–183 (2002).
74. Dallas, M. L. *et al.* Carbon Monoxide Induces Cardiac Arrhythmia via Induction of the Late Na<sup>+</sup> Current. *Am. J. Respir. Crit. Care Med.* **186**, 648–656 (2012).
75. Elies, J. *et al.* Inhibition of the Cardiac Na<sup>+</sup> Channel Nav1.5 by Carbon Monoxide. *J. Biol. Chem.* **289**, 16421–16429 (2014).
76. Doblar, D. D., Santiago, T. V. & Edelman, N. H. Correlation between ventilatory and cerebrovascular responses to inhalation of CO. *J. Appl. Physiol.* **43**, 455–462 (1977).
77. Santiago, T. V. & Edelman, N. H. Mechanism of the ventilatory response to carbon monoxide. *J. Clin. Invest.* **57**, 977–986 (1976).
78. Stuhmiller, J. H. & Stuhmiller, L. M. A mathematical model of ventilation response to inhaled carbon monoxide. *J. Appl. Physiol.* **98**, 2033–2044 (2005).

79. Kolarzyk, E. Regulation of breathing in cases of acute carbon monoxide poisoning. *Int. J. Occup. Med. Environ. Health* **8**, 89–101 (1995).
80. Davies, D. G. & McGrath, J. J. Arterial blood gas status in rats exposed to chronic CO at low and high altitude. *Respir. Physiol.* **75**, 193–198 (1989).
81. King, C. E., Cain, S. M. & Chapler, C. K. The role aortic chemoreceptors during severe CO hypoxia. *Can. J. Physiol. Pharmacol.* **63**, 509–514 (1985).
82. Gautier, H., Murariu, C. & Bonora, M. Ventilatory and metabolic responses to ambient hypoxia or hypercapnia in rats exposed to CO hypoxia. *J. Appl. Physiol.* **83**, 253–261 (1997).
83. Choi, I. S. Carbon monoxide poisoning: systemic manifestations and complications. *J. Korean Med. Sci.* **16**, 253–261 (2001).
84. Naeije, D. R., Peretz, A. & Cornil, A. Acute pulmonary edema following carbon monoxide poisoning. *Intensive Care Med.* **6**, 189–191 (1980).
85. Fein, A., Grossman, R. F., Jones, J. G., Hoeffel, J. & McKay, D. Carbon monoxide effect on alveolar epithelial permeability. *CHEST J.* **78**, 726–731 (1980).
86. Akilli, N. B. *et al.* A new marker for myocardial injury in carbon monoxide poisoning: T peak-T end. *Am. J. Emerg. Med.* **31**, 1651–1655 (2013).
87. Sinha, A. K., Klein, J., Schultze, P., Weiss, J. & Weiss, H. R. Cerebral regional capillary perfusion and blood flow after carbon monoxide exposure. *J. Appl. Physiol.* **71**, 1196–1200 (1991).
88. Lebby, T. I., Zalenski, R., Hryhorczuk, D. O. & Leikin, J. B. The usefulness of the arterial blood gas in pure carbon monoxide poisoning. *Vet. Hum. Toxicol.* **31**, 138–140 (1989).
89. Langston, P., Gorman, D., Runciman, W. & Upton, R. The effect of carbon monoxide on oxygen metabolism in the brains of awake sheep. *Toxicology* **114**, 223–232 (1996).
90. Myers, R. A. & Britten, J. S. Are arterial blood gases of value in treatment decisions for carbon monoxide poisoning? *Crit. Care Med.* **17**, 139–142 (1989).
91. Sutariya, B. B., Penney, D. G., Dunbar, J. C. & Swanson, C. J. Blood lactate and catecholamine levels in the carbon monoxide-exposed rat: the response to elevated glucose. *Toxicology* **73**, 169–178 (1992).
92. Fozo, M. S. & Penney, D. G. Dibromomethane and carbon monoxide in the rat: comparison of the cardiovascular and metabolic effects. *J. Appl. Toxicol. JAT* **13**, 147–151 (1993).
93. Åberg, A.-M., Hultin, M., Abrahamsson, P. & Larsson, J. E. Circulatory effects and kinetics following acute administration of carbon monoxide in a porcine model. *Life Sci.* **75**, 1029–1039 (2004).
94. Inoue, S. *et al.* Lactate as a prognostic factor in carbon monoxide poisoning: a case report. *Am. J. Emerg. Med.* **26**, 966.e1–3 (2008).
95. Mayevsky, A., Meilin, S., Rogatsky, G. G., Zarchin, N. & Thom, S. R. Multiparametric monitoring of the awake brain exposed to carbon monoxide. *J. Appl. Physiol.* **78**, 1188–1196 (1995).
96. Safar, P. Resuscitation from clinical death: pathophysiologic limits and therapeutic potentials. *Crit. Care Med.* **16**, 923–941 (1988).
97. Raub, J. A. & Benignus, V. A. Carbon monoxide and the nervous system. *Neurosci. Biobehav. Rev.* **26**, 925–940 (2002).

98. Mendelman, A., Zarchin, N., Rifkind, J. & Mayevsky, A. Brain multiparametric responses to carbon monoxide exposure in the aging rat. *Brain Res.* **867**, 217–222 (2000).
99. Miró, Ò., Casademont, J., Barrientos, A., Urbano-Márquez, Á. & Cardellach, F. Mitochondrial Cytochrome c Oxidase Inhibition during Acute Carbon Monoxide Poisoning. *Pharmacol. Toxicol.* **82**, 199–202 (1998).
100. Choi, Y. K., Por, E. D., Kwon, Y.-G. & Kim, Y.-M. Regulation of ROS Production and Vascular Function by Carbon Monoxide. *Oxid. Med. Cell. Longev.* **2012**, e794237 (2012).
101. GARRABOU, G. *et al.* Mitochondrial Injury in Human Acute Carbon Monoxide Poisoning: The Effect of Oxygen Treatment. *J. Environ. Sci. Health Part C* **29**, 32–51 (2011).
102. Lee, H. M., Hallberg, L. M., Greeley, G. H. & Englander, E. W. Differential inhibition of mitochondrial respiratory complexes by inhalation of combustion smoke and carbon monoxide, in vivo, in the rat brain. *Inhal. Toxicol.* **22**, 770–777 (2010).
103. Piantadosi, C. A. Carbon monoxide, reactive oxygen signaling, and oxidative stress. *Free Radic. Biol. Med.* **45**, 562–569 (2008).
104. Meyer-Witting, M., Helps, S. & Gorman, D. F. Acute carbon monoxide exposure and cerebral blood flow in rabbits. *Anaesth. Intensive Care* **19**, 373–377 (1991).
105. Lu, Y.-Y., Tsai, S.-C., Kao, C.-H. & Lin, W.-Y. Regional cerebral blood flow in patients with carbon monoxide intoxication. *Ann. Nucl. Med.* **26**, 771–776 (2012).
106. MacMillan, V. Regional cerebral blood flow of the rat in acute carbon monoxide intoxication. *Can. J. Physiol. Pharmacol.* **53**, 644–650 (1975).
107. Okeda, R. *et al.* Regional cerebral blood flow of acute carbon monoxide poisoning in cats. *Acta Neuropathol. (Berl.)* **72**, 389–393 (1987).
108. Sinha, A. K., Klein, J., Schultze, P., Weiss, J. & Weiss, H. R. Cerebral regional capillary perfusion and blood flow after carbon monoxide exposure. *J. Appl. Physiol.* **71**, 1196–1200 (1991).
109. Koehler, R., Jones, M. D. & Traystman, R. J. Cerebral circulatory response to carbon monoxide and hypoxic hypoxia in the lamb. *Heart Circ Physiol* **12**, 27–32 (1982).
110. Koehler, R., Traystman, R. J. & Jones, M. D. Role of O<sub>2</sub>-hemoglobin affinity on cerebrovascular response to carbon monoxide hypoxia. *Am. J. Physiol. - Heart Circ. Physiol.* **14**, 1019–1023 (1983).
111. Ludbrook, G. L., Helps, S., Gorman, D. F. & Reilly, P. L. The relative effects of hypoxia and carbon monoxide on brain function in rabbits. *Toxicology* **75**, 71–80 (1992).
112. Ingi, T., Cheng, J. & Ronnett, G. V. Carbon Monoxide: An Endogenous Modulator of the Nitric Oxide–Cyclic GMP Signaling System. *Neuron* **16**, 835–842 (1996).
113. Thom, S. R. *et al.* Neuronal nitric oxide synthase and N-methyl-d-aspartate neurons in experimental carbon monoxide poisoning. *Toxicol. Appl. Pharmacol.* **194**, 280–295 (2004).
114. Meilin, S. *et al.* Effects of carbon monoxide on the brain may be mediated by nitric oxide. *J. Appl. Physiol.* **81**, 1078–1083 (1996).

115. Thom, S. R., Bhopale, V. M. & Fisher, D. Hyperbaric oxygen reduces delayed immune-mediated neuropathology in experimental carbon monoxide toxicity. *Toxicol. Appl. Pharmacol.* **213**, 152–159 (2006).
116. Shprecher, D. & Mehta, L. The syndrome of delayed post-hypoxic leukoencephalopathy. *NeuroRehabilitation* **26**, 65–72 (2010).
117. Thom, S. R., Bhopale, V. M., Fisher, D., Zhang, J. & Gimotty, P. Delayed neuropathology after carbon monoxide poisoning is immune-mediated. *Proc. Natl. Acad. Sci. U. S. A.* **101**, 13660–13665 (2004).
118. Piantadosi, C. A., Zhang, J., Levin, E. D., Folz, R. J. & Schmechel, D. E. Apoptosis and Delayed Neuronal Damage after Carbon Monoxide Poisoning in the Rat. *Exp. Neurol.* **147**, 103–114 (1997).
119. Jalukar, V., Penney, D. G., Crowley, M. & Simpson, N. Magnetic resonance imaging of the rat brain following acute carbon monoxide poisoning. *J. Appl. Toxicol.* **12**, 407–414 (1992).
120. Martindale, J. L. Imaging Abnormalities Associated with Carbon Monoxide Toxicity. *J. Emerg. Med.* (2013). doi:10.1016/j.jemermed.2012.07.069
121. Md, N. K. *et al.* The utility of MRI in acute stage of carbon monoxide poisoning. *Intensive Care Med.* **18**, 371–372 (1992).
122. Gotoh, M. *et al.* Sequential changes in mr images of the brain in acute carbon monoxide poisoning. *Comput. Med. Imaging Graph.* **17**, 55–59 (1993).
123. O'Donnell, P., Buxton, P. J., Pitkin, A. & Jarvis, L. J. The magnetic resonance imaging appearances of the brain in acute carbon monoxide poisoning. *Clin. Radiol.* **55**, 273–280 (2000).
124. Wang, P. *et al.* Lipid Peroxidation was Involved in the Memory Impairment of Carbon Monoxide-induced Delayed Neuron Damage. *Neurochem. Res.* **34**, 1293–1298 (2009).
125. Thom, S. R. Carbon monoxide-mediated brain lipid peroxidation in the rat. *J. Appl. Physiol.* **68**, 997–1003 (1990).
126. Taskiran, D., Nesil, T. & Alkan, K. Mitochondrial oxidative stress in female and male rat brain after ex vivo carbon monoxide treatment. *Hum. Exp. Toxicol.* **26**, 645–651 (2007).
127. Hampson, N. B., Piantadosi, C. A., Thom, S. R. & Weaver, L. K. Practice recommendations in the diagnosis, management, and prevention of carbon monoxide poisoning. *Am. J. Respir. Crit. Care Med.* **186**, 1095–1101 (2012).
128. Weaver, L. K., Valentine, K. J. & Hopkins, R. O. Carbon monoxide poisoning: risk factors for cognitive sequelae and the role of hyperbaric oxygen. *Am. J. Respir. Crit. Care Med.* **176**, 491–497 (2007).
129. Nikkanen, H. & Skolnik, A. Diagnosis and management of carbon monoxide poisoning in the emergency department. *Emerg. Med. Pract.* **13**, 1–14; quiz 14 (2011).
130. Ilano, A. L. & Raffin, T. A. Management of carbon monoxide poisoning. *CHEST J.* **97**, 165–169 (1990).
131. Gorman, D. F., Clayton, D., Gilligan, J. E. & Webb, R. K. A longitudinal study of 100 consecutive admissions for carbon monoxide poisoning to the Royal Adelaide Hospital. *Anaesth. Intensive Care* **20**, 311–316 (1992).

132. Simini, B. Cherry-red discolouration in carbon monoxide poisoning. *The Lancet* **352**, 1154 (1998).
133. Hoppe, D. F. Ueber die Einwirkung des Kohlenoxydgases auf das Hämatoglobulin. *Arch. Für Pathol. Anat. Physiol. Für Klin. Med.* **11**, 288–289 (1857).
134. Findlay, G. H. Carbon monoxide poisoning: Optics and histology of skin and blood. *Br. J. Dermatol.* **119**, 45–51 (1988).
135. SKORODIN, M. S. Carbon Monoxide Poisoning Presenting as Hyperventilation Syndrome. *Ann. Intern. Med.* **105**, 632–632 (1986).
136. Roth, D. *et al.* Unrecognized carbon monoxide poisoning leads to a multiple-casualty incident. *J. Emerg. Med.* **45**, 559–561 (2013).
137. Nilson, D., Partridge, R., Suner, S. & Jay, G. Non-invasive carboxyhemoglobin monitoring: screening emergency medical services patients for carbon monoxide exposure. *Prehospital Disaster Med.* **25**, 253–256 (2010).
138. Jaslow, D., Ufberg, J., Ukasik, J. & Sananman, P. Routine carbon monoxide screening by emergency medical technicians. *Acad. Emerg. Med. Off. J. Soc. Acad. Emerg. Med.* **8**, 288–291 (2001).
139. Cone, D. C. *et al.* Noninvasive fireground assessment of carboxyhemoglobin levels in firefighters. *Prehospital Emerg. Care Off. J. Natl. Assoc. EMS Physicians Natl. Assoc. State EMS Dir.* **9**, 8–13 (2005).
140. Weaver, L. K. Carbon Monoxide Poisoning. *N. Engl. J. Med.* **360**, 1217–1225 (2009).
141. Hajsadeghi, S., Tavakkoli, N., Jafarian Kerman, S. R., Shahabadi, A. & Khojandi, M. Electrocardiographic findings and serum troponin I in carbon monoxide poisoned patients. *Acta Med. Iran.* **50**, 185–191 (2012).
142. Shimazu, T. *et al.* Half-life of blood carboxyhemoglobin after short-term and long-term exposure to carbon monoxide. *J. Trauma* **49**, 126–131 (2000).
143. Shimazu, T. Half-life of blood carboxyhemoglobin. *Chest* **119**, 661–663 (2001).
144. Hardy, K. R. & Thom, S. R. Pathophysiology and treatment of carbon monoxide poisoning. *J. Toxicol. Clin. Toxicol.* **32**, 613–629 (1994).
145. National EMS Education Standards. *Natl. Highw. Transit Saf. Auth.* (2010). at <<http://www.ems.gov/educationstandards.htm>>
146. Stripe, S. C. & Susman, J. A rural-urban comparison of prehospital emergency medical services in Nebraska. *J. Am. Board Fam. Pract. Am. Board Fam. Pract.* **4**, 313–318 (1991).
147. Gonzalez, R. P., Cummings, G. R., Harlan, S. M., Mulekar, M. S. & Rodning, C. B. EMS relocation in a rural area using a geographic information system can improve response time to motor vehicle crashes. *J. Trauma* **71**, 1023–1026 (2011).
148. Gonzalez, R. P., Cummings, G. R., Phelan, H. A., Mulekar, M. S. & Rodning, C. B. Does increased emergency medical services prehospital time affect patient mortality in rural motor vehicle crashes? A statewide analysis. *Am. J. Surg.* **197**, 30–34 (2009).
149. Al-Moamary, M. S. *et al.* Complications of carbon monoxide poisoning. *Saudi Med. J.* **21**, 361–363 (2000).
150. Rosenthal, L. D. B. Carbon Monoxide Poisoning: Immediate diagnosis and treatment are crucial to avoid complications. *J. Nurs. March 2006* **106**, 40–46 (2006).

151. Sluijter, M. E. THE TREATMENT OF CARBON MONOXIDE POISONING BY THE ADMINISTRATION OF OXYGEN AT HIGH ATMOSPHERIC PRESSURE. *Proc. R. Soc. Med.* **56**, 1002–1008 (1963).
152. Adamiec, L., Kamiński, B., Kwiatkowski, H., Sabiniewicz, W. & Zawadzki, A. Hyperbaric oxygen in treatment of acute carbon monoxide poisoning. *Anaesth. Resusc. Intensive Ther.* **3**, 305–313 (1975).
153. Hampson, N. B., Mathieu, D., Piantadosi, C. A., Thom, S. R. & Weaver, L. K. Carbon monoxide poisoning: interpretation of randomized clinical trials and unresolved treatment issues. *Undersea Hyperb. Med. J. Undersea Hyperb. Med. Soc. Inc* **28**, 157–164 (2001).
154. Weaver, L. K. *et al.* Hyperbaric Oxygen for Acute Carbon Monoxide Poisoning. *N. Engl. J. Med.* **347**, 1057–1067 (2002).
155. Byrne, B. T., Lu, J. J., Valento, M. & Bryant, S. M. Variability in hyperbaric oxygen treatment for acute carbon monoxide poisoning. *Undersea Hyperb. Med. J. Undersea Hyperb. Med. Soc. Inc* **39**, 627–638 (2012).
156. Taylor, C. B. *et al.* An investigation into the cost, coverage and activities of Helicopter Emergency Medical Services in the state of New South Wales, Australia. *Injury* **42**, 1088–1094 (2011).
157. Taylor, C. B. *et al.* A systematic review of the costs and benefits of helicopter emergency medical services. *Injury* **41**, 10–20 (2010).
158. Henderson, Y. & Haggard, H. The elimination of carbon monoxide from the blood after a dangerous degree of asphyxiation, and a therapy for accelerating the elimination. *J Pharmacol Exp Ther* **16**, 11–20 (1920).
159. Weaver, L. K., Howe, S., Hopkins, R. & Chan, K. J. Carboxyhemoglobin half-life in carbon monoxide-poisoned patients treated with 100% oxygen at atmospheric pressure. *Chest* **117**, 801–808 (2000).
160. Juurlink, D. N. *et al.* Hyperbaric oxygen for carbon monoxide poisoning. *Cochrane Database Syst. Rev.* CD002041 (2005). doi:10.1002/14651858.CD002041.pub2
161. Jiang, G. *et al.* Structural and functional improvement of injured brain after severe acute carbon monoxide poisoning by stem cell-based therapy in rats. *Crit. Care Med.* **37**, 1416–1422 (2009).
162. Spagnolo, F. *et al.* Delayed hyperbaric oxygen treatment after acute carbon monoxide poisoning. *J. Neurol.* **258**, 1553–1554 (2011).
163. Brvar, M., Luzar, B., Finderle, Ž., Šuput, D. & Bunc, M. The time-dependent protective effect of hyperbaric oxygen on neuronal cell apoptosis in carbon monoxide poisoning. *Inhal. Toxicol.* **22**, 1026–1031 (2010).
164. Saunders, P. J. Hyperbaric oxygen therapy in the management of carbon monoxide poisoning, osteoradionecrosis, burns, skin grafts, and crush injury. *Int. J. Technol. Assess. Health Care* **19**, 521–525 (2003).
165. Buckley, N. A., Juurlink, D. N., Isbister, G., Bennett, M. H. & Lavonas, E. J. Hyperbaric oxygen for carbon monoxide poisoning. *Cochrane Database Syst. Rev.* CD002041 (2011). doi:10.1002/14651858.CD002041.pub3
166. Oter, S. *et al.* Correlation between hyperbaric oxygen exposure pressures and oxidative parameters in rat lung, brain, and erythrocytes. *Clin. Biochem.* **38**, 706–711 (2005).



167. Korkmaz, A. *et al.* Exposure time related oxidative action of hyperbaric oxygen in rat brain. *Neurochem. Res.* **33**, 160–166 (2008).
168. Speit, G., Dennog, C., Radermacher, P. & Rothfuss, A. Genotoxicity of hyperbaric oxygen. *Mutat. Res.* **512**, 111–119 (2002).
169. Matsunami, T. *et al.* Enhancement of reactive oxygen species and induction of apoptosis in streptozotocin-induced diabetic rats under hyperbaric oxygen exposure. *Int. J. Clin. Exp. Pathol.* **4**, 255–266 (2011).
170. Matsunami, T., Sato, Y., Sato, T. & Yukawa, M. Antioxidant status and lipid peroxidation in diabetic rats under hyperbaric oxygen exposure. *Physiol. Res. Acad. Sci. Bohemoslov.* **59**, 97–104 (2010).
171. Rucker, J. *et al.* Normocapnia improves cerebral oxygen delivery during conventional oxygen therapy in carbon monoxide-exposed research subjects. *Ann. Emerg. Med.* **40**, 611–618 (2002).
172. Yokoyama, K. Effect of perfluorochemical (PFC) emulsion on acute carbon monoxide poisoning in rats. *Jpn. J. Surg.* **8**, 342–352 (1978).
173. Ireland, B. J. A case of carbon monoxide poisoning treated by replacement blood transfusion. *Med. J. Aust.* **1**, 331–332 (1952).
174. Jarcho, S. William Halsted on refusion of blood in carbon monoxide poisoning (1883). *Am. J. Cardiol.* **7**, 589–597 (1961).
175. Sun, X. *et al.* Potential use of hyperoxygenated solution as a treatment strategy for carbon monoxide poisoning. *PloS One* **8**, e81779 (2013).
176. McCunn, M., Reynolds, H. N., Cottingham, C. A., Scalea, T. M. & Habashi, N. M. Extracorporeal support in an adult with severe carbon monoxide poisoning and shock following smoke inhalation: a case report. *Perfusion* **15**, 169–173 (2000).
177. Yin, L. *et al.* Treatment of acute carbon monoxide poisoning with extracorporeal membrane trioxxygenation. *Int. J. Artif. Organs* **35**, 1070–1076 (2012).
178. Qingsong, W., Yeming, G., Xuechun, L., Hongjuan, L. & Jing, W. The free radical scavenger, edaravone, ameliorates delayed neuropsychological sequelae after acute carbon monoxide poisoning in rabbits. *Undersea Hyperb. Med. J. Undersea Hyperb. Med. Soc. Inc* **40**, 223–229 (2013).
179. Hoffman, B. M. & Petering, D. H. Coboglobins: oxygen-carrying cobalt-reconstituted hemoglobin and myoglobin. *Proc. Natl. Acad. Sci. U. S. A.* **67**, 637–643 (1970).
180. Ludwig and, M. L. & Matthews, R. G. Structure-Based Perspectives on B12-Dependent Enzymes. *Annu. Rev. Biochem.* **66**, 269–313 (1997).
181. Thompson, J. P. & Marrs, T. C. Hydroxocobalamin in cyanide poisoning. *Clin. Toxicol. Phila. Pa* **50**, 875–885 (2012).
182. Uhl, W., Nolting, A., Golor, G., Rost, K. L. & Kovar, A. Safety of hydroxocobalamin in healthy volunteers in a randomized, placebo-controlled study. *Clin. Toxicol. Phila. Pa* **44 Suppl 1**, 17–28 (2006).
183. Weinberg, J. B. *et al.* Inhibition of nitric oxide synthase by cobalamins and cobinamides. *Free Radic. Biol. Med.* **46**, 1626–1632 (2009).
184. Gerth, K., Ehring, T., Braendle, M. & Schelling, P. Nitric oxide scavenging by hydroxocobalamin may account for its hemodynamic profile. *Clin. Toxicol. Phila. Pa* **44 Suppl 1**, 29–36 (2006).

185. Borron, S. W. *et al.* Hemodynamics after intraosseous administration of hydroxocobalamin or normal saline in a goat model. *Am. J. Emerg. Med.* **27**, 1065–1071 (2009).
186. Greenberg, S. S., Xie, J., Zatarain, J. M., Kapusta, D. R. & Miller, M. J. Hydroxocobalamin (vitamin B12a) prevents and reverses endotoxin-induced hypotension and mortality in rodents: role of nitric oxide. *J. Pharmacol. Exp. Ther.* **273**, 257–265 (1995).
187. Roderique, J. D. *et al.* The Use of High-Dose Hydroxocobalamin for Vasoplegic Syndrome. *Ann. Thorac. Surg.* **97**, 1785–1786 (2014).
188. Stücker, M. *et al.* Topical vitamin B12—a new therapeutic approach in atopic dermatitis—evaluation of efficacy and tolerability in a randomized placebo-controlled multicentre clinical trial. *Br. J. Dermatol.* **150**, 977–983 (2004).
189. Wheatley, C. A scarlet pimpernel for the resolution of inflammation? The role of supra-therapeutic doses of cobalamin, in the treatment of systemic inflammatory response syndrome (SIRS), sepsis, severe sepsis, and septic or traumatic shock. *Med. Hypotheses* **67**, 124–142 (2006).
190. Schrauzer, G. N. & Lee, L. P. The reduction of vitamin B12a by carbon monoxide. *Arch. Biochem. Biophys.* **138**, 16–25 (1970).
191. Roderique, J. D. STUDIES ON THE REACTION OF HIGH-DOSE HYDROXOCOBALAMIN AND ASCORBIC ACID WITH CARBON MONOXIDE: IMPLICATIONS FOR TREATMENT OF CARBON MONOXIDE POISONING. (2013).
192. Barness, L. A. Safety considerations with high ascorbic acid dosage. *Ann. N. Y. Acad. Sci.* **258**, 523–528 (1975).
193. Somera, L. HYDROXOCOBALAMIN TREATMENT FOR CARBON MONOXIDE EXPOSURES: CHARACTERIZING HEMOGLOBIN CHANGES AND TESTING FOR NEUROLOGICAL SEQUELAE. (2014).
194. Dora, E., Chance, B., Kovach, A. G. & Silver, I. A. Carbon monoxide-induced localized toxic anoxia in the rat brain cortex. *J. Appl. Physiol.* **39**, 875–878 (1975).
195. Schroeder, J. L., Highsmith, J. M., Young, H. F. & Mathern, B. E. Reduction of hypoxia by perfluorocarbon emulsion in a traumatic spinal cord injury model. *J. Neurosurg. Spine* **9**, 213–220 (2008).
196. Sarrafzadeh, A. S., Sakowitz, O. W., Callsen, T. A., Lanksch, W. R. & Unterberg, A. W. Detection of secondary insults by brain tissue pO<sub>2</sub> and bedside microdialysis in severe head injury. *Acta Neurochir. Suppl.* **81**, 319–321 (2002).
197. Sarrafzadeh, A. S., Klening, K. L., Callsen, T.-A. & Unterberg, A. W. Metabolic changes during impending and manifest cerebral hypoxia in traumatic brain injury. *Br. J. Neurosurg.* **17**, 340 (2003).
198. Dengler, J., Frenzel, C., Vajkoczy, P., Wolf, S. & Horn, P. Cerebral tissue oxygenation measured by two different probes: challenges and interpretation. *Intensive Care Med.* **37**, 1809–1815 (2011).
199. Nortje, J. & Gupta, A. K. The role of tissue oxygen monitoring in patients with acute brain injury. *Br. J. Anaesth.* **97**, 95–106 (2006).
200. Nemani, V. M. & Manley, G. T. Brain tissue oxygen monitoring: physiologic principles and clinical application. *Oper. Tech. Neurosurg.* **7**, 2–9 (2004).
201. Verweij, B. H., Amelink, G. J. & Muizelaar, J. P. in *Prog. Brain Res.* (ed. John T. Weber and Andrew I.R. Maas) **Volume 161**, 111–124 (Elsevier, 2007).

202. Jespersen, B., Knupp, L. & Northcott, C. A. Femoral Arterial and Venous Catheterization for Blood Sampling, Drug Administration and Conscious Blood Pressure and Heart Rate Measurements. *J. Vis. Exp.* (2012). doi:10.3791/3496
203. Lee, J. *et al.* Potential Interference by Hydroxocobalamin on Cooximetry Hemoglobin Measurements During Cyanide and Smoke Inhalation Treatments. *Ann. Emerg. Med.* **49**, 802–805 (2007).
204. Carlsson, C. J. *et al.* An evaluation of the interference of hydroxycobalamin with chemistry and co-oximetry tests on nine commonly used instruments. *Scand. J. Clin. Lab. Invest.* **71**, 378–386 (2011).
205. Subramanian, R. K. *et al.* Normative data for arterial blood gas and electrolytes in anesthetized rats. *Indian J. Pharmacol.* **45**, 103–104 (2013).
206. Martini, R. P., Deem, S. & Treggiari, M. M. Targeting Brain Tissue Oxygenation in Traumatic Brain Injury. *Respir. Care* **58**, 162–172 (2013).
207. Mopett, I. K. D. & Hardman, J. G. D. Modeling the Causes of Variation in Brain Tissue Oxygenation. *Anesth. Analg.* Oct. 2007 **105**, 1104–1112 (2007).
208. Cipolla, M. *The Cerebral Circulation*. (Morgan & Claypool Life Sciences, 2009). at <<http://www.ncbi.nlm.nih.gov/books/NBK53082/>>
209. Hernández, M. J., Brennan, R. W. & Bowman, G. S. Cerebral blood flow autoregulation in the rat. *Stroke* **9**, 150–154 (1978).
210. Hagendorff, A. *et al.* Myocardial and cerebral hemodynamics during tachyarrhythmia-induced hypotension in the rat. *Circulation* **90**, 400–410 (1994).
211. Critchley, G. R. & Bell, B. A. Acute cerebral tissue oxygenation changes following experimental subarachnoid hemorrhage. *Neurol. Res.* **25**, 451–456 (2003).
212. Hemphill, J. C. I., Knudson, M. M., Derugin, N., Morabito, D. R. N. & Manley, G. T. M. D. Carbon Dioxide Reactivity and Pressure Autoregulation of Brain Tissue Oxygen. [Miscellaneous Article]. *Neurosurg. Febr. 2001* **48**, 377–384 (2001).
213. Edelman, G. J., Hoffman, W. E., Rico, C. & Ripper, R. Comparison of brain tissue and local cerebral venous gas tensions and pH. *Neurol. Res.* **22**, 642–644 (2000).
214. Gupta, A. K. *et al.* Measuring brain tissue oxygenation compared with jugular venous oxygen saturation for monitoring cerebral oxygenation after traumatic brain injury. *Anesth. Analg.* **88**, 549–553 (1999).
215. Fortune, J. B., Feustel, P. J., Weigle, C. G. & Popp, A. J. Continuous measurement of jugular venous oxygen saturation in response to transient elevations of blood pressure in head-injured patients. *J. Neurosurg.* **80**, 461–468 (1994).
216. Sheinberg, M. *et al.* Continuous monitoring of jugular venous oxygen saturation in head-injured patients. *J. Neurosurg.* **76**, 212–217 (1992).
217. Van den Brink, W. A. *et al.* Brain Oxygen Tension in Severe Head Injury. *Neurosurg. April 2000* **46**, 868–878 (2000).
218. Pal, D. *et al.* Determination of minimum alveolar concentration for isoflurane and sevoflurane in a rodent model of human metabolic syndrome. *Anesth. Analg.* **114**, 297–302 (2012).
219. Eger, E. I. The pharmacology of isoflurane. *Br. J. Anaesth.* **56 Suppl 1**, 71S–99S (1984).
220. Marano, G., Grigioni, M., Tiburzi, F., Vergari, A. & Zanghi, F. Effects of isoflurane on cardiovascular system and sympathovagal balance in New Zealand white rabbits. *J. Cardiovasc. Pharmacol.* **28**, 513–518 (1996).

221. Strebel, S. *et al.* Dynamic and static cerebral autoregulation during isoflurane, desflurane, and propofol anesthesia. *Anesthesiology* **83**, 66–76 (1995).
222. Hoffman, W. E. *et al.* Cerebral autoregulation in awake versus isoflurane-anesthetized rats. *Anesth. Analg.* **73**, 753–757 (1991).
223. Avram, M. J. *et al.* Isoflurane alters the recirculatory pharmacokinetics of physiologic markers. *Anesthesiology* **92**, 1757–1768 (2000).
224. Duong, T. Q., Iadecola, C. & Kim, S. G. Effect of hyperoxia, hypercapnia, and hypoxia on cerebral interstitial oxygen tension and cerebral blood flow. *Magn. Reson. Med. Off. J. Soc. Magn. Reson. Med. Soc. Magn. Reson. Med.* **45**, 61–70 (2001).
225. Aksenov, D., Eassa, J. E., Lakhoo, J., Wyrwicz, A. & Linsenmeier, R. A. Effect of isoflurane on brain tissue oxygen tension and cerebral autoregulation in rabbits. *Neurosci. Lett.* **524**, 116–118 (2012).
226. Berry, P. D., Sessler, D. I. & Larson, M. D. Severe carbon monoxide poisoning during desflurane anesthesia. *Anesthesiology* **90**, 613–616 (1999).
227. Nielsen, T. H., Olsen, N. V., Toft, P. & Nordström, C. H. Cerebral energy metabolism during mitochondrial dysfunction induced by cyanide in piglets. *Acta Anaesthesiol. Scand.* **57**, 793–801 (2013).
228. Collison, H. A., Rodkey, F. L. & O'Neal, J. D. Determination of Carbon Monoxide in Blood by Gas Chromatography. *Clin. Chem.* **14**, 162–171 (1968).
229. Guillot, J. G., Weber, J. P. & Savoie, J. Y. Quantitative determination of carbon monoxide in blood by head-space gas chromatography. *J. Anal. Toxicol.* **5**, 264–266 (1981).
230. Hao, H., Zhou, H., Liu, X., Zhang, Z. & Yu, Z. An accurate method for microanalysis of carbon monoxide in putrid postmortem blood by head-space gas chromatography-mass spectrometry (HS/GC/MS). *Forensic Sci. Int.* **229**, 116–121 (2013).

## Vita

Alden Hemenway Newcomb was born in Fredericksburg, VA on July 27<sup>th</sup>, 1990. Following graduation from Colonial Forge High School in Stafford, VA he attended Virginia Polytechnic Institute & State University where he received a Bachelor of Science degree in biochemistry in May, 2012. He continued his studies at Virginia Commonwealth University in pursuit of a Master of Science in Physiology & Biophysics that he is scheduled to receive in August 2014. During his time in graduate school he worked as a medic in the emergency department at VCU Medical Center<sup>3</sup>. He is currently living in Richmond and will be entering the VCU School of Medicine as a member of the class of 2018 in August, 2014.